

https://dspace.org/

Application of fate and transport models to evaluate the efficiency of a Cr(VI) remediation pump and treat system

Nkosi, Sifiso Collen

2016

http://hdl.handle.net/10539/21234

Nkosi, Sifiso Collen (2016) Application of fate and transport models to evaluate the efficiency of a Cr(VI) remediation pump and treat system, University of Witwatersrand, Johannesburg, <http://wiredspace.wits.ac.za/handle/10539/21234>

Downloaded from a DSpace repository. https://dspace.org/

Application of fate and transport models to evaluate the efficiency of a Cr(VI) remediation pump and treat system

Sifiso Collen Nkosi

Student number: 0702199P

GEOL 7028 – Research Project

For partial fulfillment of the Master of Science in Hydrogeology

23 May 2016



School of Geosciences

University of the Witwatersrand

Johannesburg, South Africa

I declare that this research project is my own, independent work. This research report is being submitted in partial fulfilment of the requirements for the degree, Master of Science (coursework and research) in Hydrogeology at the University of the Witwatersrand, Johannesburg. It has not been submitted for degree awarding or examination purposes at any other university.

(Signature)

Sifiso Collen Nkosi; BSc (Hons), Cand.Sci.Nat. (No 100105/13)

Candidate Natural Scientist

ACKNOWLEDGEMENTS

I would like to thank Morne Burger and the management of Geo Pollution Technologies for allowing me to undertake this study and for their continued support throughout the project. Morne Burger conceptualised and designed the remedial system and I congratulate him on his innovative thinking and sound scientific knowledge and expertise. Altus Huisamen for the guidance on the use of the Geochemist's Workbench and its capabilities. A big thank you to Leske van Dyk for assistance with the use of specialised GIS software. My colleagues, Christo Gouws and Vevanya Naidoo for assistance with the fieldwork and continued support.

I would like to thank my partner, Simphiwe Khumalo and my family for their support during my time at the University of the Witwatersrand.

Thank you to the UNESCO HOPE Initiative for providing training and software for the ModelMuse interface for MODFLOW 2005.

A special word of thanks to my supervisor Prof. T. Abiye and his support staff for sharing his knowledge and experience for the good of the African continent and the world at large. I appreciate his time and patience. I would also like to congratulate him on initiating the hydrogeology course at Wits University and I am very proud to have been a part of the first class of MSc in Hydrogeology by coursework and research at Wits University. I look forward to future co-operation with this newly founded department.

ABSTRACT

Groundwater treatment by chemical precipitation is a popular form of remediation at mines that are in operation. The water quality status at the implementation of the PAT in this study was compared to the water quality status after a six-month period of active remediation. Chromium is very important as an industrial metal owing to its numerous uses in a variety of industries. The objective of the remedial action is to intercept the Cr(VI) plume, abstract contaminated groundwater and chemically treat it on the surface. The long-term (15-year) objective is to eventually reduce Cr(VI) concentrations in the aquifer(s) to below 0.05 mg/ℓ. The PAT system was implemented as a medium-term (5-year) strategy to intercept the Cr(VI) contamination plume during migration to prevent it from negatively impacting on groundwater users downstream of the mine.

In the vicinity of the three PAT systems' abstracting wells, water levels declined by an average of 2 m compared to the same period in 2014. Periodical fluctuations in the fractured aquifer are reflective of the influence of fractures on groundwater flow. In the aquifer, hydrochemical signatures show evidence of mixing between the primary and secondary aquifers. The treatment system has been successful in reducing Cr(VI) to Cr(III) and precipitating $Cr(OH)_3$. The treatment system was designed to treat Cr(VI), other elevated constituents and generally high dissolved ions are not treated in this remedial process. Sulphate concentrations increase after treatment as a result of the addition of $Fe(II)SO_4$ for chromate contamination treatment purposes.

The simulated reaction path shows that the transformation of CrO_4^{2-} to Cr_2O_3 in the treatment system is not immediate. The Cr(VI) to Cr(III) transformation is irreversible, this is beneficial as the water is abstracted from more reducing conditions, and the treatment ponds are open to the atmosphere thus the conditions following dosing with $Fe(II)SO_4$ are oxic and chromate complexes are stable over a wider range of Eh-pH conditions than Cr(III) compounds. This ensures that the efficiency of the dosing system is not reversed in Settling Pond B. The modelled flow paths are similar to the inferred flow vectors in the plume capture zone. Fracture flow is the dominant type of flow, the fault zones and dykes create high permeability conduits to flow. Flow paths are parallel to fault lines or the lateral dimension of dykes; flow occurs along fractures and deformation zones.

The reduction of Cr(VI) concentrations in some of the peripheral sampling points indicates that the PAT system has been successful in capturing the chromate contaminated water through pumping.

Keywords: Hexavalent chromium, groundwater pollution, remediation, pump-and-treat, fractured aquifers

TABLE OF CONTENTS

Page

1. INTRODUCTION 11
1.1 THE RESEARCH PROBLEM 14
1.2 THE PURPOSE OF THE STUDY 14
1.3 SCOPE OF WORK 14
2. LITERATURE REVIEW 15
2.1 GEOCHEMISTRY OF CHROMIUM 19
2.2 FATE AND TRANSPORT OF CR(VI) IN THE ENVIRONMENT 21
2.3 NUMERICAL MODELLING 22
2.4 CASE STUDIES 25
3. STUDY METHODOLOGY 27
3.1 SAMPLE COLLECTION 27
3.2 LABORATORY ANALYSES 27
3.2.1 Inorganic Chemistry 28
3.2.2 Cr(VI) Analysis 28
3.2.3 Environmental Isotope Analysis 29
3.3 QUALITY CONTROL AND QUALITY ASSURANCE 29
3.4 FATE AND TRANSPORT MODELLING 30
3.5 NUMERICAL MODELLING 30
3.6 ENVIRONMENTAL ISOTOPES AND GROUNDWATER TRACERS 31
3.7 SWOT ANALYSIS 31
4. SITE DESCRIPTION 32
4.1 SITE LOCATION 32
4.2 CLIMATE AND DRAINAGE 35
4.3 LOCAL GEOLOGY 39
4.4 LOCAL HYDROGEOLOGY 41
5. HISTORICAL DATA REVIEW 44
5.1 CLASSIFICATION OF CONTAMINATED SITE 44
5.2 INITIAL TESTING PROGRAMME 46
5.2.1 Aquifer tests 46
5.3 SYSTEM DESIGN 48
5.4 OBJECTIVES OF THE PAT TECHNOLOGY 50
5.5 EXPECTED OUTCOMES 50
5.6 IMPLEMENTATION OF TREATMENT TECHNOLOGY 51
5.6.1 Step 1 - Pumped Cr (VI)- contaminated groundwater 51

5.6.2 Step 2 – Settling pond A to Dosing Pump 51
5.6.3 Step 3 – Dosing Pump to Settling pond B 51
5.7 GROUNDWATER MONITORING NETWORK 52
6. RESULTS AND INTERPRETATION 56
6.1 CONCEPTUAL SITE MODEL 56
6.2 WATER LEVELS 58
6.3 HYDROCHEMICAL CHARACTERISATION 63
6.3.1 Water types 64
6.3.2 ^{2}H and ^{18}O 67
6.3.3 Tritium 69
6.4 ASSESSMENT OF TREATMENT SYSTEM 70
6.5 GEOCHEMICAL MODELLING 73
6.6 NUMERICAL MODELLING 77
6.6.1 Assumptions and Limitations 77
6.6.2 Boundary Conditions 77
6.6.3 Elevation Data 78
6.6.4 Aquifer parameters 78
6.6.5 Calibration of the Model 78
6.6.6 Groundwater Flow 82
7. DISCUSSION 84
7.1 STRENGTHS 84
7.2 WEAKNESSES 84
7.3 OPPORTUNITIES 84
7.4 THREATS 84
8. CONCLUSIONS 85
9. RECOMMENDATIONS 88

LIST OF FIGURES

Page

FIGURE 1: WORLD CHROMIUM PRODUCTION (ICDA, 2015)..... 15
FIGURE 2: SIMPLIFIED STRATIGRAPHIC COLUMN THROUGH THE WESTERN AND EASTERN LIMBS OF THE BUSHVELD IGNEOUS COMPLEX (VAN DER MERWE AND CAWTHORN, 2005)..... 17
FIGURE 3: FLOW CHART OF THE COMMON STEPS TAKEN BY FERROCHROME PRODUCERS IN SOUTH AFRICA TO EXCTRACT FECR PRODUCT (BEUKES ET AL., 2010)..... 18
FIGURE 4: ILLUSTRATION OF PRECIPITATION OF A SOLUTE OUT OF SOLUTION (SCHAFFER AND HERMAN, 2015)..... 26
FIGURE 5: LOCATION OF THE STUDY AREA AND LAYOUT OF THE STUDY AREA SHOWING THE CHROMATE CONTAMINATION PLUME PRIOR TO THE COMMENCEMENT OF TREATMENT..... 33
FIGURE 6: LAND USE MAP AROUND THE MINE AND STUDY AREA, SHOWING A 2 KM RADIUS AROUND THE SOURCE AREA. 34
FIGURE 7: DIGITAL ELEVATION MODEL (DEM) OF THE UPPER CROCODILE SUB-CATCHMENT SHOWING THE STUDY AREA AND NATURAL DRAINAGE FEATURES.36
FIGURE 8: MEAN MONTHLY RAINFALL AND EVAPORATION DATA AS RECORDED AT THE KROONDAL METEOROLOGICAL STATION (SOURCE: DWA, 2015). 38
FIGURE 9: SITE GEOLOGY MAP. 40
FIGURE 10: FAULT ZONE POTENTIAL INFLUENCES ON HYDRAULIC HEAD GRADIENTS AND GROUNDWATER FLOW (SOURCE: BENSE ET AL., 2013). 42
FIGURE 11: STRATIGRAPHY OF THE CHROMITITE BEARING LAYERS OF THE RLS (NOT TO SCALE; SOURCE CAWTHORN, 1999). 43
FIGURE 12: SITE ASSESSMENT AS PER THE BEST PRACTICE GUIDELINES AS SET BY THE SOUTH AFRICAN ENVIRONMENTAL AUTHOROTIES (DWAF, 1998)..... 45
FIGURE 13: TREATMENT SYSTEM DESIGN (GEO POLLUTION TECHNOLOGIES, 2013). 49
FIGURE 14: CONCEPTUAL GROUNDWATER PLUME SHOWN THROUN AND W-E CROSS SECTION THROUGH THE WEATHERED AND FRACTURED AQUIFERS, CONCEPTUALISING THE POTENTIAL FLOW PATHS THROUGH THE SUBSURFACE.. 57
FIGURE 15: WATER LEVEL TRENDS OVER A PERIOD OF ONE YEAR SHOWING CHANGES IN AQUIFER STORAGE. BH-SM3 WAS DESTROYED IN APRIL 2015. 60
FIGURE 16: CONTOURED WATER LEVEL ELEVATIONS ALSO SHOWING INFERRED GROUNDWATER FLOW VECTORS PRIOR TO PUMPING (JANUARY 2015)..... 61

FIGURE 17: CONTOURED WATER LEVEL ELEVATIONS ALSO SHOWING INFERRED GROUNDWATER FLOW VECTORTS (JULY 2015)..... 62
FIGURE 18: STIFF DIAGRAMS SHOWING THE SPATIAL DISTRIBUTION OF MAJOR IONS AND WATER SIGNATURES IN THE STUDY AREA. 65
FIGURE 19: CLASSIFICATION DIAGRAM OF THE HYDROCHEMICAL FACIES IN THE PIPER DIAGRAM (HISCOCK, 2005). 66
FIGURE 20: WATER SAMPLES FOR GROUNDWATER AND SURFACE WATER SAMPLES PLOTTED AGAINST THE PIPER DIAGRAM. 66
FIGURE 21: STABLE ISOTOPE DATA ($\Delta^{18}O$ (‰) VS. $\Delta^{2}H$ (‰)) PLOTTED RELATIVE TO THE GMWL AND PLMWL. 68
FIGURE 22: TRENDS IN CR AND CR(VI) CONCENTRATIONS IN THE TREATMENT SYTEM BEFORE AND AFTER CHEMICAL TREATMENT OVER A SIX-MONTH PERIOD. 70
FIGURE 23: TRENDS IN MAJOR ION CHEMISTRY BEFORE CHEMICAL TREATMENT OVER A SIX-MONTH PERIOD. 71
FIGURE 24: TRENDS IN MAJOR ION CHEMISTRY AFTER CHEMICAL TREATMENT OVER A SIX-MONTH PERIOD. 72
FIGURE 25: CHEMICAL AND MINERALOGICAL SPECIATION DURING TREATMENT (REACTION PATH FROM CRO_4^{--} AQUEOUS PHASE TO CR_2O_3 MINERAL PHASE)..... 74
FIGURE 26: RESULTS OF THE MODELLING OF THE CRO_4^{2-} TRANSITION CR_2O_3 IN GWB IN TERMS OF CHROMATE CONCENTRATIONS OVER TIME. 75
FIGURE 27: STABILITY FIELD DIAGRAM FOR CR SPECIES IN WATER AT 25°C AND 1 ATM ON EH AND PH AXES. 76
FIGURE 28: CALIBRATION GRAPH (HYDRAULIC HEAD IN M.A.M.S.L.). 79
FIGURE 29: ELEVATION CONTOURS. 80
FIGURE 30: MODEL BOUNDARY. 81
FIGURE 31: MODELLED GROUNDWATER HEAD CONTOURS SHOWING FLOW VECTORS. 83

LIST OF TABLES

Page

TABLE 1: THE VARIOUS OXIDATION STATES OF CHROMIUM WITH COMMON COMPOUND EXAMPLES FOR EACH OXIDATION STATE. 20
TABLE 2: MEAN MONTHLY RAINFALL AND EVAPORATION DATA AS RECORDED AT THE KROONDAL METEOROLOGICAL STATION OVER A 70-YEAR PERIOD BETWEEN 2015 AND 1945 (SOURCE: DWA, 2015). 37

TABLE 3: MONITORING POINTS. 54
TABLE 4: MONITORED INDICATOR PARAMETERS. 55
TABLE 5: A COMPARISON OF THE WATER LEVEL DATA MEASURED OVER A PERIOD OF A YEAR (JULY 2014 TO JULY 2015). THE DIFFERENCE IN WATER LEVELS AFTER A YEAR OF PERIODICAL WATER LEVEL MONITORING REPRENTS A WATER LEVEL DECLINE FOR A POSITIVE VALUE AND VICE VERSA. 59
TABLE 6: LIKELY SOURCES OF DISSOLVED CONSTITUENTS UN THE STUDY AREA. 63
TABLE 7: RESULTS OF THE STABLE ISOTOPE ANALYSIS. 67
TABLE 8: RESULTS OF THE TRITIUM ANALYSIS FOR MONITORING BOREHOLES. 69

LIST OF APPENDICES

Page
APPENDIX I: ANALYTICAL DATA 92
APPENDIX II: AQUIFER TEST ANALYSIS 99
APPENDIX III: BOREHOLE CONSTRUCTION 104

LIST OF ABBREVIATIONS

Abbreviation	**Explanation**
Cr	Total chromium
Cr(III)	Tetravalent chromium
Cr(VI)	Hexavalent chromium
CSM	Conceptual site model
EC	Electrical conductivity
Km^2	Square Kilometre
ℓ/s	Litres per second
m a.m.s.l.	Meters above mean sea level
m. b.g.l.	Meters below ground level
m	Meter
Mg/ℓ	Milligrams/litre
mm	Millimetre
mm/a	Millimetres per annum
mS/m	MilliSiemens per metre
m^3	Cubic metres
MAE	Mean Annual Evaporation
MAP	Mean Annual Precipitation
PAT	Pump And Treat
ppm	Parts per million
TDS	Total Dissolved Solids

1. INTRODUCTION

The Cr(VI) groundwater contamination plume in the study area extends over a large lateral and vertical extent. Metal contamination in a populated area that depends on groundwater is a major environmental problem. Thus, it is important to ensure that remedial objectives are met and the risk of further potential contamination of the groundwater resource is minimised. Active groundwater remediation strategies have to be adapted to the area that is impacted by toxic chemicals. The successful remediation of contaminated groundwater should address primarily the contamination source as well as the contaminant plume (Hiscock, 2005). The remedial method employed for the site under investigation is a pump-and-treat (PAT) system. The conventional pump-and-treat method of aquifer treatment is to abstract the contaminated groundwater then chemically treat it on the surface. Following the treatment of contaminants of concern, in this case CR(VI), the water is disposed of by discharging it into surface water resources or injecting it back into the aquifer (Hiscock, 2005). The first step in the treatment process is to minimise the potential for further contamination from the source of contamination. The contamination source under investigation has been decommissioned and contained over a period of 12 years. The presence of receptors and the contamination plume having impacted upon privately owned abstraction boreholes rendered remediation necessary.

Chromium (Cr) occurs in the natural environment in two valence states, i.e. Cr(III) and Cr(VI). Cr(VI) is very soluble and highly toxic, whereas Cr(III) is less soluble and an essential nutrient to the human diet. Cr(III) occurs as chromium oxide (Cr_2O_3) and chromium hydroxide [$Cr(OH)_3$] or as dissolved $CrOH^{2+}$ and $Cr(OH)^{2+}$ cations (Economou-Eliopoulos et al., 2011). Cr(VI) generally occurs as dissolved dichromate ($Cr_2O_7^{2-}$) and chromate (CrO_4^{2-}) anions (Motzer and Todd Engineers, 2005). Cr(VI) is highly soluble at near neutral and alkaline pH waters and can thus be transported over great distances (Stanin and Pirnie, 2005).

Cr(VI) is generally classified as a carcinogen, with up to 20 years cancer latency. The drinking water limit for Cr(VI) concentration is nationally set at 0.05 mg/ℓ above which water consumers may experience negative health effects with short- and long-term intake (Motzer and Todd Engineers, 2005). The contaminated site monitoring boreholes showed Cr(VI) concentrations ranging from 0.00 to 1.16 mg/ℓ before implementation of the remedial technology. These are relatively small concentrations in the context of groundwater contamination and remediation, which makes it difficult to effectively and efficiently treat Cr(VI)-contaminated groundwater (Watts et al., 2015).

The construction of the pilot plant was completed by the end of February 2015 and was operational immediately after construction. The treatment of Cr(VI) contaminated groundwater is to be achieved by the reduction of Cr(VI) to Cr(III) using aqueous ferrous sulphate [$Fe(II)SO_4$]. The operational schedule includes water level and water quality monitoring, and inspection and maintenance of infrastructure.

Groundwater treatment by chemical precipitation is a popular form of remediation at mines, which are in operation (Fenglian and Wang, 2011). Chromium is to be precipitated as a hydroxide, viz. chromium hydroxide [$Cr(OH)_3$]. The removal of chromium can be achieved by the addition of ferrous sulphate (Dossing et al., 2011).

The technology is simple to operate and cost effective (Barcelona et al., 2005). However, its success is dependent on some hydrochemical conditions in the dosing system and treatment ponds as well as transient hydrogeochemical and physical hydrogeological conditions (Wanner et al., 2012). Consequently, the efficiency of the treatment technology may be affected negatively under conditions of basic, acidic or ultra-basic pH, and oxidising conditions (Mukhopadhyay et al., 2007). Quarterly monitoring of the entire monitoring network is already in place and is set to continue under the management of the mine environmental officer. Water abstracted for treatment and the treated water will be monitored for Cr and Cr(VI) at a high frequency, i.e. weekly and as part of the quarterly monitoring programme. The water quality status at the implementation of the remedial technology will be compared to the water quality status after a six month period.

The efficiency of the active treatment of Cr(VI) contaminated aquifers by chemical precipitation using dissolved Ferrous ion (Fe^{2+}) as the reactive agent will be evaluated using geochemical and numerical models. High frequency hydrochemical monitoring data and isotopic data will be assessed and integrated into a transport model using ModelMuse interface for MODFLOW 2005 and geochemical modelling using the Geochemist's Workbench programme. The assessment will culminate in a SWOT (strengths, weaknesses, opportunities and threats) analysis, examining associated expected outcomes, risks and possible improvements (Theis et al., 2003).

Environmental isotopes (^2H, ^3H and ^{18}O) are useful to trace mixing of different types of groundwater to determine the origin of dissolved constituents (Geyh, 2000; Wanner et al., 2011). ^2H, ^3H and ^{18}O are integral parts of the hydrological cycle. Thus they are useful in tracing groundwater movement, including its dissolved constituents when used in conjunction with major ion chemistry. Unlike most chemical tracers, environmental isotopes are relatively conservative in reactions with catchment materials. This is especially true for oxygen and hydrogen isotopes in water; meteoric waters retain their distinctive fingerprints until they mix with waters of different compositions or, in the case of isotopes of dissolved species, there are reactions with minerals or other fluids.

The data utilised in this study were collected from a comprehensive water monitoring network, consisting of 13 monitoring boreholes, six privately owned abstraction boreholes and three surface water monitoring points. *Kareespruit* is a tributary of the Crocodile River and is located at about 2 km west of the contamination source and is considered as a critical receptor. The research project made use of frequently monitored groundwater level and hydrochemical data. Thus this

research project is essentially a phase III monitoring and control exercise. The hydrochemical data used consists of major and minor ions and metals. The environmental isotopes consist of 18-O, 2-H and ^{3}H. The data set was used in conjunction with fundamental hydrogeological information to model the fate and transport of Cr(VI). The transient groundwater level data was used to calibrate a mathematical model to determine the capture zones of the abstracting boreholes used for the PAT system.

The technical success of the PAT system depends on the interaction between various factors viz.: engineering design, housekeeping and resource availability. It is important to ensure that systems are not allowed to get too complex and that they are adapted to prevailing conditions through analytical studies. Groundwater flow dynamics and the movement of contaminants in the groundwater regime are complex processes (Singhal and Gupta, 2009). Thus it is important to develop remedial techniques that are adaptable to the area of application and to meet remedial objectives.

1.1 The Research Problem

The current research problem is to evaluate the efficiency of the dosing system in treating Cr(VI) by reduction to Cr(III); precipitation of Cr(III) in the reaction pond; effectiveness of abstraction in capturing the contamination plume; the effect of pumping on groundwater flow and reactions.

1.2 The Purpose of the Study

The research project focuses on the hydrogeological study that is being undertaken as part of the remedial action plan to address Cr(VI) groundwater contamination at an operational mine and surrounding environment. The reasons as to why this study that several areas of uncertainty exist regarding groundwater contamination by Cr(VI) which requires further research in order to better quantify risks and enhance effectiveness of mitigation and remedial steps (Beukes et al., 2010).

1.3 Scope of Work

In order to generate the required information and to assess the efficiency of the treatment system in treating Cr(VI) contamination, the following tasks were completed:

- Weekly sampling of the treatment ponds and quarterly sampling of the entire monitoring network over a 6-month period from the implementation of the treatment technology.
- Laboratory analysis, data capturing and data processing.
- Hydrochemical characterisation using major element chemistry, stable isotopes and tritium (Kitchen et al., 2012).
- Determining the fate and transport of Cr(VI) in the aquifer(s) (Wanner et al., 2011).
- To characterise the pH, Eh and temperature conditions and naturally occurring reactions in the treatment ponds' aqueous system and contaminated aquifers.
- Assess water level monitoring data and effect of abstraction for treatment on groundwater storage.
- Evaluate the efficiency of the treatment technology and dosing system in effectively reducing Cr(VI) and precipitating $Cr(OH)_3$.
- Perform a SWOT analysis to identify associated risks and possible improvements that can be made to the treatment system (Theis et al., 2003).

2. LITERATURE REVIEW

Chromium is very important as an industrial metal due its numerous uses in a variety of products. Of the three Cr oxidation states that occur in nature, viz.: Cr(0), Cr(III) and Cr(VI), Cr(VI) as dissolved chromate is considered toxic to living organisms (Motzer and Todd Engineers, 2005). Cr(VI) occurs as soluble dichromate ($Cr_2O_7^-$) and chromate (CrO_4^{2-}) anions. The ingestion of these anions results in severe gastrointestinal disorders, hemorrhagic diathesis and convulsions at concentrations exceeding 1 g/ℓ. At concentrations below 0.05 mg/ℓ Cr(VI) is reduced to Cr(III) in the digestive tract (Guertin, 2005). Ingestion pathways may be through ingestion, dermal contact or inhalation. Only the effects of ingestion through drinking Cr(VI) contaminated water are considered in this research project. Water-borne Cr(VI) is not considered carcinogenic, but has been proven to cause illness and ultimately death in humans (Guertin, 2005). Due to the high carcinogenic risk associated with air-borne Cr(VI), Cr(VI)-bearing dusts and fumes are mixed with water increasing the advent of water contamination (Beukes et al., 2010).

South Africa accounts for 45% of the 15 100 000 tons of chromium produced worldwide. Chromite ore is used in the metallurgical, chemical and refractory industries. Up to 90% of all chrome ore is used in the metallurgical industry to produce stainless steel, alloyed steel and non-ferrous alloys. Several areas of uncertainty still exist in chromium-related environmental problems in the South African ferrochrome industry. It has become increasingly important to quantify risks and redress environmental contamination. Metallic Cr is not considered toxic, however in its more soluble and mobile Cr(VI) oxidation state it has been proven to cause acute health effects when ingested.

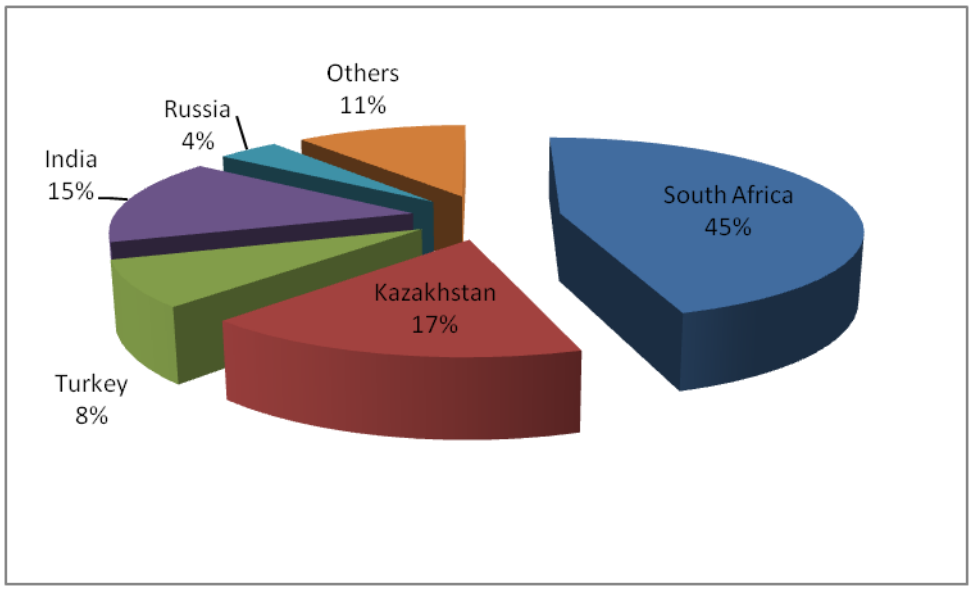


Figure 1: World chromium production (ICDA, 2015).

Cr(VI) is unintentionally generated in the South African ferrochrome industry during the dry milling and agglomeration processes (Beukes et al., 2010). Agglomeration is a necessary pre-treatment step typical of the South African metallurgical extraction process. Agglomeration of fine-grained ore feed

serves to ensure a permeable furnace bed, without gas eruptions and bed turnovers improving furnace efficiency and reducing downtime. The dry milling and agglomeration processes are conducted at high temperatures under highly reducing conditions. Since oxygen cannot be excluded from high temperature processes, Cr(VI) is formed by the oxidation of Cr(III) (Beukes et al., 2010). The smelting process of chromite ore at the contaminated site in an open/semi-closed furnace generated FeCr (product), slag and baghouse dust as the final and by-products.

Cr(VI) generation potential during ore processing is controlled by a number of factors, viz.: furnace design, the presence of alkaline compounds and fines in the furnace feed. (Beukes et al., 2010) suggests practices that can reduce the risk of Cr(VI) generation during ore processing. Namely, operating a closed furnace; acidic slag operation; and low fine chromite ore content. The influence of temperature may be disregarded as high temperatures during chromite ore processing cannot be averted. However Cr(VI) generation is largely inevitable in some industries including the electroplating and manufacturing industries. Even if waste management practices are sound, spills and leaks are still possible due to poor housekeeping. Thus it is imperative to learn from existing cases of contamination and develop effective remedial methods and management systems. Jones and Geldenhuys (2011) state that the addition carbon as a reductant in the smelting process for Upper Group 2 (UG2) reef chromite helps keep the oxidation state of Cr as Cr(II). In the form CrO, residual chromium in furnace is soluble in the slag and greatly reduces the potential for Cr(VI) dust generation.

Chromite ore exploited in the South African ferrochrome industry contains chromium as a spinel ($FeCr_2O_3$) (Beukes et al., 2010). Chromite ore [$(Fe, Mg)(Cr, Al)_2O_4$] in the Bushveld Igneous Complex (BIC) is preferentially concentrated in the chromitite layers in the Critical Zone of the Rustenburg Layered Suite (Clarke et al., 2008). The UG2 chromitite layer occurs in both the western and eastern limbs of the BIC in the Upper Cirtical Zone (C_uZ). A simplified section through the western and eastern limbs of the BIC is shown in Figure 2. Concentration of Cr(VI) in the contaminated aquifer(s) is due to a known point source, i.e a baghouse slimes dam. Baghouse dust was produced during the extractive metallurgical smelting produces. The technical aspects of Cr(VI) generation in the South African ferrochrome industry are described in a later section. Baghouse dust refers to electric furnace dust generated during the smelting process. Baghouse dust is made up of fine particles from which Cr(VI) can be leached into the subsurface reaching the shallow groundwater table (Beukes et al., 2010).

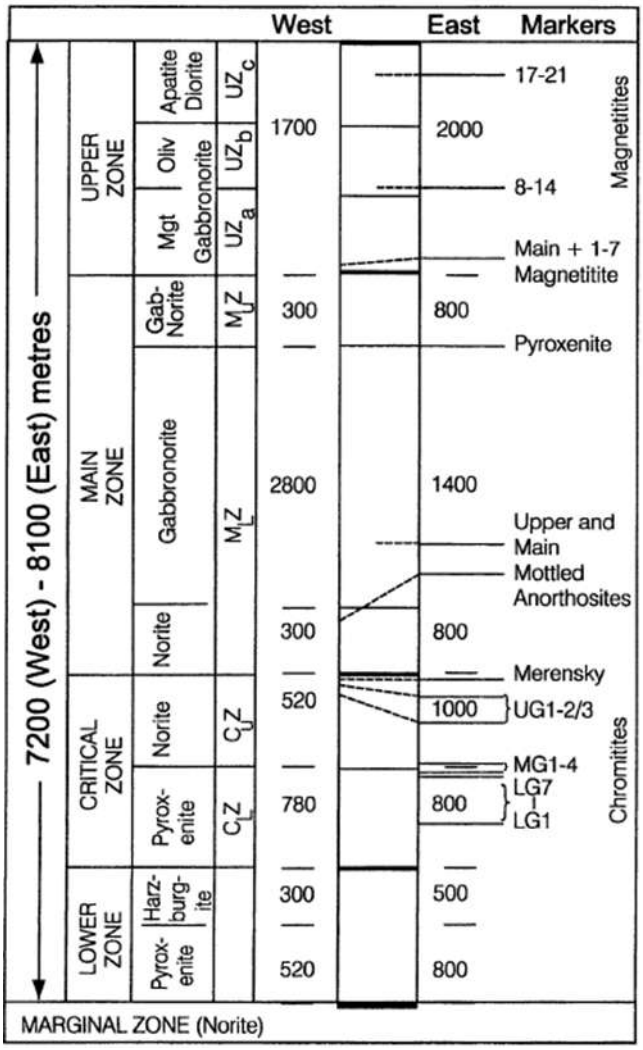


Figure 2: Simplified stratigraphic column through the western and eastern limbs of the Bushveld Igneous Complex (van der Merwe and Cawthorn, 2005).

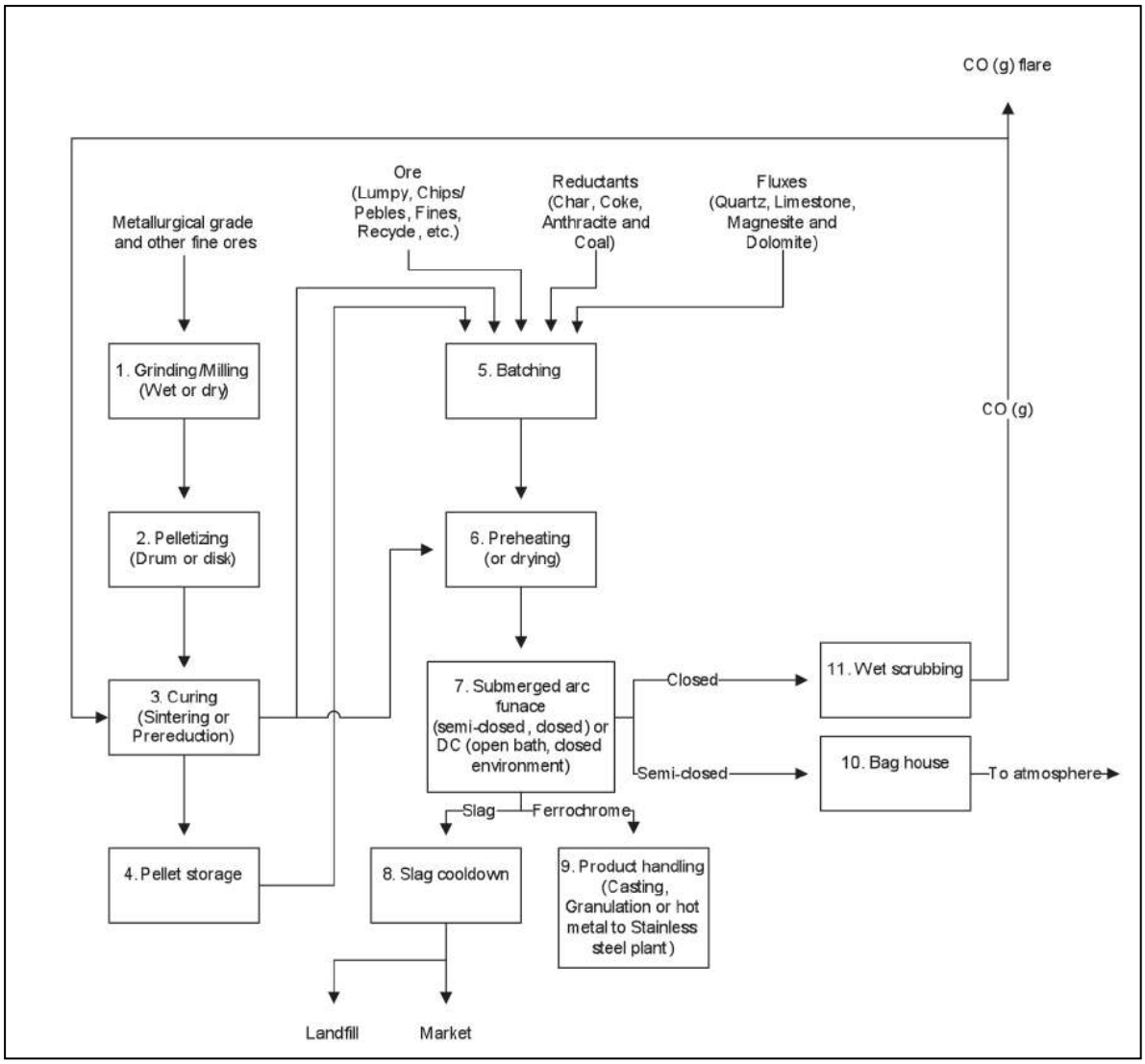


Figure 3: Flow chart of the common steps taken by ferrochrome producers in South Africa to exctract FeCr product (Beukes et al., 2010).

2.1 Geochemistry of Chromium

Chromium occurring as Cr_2O_3 is thought to have originated in the upper mantle or crust-mantle transition zones such as supra-subduction zones (Motzer and Todd Engineers, 2005). There are 82 officially recognised chromium minerals, which are mostly unique to locations of occurrence. The most widely occurring chromium ore mineral is chromite in the form: $(Mg, Fe)(Al, Cr, Fe)_2O_4$. The chromic oxide portion varies between 15 and 65% mainly due to substitution of Cr with Fe or Al. The recoverable chromium averages 46% of the chromium mineral. 23 chromium minerals are Cr(VI)-bearing (Motzer and Todd Engineers, 2005). Chromite ore deposits occur in ultramafic rocks or closely-related anorthositic rocks either as stratified layered intrusions or as podiform deposits. In South Africa exploited chromium ore is found in the Bushveld Igneous Complex discussed in a later section of this report.

Under conditions of normal pressure and temperature in groundwater Cr(III) is insoluble and rarely occurs above concentrations that constitute contamination. Cr(III) is stable over wide pH and Eh ranges. It occurs as Cr_2O_3 between a pH range of 5 to 13.5 and an Eh range of +0.8 to -0.75 V. Cr(III) is soluble at a pH<5 and pH>13.5. In the Cr-H_2O-O_2 system in groundwater the governing reactions are (Motzer and Todd Engineers, 2005):

$$Cr^{3+} + H_2O \rightarrow CrOH^{2+} + H^+$$
$$CrOH^{2+} + H_2O \rightarrow Cr(OH)_2^+ + H^+$$
$$Cr(OH)_2 + H_2O \rightarrow Cr(OH)_3 + H^+$$
$$Cr(OH)_3 + H_2O \rightarrow Cr(OH)_4^- + H^+$$

Under conditions of normal pressure and temperature in the Cr-H_2O-O_2 system Cr(VI) is stable over narrower pH and Eh ranges. Cr(VI) species are limited to oxidising (Eh>0) and alkaline conditions as chromate or dichromate (pH>6). The governing reaction occurs as (Motzer and Todd Engineers, 2005):

$$HCrO_4^- \rightarrow CrO_4^{2-} + H^+$$

The reaction rate for the reduction of Cr(VI) to Cr(III) is rapid with $t_{1/2}$ ranging from instantaneous to 53 days under anoxic or reducing conditions. Under oxic conditions $t_{1/2}$ ranges from 15 min to 22 days. The oxidation of Cr(III) to Cr(VI) is much slower with $t_{1/2}$ ranging from 0.6 to 37.2 yr. Cr(VI) reduction by Fe(II) involves a three-step process as (Motzer and Todd Engineers, 2005):

$$Fe^{2+} + Cr^{6+} \rightarrow Fe^{3+} + Cr^{5+}$$
$$Fe^{2+} + Cr^{5+} \rightarrow Fe^{3+} + Cr^{4+}$$
$$Fe^{2+} + Cr^{4+} \rightarrow Fe^{3+} + Cr^{3+}$$

In solution sulphate anions can substitute for chromate and dichromate anions. Cr(VI) and S(VI) anions have similar ionic radii, 0.0325 – 0.052 and 0.029 – 0.034, respectively (Motzer and Todd Engineers, 2005).

Table 1: The various oxidation states of chromium with common compound examples for each oxidation state.

Oxidation state	Common compound	Formula
-2	Sodium chromium (-II) carbonyl	$Na_2[Cr(CO)_5]$
-1	Sodium chromium (-I) carbonyl	$Na_2[Cr_2(CO)_{10}]$
0	Chromium (0) (metal)	Cr
+1	Chromium oxide	CrO
+2	Chromium difluoride	CrF_2
+3	Chromium hydroxide	$Cr(OH)_3$
+4	Chromium dioxide	CrO_2
+5	Chromium pentafluoride	CrF_5
+6	Chromate anion	Cr_2O7^-
	Dichromate anion	Cr_2O7^{2-}

2.2 Fate and Transport of Cr(VI) in the Environment

Stanin and Pirnie (2005) stress the importance of contaminant fate and transport assessments in environmental restoration projects. The most important processes controlling the behaviour of Cr(VI) in the subsurface are: Eh, precipitation-dissolution; and sEhtion-desEhtion (Stanin and Pirnie, 2005). Naturally-occurring high concentrations of Cr in groundwater are generally rare but have been observed in certain instances (Guertin, 2005). The high Cr concentrations were observed in shallow porous aquifers located down gradient of mafic provinces. Cr also occurs naturally as the insoluble mineral, chromite ($FeCr_2O_4$) (Stanin and Pirnie, 2005).

It is inadequate to assess chromium in wastewater as $Cr_{(total)}$ as the geochemical properties and behaviour of Cr(III) and Cr(VI) are highly contrasting (Stanin and Pirnie, 2005). Cr speciation in groundwater is controlled by Eh and pH. Generally, Cr(VI) will dominate under oxidising conditions, whereas Cr(III) dominates under reducing conditions (Stanin and Pirnie, 2005). In dissolved phases Cr(III) can be present as Cr^{3+}, $Cr(OH)^{2+}$, $Cr(OH)_2^{+}$, and $Cr(OH)_4^{-}$. In the solid phase Cr(III) occurs as Cr_2O_3 and $Cr(OH)_3$ (Stanin and Pirnie, 2005). In the subsurface Cr(III) forms a small percentage of total Cr as Cr(III) solid species have low solubility. In contrast Cr(VI) cannot occur in aqueous systems as a free cation and is present as chromate -2 anions. Chromate (CrO_4^{-}) and dichromate ($Cr_2O_7^{2-}$) are the most common aqueous Cr(VI) complexes at pH ranges between 6 and 8. Dichromate becomes more dominant as Cr(VI) concentrations increase due variable degrees of solubility and sorption tendencies (Stanin and Pirnie, 2005). In the solid phase Cr(VI) is found in chromate salts formed with divalent cations (e.g. Ba^{2+}, Sr^{2+}, Pb^{2+}, Zn^{2+} and Cu^{2+}) with a variable degree of solubility (Stanin and Pirnie, 2005).

The redox transformations between Cr(III) and Cr(VI) are controlled by redox conditions and require another redox pair to facilitate the transfer of electrons. In natural aquatic environments the significant redox pairs or agents are (Stanin and Pirnie, 2005):

- H_2O/O_2
- Mn(II)/Mn(IV)
- NO_2/NO_3
- Fe(II)/Fe(III)
- S^{2-}/SO_4^{2-}
- CH_4/CO_2

The oxidation of Cr(III) to Cr(VI) in the subsurface is limited by insufficient concentrations of oxidising agents. Conversely reducing agents for the transformation of Cr(VI) to Cr(III) are abundant

in sufficient concentrations (Stanin and Pirnie, 2005). In groundwater Cr(VI) can be transported for great distances. It can be reduced and precipitated as Cr(III) by organic matter, Fe(II) or dissolved sulphides at low Eh and pH (Stanin and Pirnie, 2005).

In the subsurface –sorption/desorption may serve to retard contaminant migration or increase contaminant concentrations. Chromate anions can be sorbed by positively charged surfaces such as Mn, Al and Fe oxides, clay minerals, colloids and natural solids coating aquifer materials. Amorphous Fe is the most abundant chromate adsorbate in the groundwater regime. Chromate sorption increases with decreasing pH, i.e. lower pH results in higher Partition Coefficient (Kd) values. Kd, the partition coefficient, is a measure of the ratio of solubility between immiscible phases of a certain compounds, applied to fate and transport modelling (Stanin and Pirnie, 2005). Sorption of chromate is low to moderate at pH ranges common to the groundwater environment (Stanin and Pirnie, 2005). Importantly it has been observed that the sorption of Cr(VI) is not totally reversible, reducing the potential of monitored concentration to increase following periods of decline(Stanin and Pirnie, 2005).

Biota play an important role in the removal of Cr(VI) as they accumulate chromium and reduce Cr(VI) to Cr(III). However, high levels of Cr(VI) are also toxic to plants, bacteria, aquatic animals and terrestrial animals. In situ microbial remediation of chromate contaminated aquifers is possible under both oxic and anoxic conditions. The method aims to retard plume migration through the reduction of Cr(VI) to Cr(III) and precipitating $Cr(OH)_3$.

2.3 Numerical Modelling

Understanding of flow dynamics under non-steady state conditions in the plume capture zone is essential in assessing the efficiency of a PAT system. Besides, the influence of abstraction on contaminant transport and attenuation is important for fate and transport assessments. Groundwater modelling provides an analytical tool for investigating the influence of pumping time for multi-dimensional contaminant transport (Mustafa et al., 2015). The purpose of the groundwater model is to understand how pumping rates and time, control flow paths.

Groundwater models are tools used to make predictions about possible future impacts on groundwater resources associated with proposed activities or existing problem. Modelling approaches can either be analytical, stochastic or numerical. Analytical models are mathematically solvable; stochastic models are statistically solvable; and numerical models are solvable through computational methods. An intrinsic problem associated with groundwater models is inaccuracies as models are based on simplifying assumptions. Thus it is important to calibrate models with measured field data representative of the natural conditions. A high degree of certainty can be achieved through deterministic modelling as opposed to probabilistic (stochastic) modelling. A stochastic model is based on statistical values of the output variables, e.g. solute distribution, hydraulic conductivity or

porosity. Conversely, for a deterministic model the partial differential equation is solved numerically or analytically for a known set of input variables, aquifer parameters and boundary conditions. The output variables therefore have specific values at any given place in the aquifer.

Groundwater modelling is by far the only effective way to test groundwater management strategies. Models can be conceptualised in and calibrated with steady state or transient (non-steady state) conditions. To design a model the following steps are commonly followed: (1) Establish the purpose of the model; (2) Develop conceptual model of the system; (3) Select governing equations and computer code; (4) Design model; (5) Calibrate model. Hiscock (2005) describes calibration as the process of modifying the input parameters to a model until the output from the model matches an observed set of data. The point is to show that the model can reproduce field-measured heads, flow or solute concentrations. This results in a parameter data set that best represents the field-measured conditions.

Numerical models have been applied in hydrogeological and environmental applications since the 1960s. There are two types of mathematical solutions in numerical modelling, i.e. the finite difference and finite element methods. The Finite Difference Modular Flow Model (MODFLOW) domain uses the finite difference approach. 3D finite difference models entail vertical layering of the model. MODFLOW is a computer programme that numerically solves 3D groundwater flow equations for a porous medium. The model area is overlain by a rectangular grid and the partial differential equation is replaced by a set of finite difference equations in terms of piezometric heads at the nodes of the grid model. The general 3D governing equation is given as:

$$\frac{\partial}{\partial x}\left(Kxx\frac{\partial h}{\partial x}\right)+\frac{\partial}{\partial y}\left(Kyy\frac{\partial h}{\partial y}\right)+\frac{\partial}{\partial z}\left(Kzz\frac{\partial h}{\partial z}\right)-W=Ss\frac{\partial h}{\partial t}-R$$

Where: K_{xx}, K_{yy}, K_{zz} = Values of hydraulic conductivity along the x, y and z axes

h = Total head

W = Sources and sinks

S_s = Specific storage

t = Time

R = Recharge

In 2D for a confined aquifer the LaPlace equation is given as:

$$\frac{\partial}{\partial x}\left(Tx\frac{\partial h}{\partial x}\right)+\frac{\partial}{\partial y}\left(Ty\frac{\partial h}{\partial y}\right)=S\frac{\partial h}{\partial t}-R$$

In 2D for an unconfined aquifer the LaPlace equation is given as:

$$\frac{\partial}{\partial x}\left(hKx\frac{\partial h}{\partial x}\right)+\frac{\partial}{\partial y}\left(hKy\frac{\partial h}{\partial y}\right)=S\frac{\partial h}{\partial t}-R$$

Where, S (storage coefficient) is either storativity or specific yield, given by $S = S_s*b$. Where, b is aquifer thickness. T (transmissivity) is given by the equation. $T = K*b$.

Transient conditions will be modelled due to pumping for abstraction. Under transient conditions, heads and flows change over time as a result of stresses such as pumping of the aquifer.

2.4 Case Studies

Successful remediation of chromate contaminated groundwater has been demonstrated by numerous studies. The choice of remedial technique for a specific site can only be made following intensive site investigation and continuous monitoring (Hiscock, 2005). Remedial action is taken in order to manage environmental risk. Groundwater remediation ultimately aims at a total restoration of the contaminated aquifer to background water quality. Hauley, et al. (2005) classified possible treatment technologies into three broad classes based on the principal mechanism to reduce toxicity, as listed below:

- Reduction of toxicity
- Destruction and removal of contaminant
- Containment

Guertin (2005) concluded that the destruction and removal of Cr is not practical as elemental Cr requires great energy and further treatment would be required before disposal at a new site. The reduction of Cr(VI) toxicity may occur through natural attenuation or manipulation of environmental conditions (e.g. bioaugmentation). Containment essentially aims to prevent contamination from spreading to a large area. Various methods have been rendered successful in the remediation of chromate contaminated groundwater. Namely: Chemical precipitation; adsorption or biosorption; reverse osmosis; ion exchange, electrodialysis and photo-catalysis. Hashim et al. (2011) summarises remediation technologies applicable to heavy metals mobilising together as a result of elevated acidity in aqueous systems.

Chemical precipitation is regarded as the most practical, efficient and cost-effective method. Chemical precipitation entails containment by reduction of toxicity of Cr. Soluble Cr(VI) is converted to insoluble Cr(III) by the addition of ferrous sulphate (Stanin and Pirnie, 2005). Cr(VI) is reduced to Cr(III) while Fe(II) is oxidised to Fe(III) and the products are precipitated as hydroxides. Chemical precipitation may be applied by the addition of chemicals in situ in the aquifer or ex situ through PAT technologies (Stanin and Pirnie, 2005). PAT systems conventionally entail abstraction of contaminated groundwater, which is then chemically treated on the surface (Hiscock, 2005). This method has been applied in numerous cases across the world to address Cr(VI) groundwater contamination. Ex-situ chemical treatment of Cr(VI) is well established and has been proven to be highly successful, thus full-scale implementation is possible without pilot plant testing. (Stanin and Pirnie, 2005).

Stanin and Pirnie (2005) summarises some major Cr(VI) contamination case studies in North America. The Cr(VI) sources have a wide range from industrial waste landfills to mining and milling operations. These cases helped develop our current understanding of Cr(VI) geochemistry and Cr(VI)

toxicity. Wanner et al. (2012), Kitchen et al. (2012),and Trois et al. (2007) demonstrate that addition of Fe(II) to treat Cr(VI) contaminated groundwater is effective.

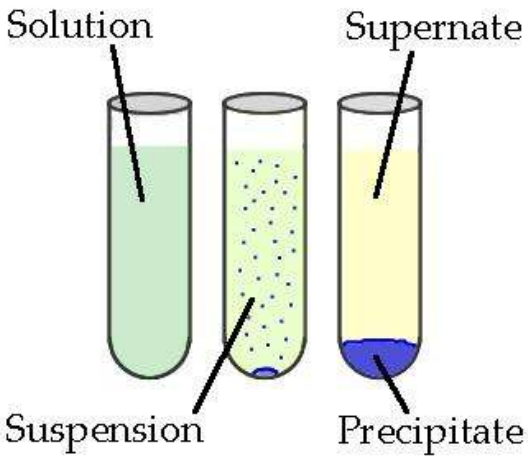


Figure 4: Illustration of precipitation of a solute out of solution (Schaffer and Herman, 2015).

3. STUDY METHODOLOGY

All the data used in this study includes new data collected specifically to monitor the PAT system and historical groundwater monitoring data prior to the implementation of the PAT system. The study uses monitoring data to assess the response of the groundwater environment to the PAT system (Wanner et al., 2011). The impacts of the continuous pumping of the surrounding aquifer system during remediation will be assessed through quarterly water level measurement (Watts et al., 2015). The effectiveness of the treatment technology was evaluated against changes in hydrochemistry (Watts et al., 2015).

3.1 Sample Collection

Groundwater and surface water monitoring points and their descriptions are listed in Table 3. All samples were collected by purging using a low-flow rate pump or by grab sampling using a polyethylene double valve bailer, depending on borehole use and depth. The borehole is purged to remove a one meter column of water. Prior to sampling all sampling equipment were cleaned with appropriate detergent and rinsed with distilled water. A new bailer is used for every groundwater or surface water sampling point. The equipment used during sampling is listed below:

- Temperature-Level-Conductivity (TLC) meter to measure in situ water temperature; water depth and borehole depth; and electrical conductivity.
- Multi parameter metre to measure pH and DO.
- Eh meter to measure redox potential.

All field data are recorded in pre-prepared forms and captured into an electronic database. Groundwater and surface water samples were submitted to the analytical laboratories using PVC containers. For non-metal sampling a PVC sampling bottle was used. For chromium and other metals sampling PVC sample liners were used with nitric acid. For stable isotope analysis all samples were collected in 10 mℓ glass bottles and tritium analysis samples were collected in 1 ℓ polyethylene bottles. Sealed and labelled samples are placed into a cooler box with frozen gel packs until delivered to a laboratory.

3.2 Laboratory Analyses

The analytical methods applied by the assigned laboratories are briefly described below. The collected samples were analysed for selected major ions, elements, metals and the environmental isotopes (^{2}H, ^{3}H and ^{18}O).

3.2.1 Inorganic Chemistry

The method used to analyse for all cations and free elements (including metals) was the inductively coupled plasma optical spectrometry (ICP-OES scan). The ICP-OES scan is essentially an atomic emission technique. Manahan (2000) describes the technique in the following words: "The analyte atoms are excited in plasma emission consisting of incandescent plasma (ionised gas) of argon (Ar) heated inductively by radiofrequency energy at 4 – 50 Mhz and 2 – 5 kW. The energy is transferred to a stream of Ar through an induction coil, producing temperatures up to 10 000 K. The sample atoms are subjected to temperatures around 7 000 K, twice that of conventional flames." The technique allows for high degrees of accuracy and precision as the emission of light increases exponentially with increasing temperature. The technique is a modern combination of plasma atomisation with mass spectrometric measurement and has been proven to be an efficient multi-element analytical technique.

The method used to analyse for all anions was spectrophotometry. Manahan (2000) describes absorption spectrophotometry as a useful method for the determination of water contaminants. Absorption spectrophotometry of light-absorbing species in solution consists of measuring the percent transmittance (%T) of monochromatic light passing through a blank solution as compared to a solution containing everything but the constituent being measured. The absorbance (A) is given by the following equation:

$$A = \log (100/\%T)$$

The relationship between A and the concentration (C) of the absorbing substance is given by Beer's law:

$$A = abC$$

Where a, is the absorptivity, a wavelength-dependent parameter which is a natural characteristic of the specific absorbing substance; and b is the path length of the light through the absorbing solution.

3.2.2 Cr(VI) Analysis

The method used to analyse for Cr(VI) is the ion chromatographic method equipped with a pump capable of precisely delivering a flow of 1 to 5 mℓ/min. The water sample was preserved in nitric acid and filtered through a 0.45 µm filter. The solubility of Cr(III) was reduced, preserving the Cr(VI) oxidation state. The filtered sample was brought to room temperature and brought into the chromatograph's running aqueous stream of ammonium sulphate and ammonium hydroxide. Cr(III) and Cr(VI) were separated by a column and Cr(VI) was allowed to react with an azide dye to produce

a chromogen measured at 530 nm. Cr(VI) was determined on the basis of time retention. The detection limit for groundwater, drinking water and waste water effluent was 0.3 µg/ℓ.

3.2.3 Environmental Isotope Analysis

All monitoring boreholes and treatment ponds were analysed for the stable environmental isotopes, oxygen-18 (^{18}O) and deuterium (^{2}H), and radiogenic isotope, tritium (^{3}H). To analyse for tritium was conducted in the hydrogeology laboratory of the School of Geosciences, University of the Witwatersrand. The instrument used was LGR Liquid Water Isotope Analyser (model 45-EP) which is an automated a laser machine. Stable isotope compositions have been reported as delta-values (δ-values). The values are reported in units of parts per thousand or parts per mil denoted as ‰. The measured $\delta^{18}O$ and ^{2}H isotope ratios were determined relative to the Vienna Standard Mean Ocean Water (VSMOW) standard and are calculated using the general equation:

$$\delta \text{ (in ‰)} = (R_x / R_s - 1)/1000$$

Where R denotes the ratio of the heavy to light isotope and R_x and R_s are the ratios in the sample (x) and standard (s). The ratios between the heavy and light stable isotopes were measured for $^{18}O/^{16}O$ and $^{2}H/^{1}H$ and the respective abundances were calculated using the equations:

$$\delta^{18}O = \left(\frac{\left(\frac{^{18}O}{^{16}O}\right)_{sample}}{\left(\frac{^{18}O}{^{16}O}\right)_{VSMOW}} - 1 \right) 1000 ,$$

$$\delta^{2}H = \left(\frac{\left(\frac{^{2}H}{^{1}H}\right)_{sample}}{\left(\frac{^{2}H}{^{1}H}\right)_{VSMOW}} - 1 \right) 1000 .$$

The results were immediately plotted on a δD vs. $\delta^{18}O$ diagram to note data outliers, especially ones that plot significantly above the global meteoric water line (GMWL) defined by the Global meteoric water line "$\delta D = 8\ \delta^{18}O + 10‰$" (Craig, 1961).

3.3 Quality Control and Quality Assurance

Best practice quality control measures were followed according to internationally accepted protocols. The potential for cross contamination of monitoring boreholes was minimised through using

a new polyethylene bailer for every monitoring point. The TLC meter was rinsed with detergent between sampling points. All samples were stored at 4°C and delivered to a laboratory within 48 hours of sampling for temporary storage prior to analysis. Field measurements were recorded at every sampling point to ensure that the sample collected were representative of the in situ conditions. All samples analysed for major ions and metals were filtered before analysis.

3.4 Fate and transport modelling

The objective for the geochemical modelling is to model the fate and transport of Cr(VI) in the aquifer and treatment ponds during treatment . Geochemical modelling serves as input for further contaminant transport numerical flow modelling (Stanin and Pirnie, 2005).

The reactions between gases, solutes and solids were modelled using the Geochemist's Workbench geochemical modelling software package. This model solves the hydrochemical and mineral reactions with an equilibrium thermodynamic model, taking mineral dissolution/precipitation kinetics into account and aids in the evaluation of the concentrations of stable and metastable species and minerals that may form in a chemical system in various simulated scenarios (Wanner et al., 2012). The Geochemist's Workbench programme allows for the following functions:

- Plotting and manipulating geochemistry data;
- Balancing of chemical reactions and the calculation of equilibrium constants, temperatures and equations;
- Generating stability diagrams on activity, Eh, pH and fugacity axes.

3.5 Numerical modelling

Numerical groundwater modelling is considered to be the most reliable method of anticipating and quantifying the likely impacts on the groundwater regime. The impact of abstraction for treatment was simulated using the ModelMuse interface for MODFLOW-2005 (Davis and Putman, 2013). MODFLOW is a two- and three-dimensional, cell-centred, finite difference, saturated flow model developed by the United States Geological Survey (USGS). The ModelMuse interface for MODFLOW-2005 can perform both steady state and transient analyses and has a wide variety of boundary conditions and input options (Davis and Putman, 2013). The numerical model was used in conjunction with major ion chemistry, stable isotope data, and was calibrated with transient water level monitoring data and a lumped-parameter conceptual site model.

3.6 Environmental Isotopes and Groundwater Tracers

The application of environmental isotopes in understanding hydrological processes in small catchments has been demonstrated to be successful in a wide variety of studies. In the context of fate and transport assessments they are used because they allow us to understand catchment-scale processes from small-scale sampling. Environmental isotopes (^{2}H, ^{3}H and ^{18}O) are useful to trace the mixing of different types of groundwater to determine the origin of dissolved constituents (Geyh 2000; Wanner et al., 2011). ^{2}H, ^{3}H and ^{18}O are integral parts of the hydrological cycle. Thus they are useful in tracing groundwater movement, including its dissolved constituents when used in conjunction with major ion chemistry.

Environmental isotopes were used as tracers of waters and solutes in the groundwater regime as well as in the treatment ponds with the following objectives (Geyh, 2000):

- To determine whether mixing through vertical inflows into monitoring boreholes is possible as waters recharged at different times have different isotopic signatures.
- To determine the role of atmospheric deposition in controlling water chemistry.
- To determine the evolution of groundwater in the hydrologic cycle.

3.7 SWOT analysis

The success of the pump and treat system is controlled by various factors and environmental conditions. These include the reactivity of Cr(VI) which is decreased with declining Cr(VI) concentration, or the fact the settling ponds are open systems (open to the atmosphere). Further the chemistry of the groundwater in the contaminated aquifer may be affected by many natural processes or physico-chemical parameters along the new flow paths (Theis et al., 2003).

A holistic analysis of the operation of the system is required in order to achieve the most desirable result. The SWOT analysis will evaluate the strengths, weaknesses, opportunities and threats associated with the entire remedial action (Theis et al., 2003).

4. SITE DESCRIPTION

A description of the regional area information is described under the headings below. The site is located in the Bushveld region of the North West province, South Africa.

4.1 Site Location

The site is located in the North West Province of South Africa in a region dominated by industrial (including mining of chromite and PGEs) and agricultural land use. An informal settlement sprung up over the past few years downstream of the contamination source due to a demand for employment at the ferrochrome producer. The majority of the land within a 2 km radius is classified as mixed land use, ranging from agricultural, residential, industrial and vegetated (River Health Programme, 2005). Monitoring studies revealed that all farmers with a 2 km radius made use of groundwater and alternatively, water channelled through a canal sourced from the Crocodile River. Industrial land use is limited to the east and north of the contamination source. The site locality in South Africa and study area layout are shown in Figure 5 and a land use map is shown in Figure 6

Farmers downstream of the contamination source abstract contaminated groundwater for agricultural and domestic purposes. Pivot irrigation schemes are used for commercial farming.

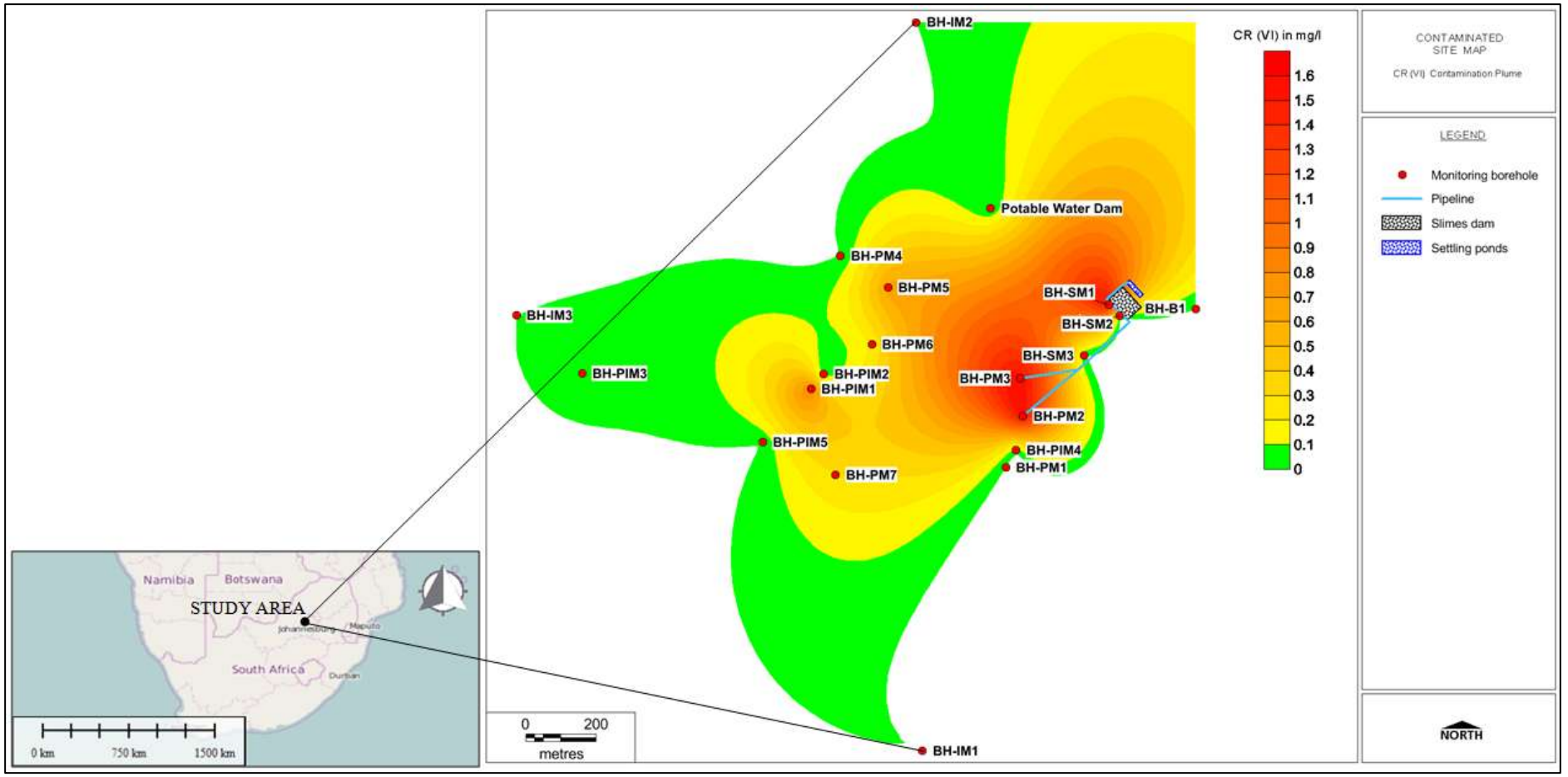


Figure 5: Location of the study area and layout of the study area showing the chromate contamination plume prior to the commencement of treatment.

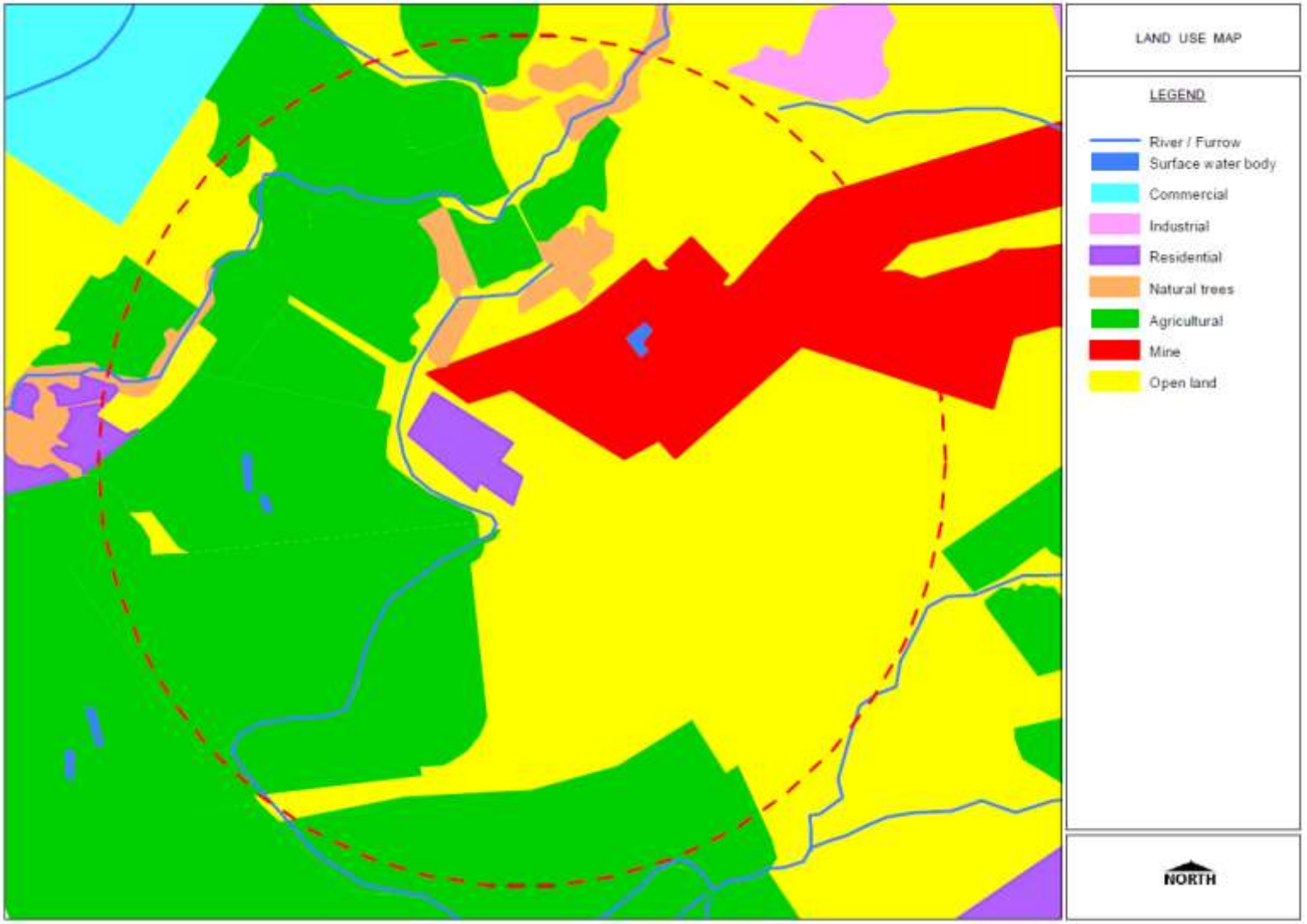


Figure 6: Land use map around the mine and study area, showing a 2 km radius around the source area.

4.2 Climate and Drainage

The site is located in the summer rainfall region of Southern Africa. The climate of the area is classified as arid to semi-arid. Precipitation is understood to be uniform across the area. Precipitation and temperature records for over 40 years show that mean annual precipitation is 642 mm and mean annual potential evaporation is 2200 mm (DWA, 2015). The highest precipitation occurs between the months of September and February (wet season), with the lowest precipitation occurring between March and August (dry season). The mean monthly precipitation is listed in Table 2 and graphically displayed in Figure 8.

The site is located in the western Crocodile River Basin, within the Upper Crocodile River Catchment. The Crocodile River flows north-west and its closest bank is located approximately 4 km south-west of the contamination source. The *Kareespruit* a tributary of the Crocodile River, is located 2 km north-west of the contamination source. Local surface drainage is north-westerly towards the Crocodile River, i.e. topographical highs are located to the north-east of the contamination source. The area is characterised by generally flat relief with slopes in the order of 1:50 (0.02). The site is located approximately 6 km north to north west of the Magaliesberg Mountain Range. The Magaliesberg forms a regional groundwater divide and also a watershed for the Crocodile River Catchment Area. The Upper Crocodile Sub-catchment has within the densely populated West, East and Central Rand areas of Greater Johannesburg in Gauteng. Major tributaries of the Crocodile River within the Upper Crocodile Sub-catchment include the Sterkstroom, Magalies, Bloubankspruit, Jukskei, Steekspoort, *Kareespruit*, Rose and Hennops rivers. This sub-catchment area is characterised by high population density and the highest level of industrial development in South Africa. The environmental statuses of the tributaries are generally poor (River Health Programme, 2005). Dewatering of mines, agricultural return flows, industrial effluents, domestic wastes and sewage spills have all contributed to deteriorating water quality in the sub-catchment (Abiye et al., 2015).

The Crocodile River has a perennial flow in the area. Abiye et al. (2015) found that groundwater contributed to streamflow through baseflow in the Upper Crocodile Sub-catchment through the application of environmental tracers. In the study area a canal system from the Crocodile River supplies water for industrial and agricultural applications.

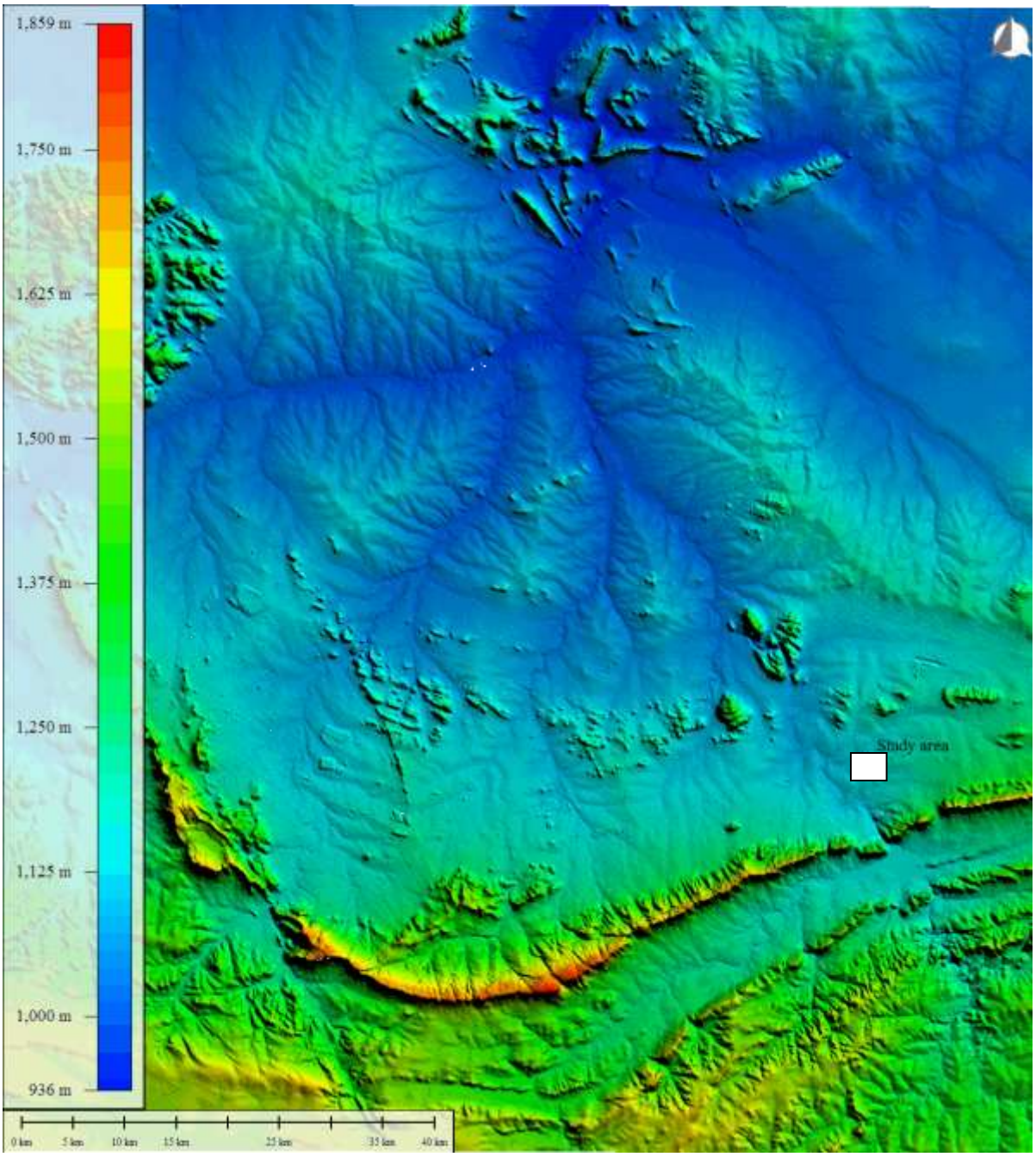


Figure 7: Digital elevation model (DEM) of the Upper Crocodile Sub-catchment showing the study area and natural drainage features.

Table 2: Mean monthly rainfall and evaporation data as recorded at the Kroondal Meteorological Station over a 70-year period between 2015 and 1945 (Source: DWA, 2015).

Month	Mean monthly precipitation (mm)	Mean monthly evaporation (mm)
January	119.8	185.8
February	100.8	157.7
March	71.3	150.8
April	47.6	113.3
May	15.7	101.1
June	10.1	79.7
July	3.1	92
August	5.7	121.3
September	18.9	159.3
October	55.1	181.72
November	91.1	178.1
December	105.7	188.7

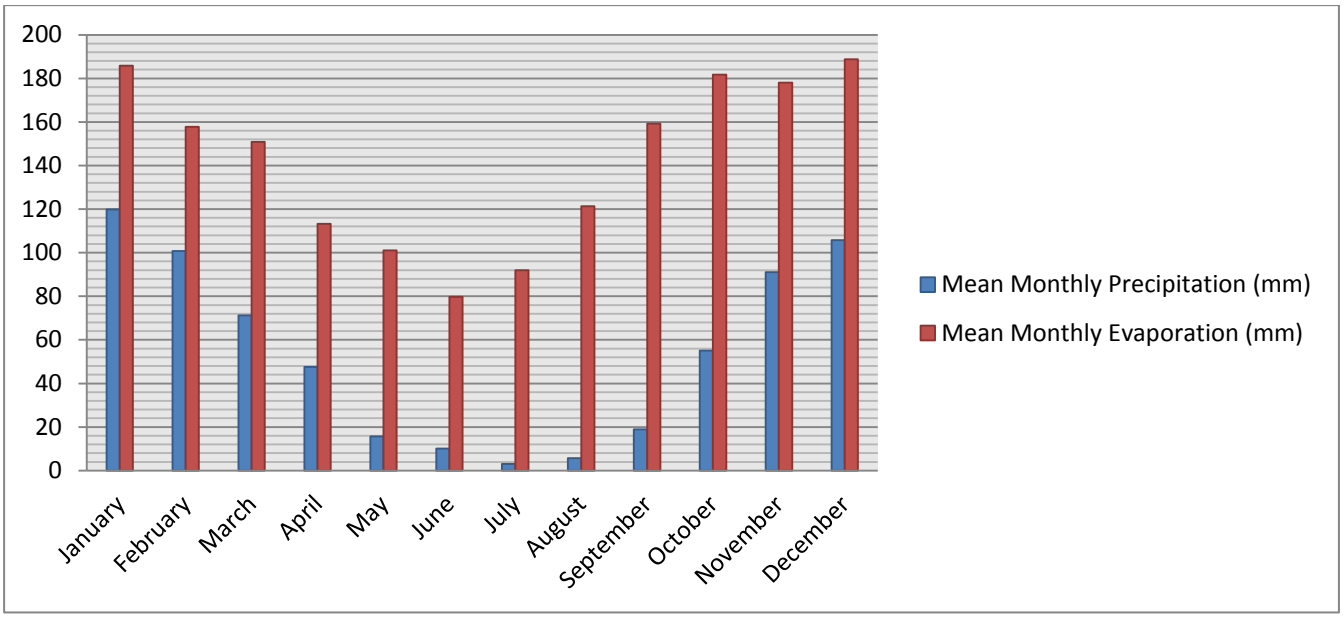


Figure 8: Mean monthly rainfall and evaporation data as recorded at the Kroondal Meteorological Station (Source: DWA, 2015).

4.3 Local Geology

The site is underlain by the Rustenburg Layered Suite (RLS) mafic rocks of the Bushveld Igneous Complex (BIC). The BIC is situated on the Kapvaal Craton of South Africa. The Palaeoprotorozoic (2.6 Ga) BIC is a layered mafic and felsic igneous province. The BIC is the largest igneous province in the world covering approximately 66 000 km^2 measured along the long axes (Du Plessis and Walvaren, 1990). The BIC is of economic important due to extensive mineral deposits of chrome, iron and platinum-group elements (PGEs). The BIC is divided into two main layers, the felsic Lebowa Granite Suite (LGS) and the mafic RLS. The RLS is a layered sequence of high-density mafic to ultramafic rocks while the LGS is a sequence of granitic rocks (Cole et al., 2014). The basal rocks in the study area are the metamorphic quartzites of the Magaliesberg Formation of the Pretoria Group of the Transvaal Supergroup (Cole et al., 2014).

The RLS is further divided into five zones, viz.: Upper, Main, Critical, Lower and Marginal zones (Zingg, 1996). Chromitite layers at the Cr(VI) contaminated site occur in UG2 layer. The accumulation of major chromitite is considered to have been caused by density stratification. Chromite is associated with ultramafic rocks owing to similar physical characteristics. At the study area the site was found to be underlain by pyroxenite [$Ca(Mg,Fe,Al)(AlSi_2O_6)$], anorthosite [$(Ca, Na)(Al,Si)(Si_2O_8)$], dolerite dykes, tuffs and chromite (Clarke et al., 2008).

BIC emplacement occurred in an intra-cratonic tectonic setting away from active margins suggesting rift-controlled intrusion attached to a mantle plume. The RLS dips between 8° and 20° towards the centre of the BIC due to thermal subsidence (Cole et al., 2014). Tilting towards the centre of the BIC was also imposed on the underlying Transvaal sediments (Cole et al., 2014). The layered RLS lithological units at the study area were found to dip 8° towards the centre of the BIC. The Magaliesberg Formation is characterised by large-scale open folds commonly with a fold wavelength in the order of several hundred meters. Dolerite intrusion, normal faulting and strike-slip movement in the BIC are thought to have occurred during different periods of emplacement as layered intrusions are thought to cool over long periods of time (Zingg, 1996). The RLS lithological units at the site are characterised by a high degree of fracturing. Figure 9 shows a site geology map of the study area. A NNE-NNW trending dyke and regional strike-slip and normal faulting are the major linear geological features.

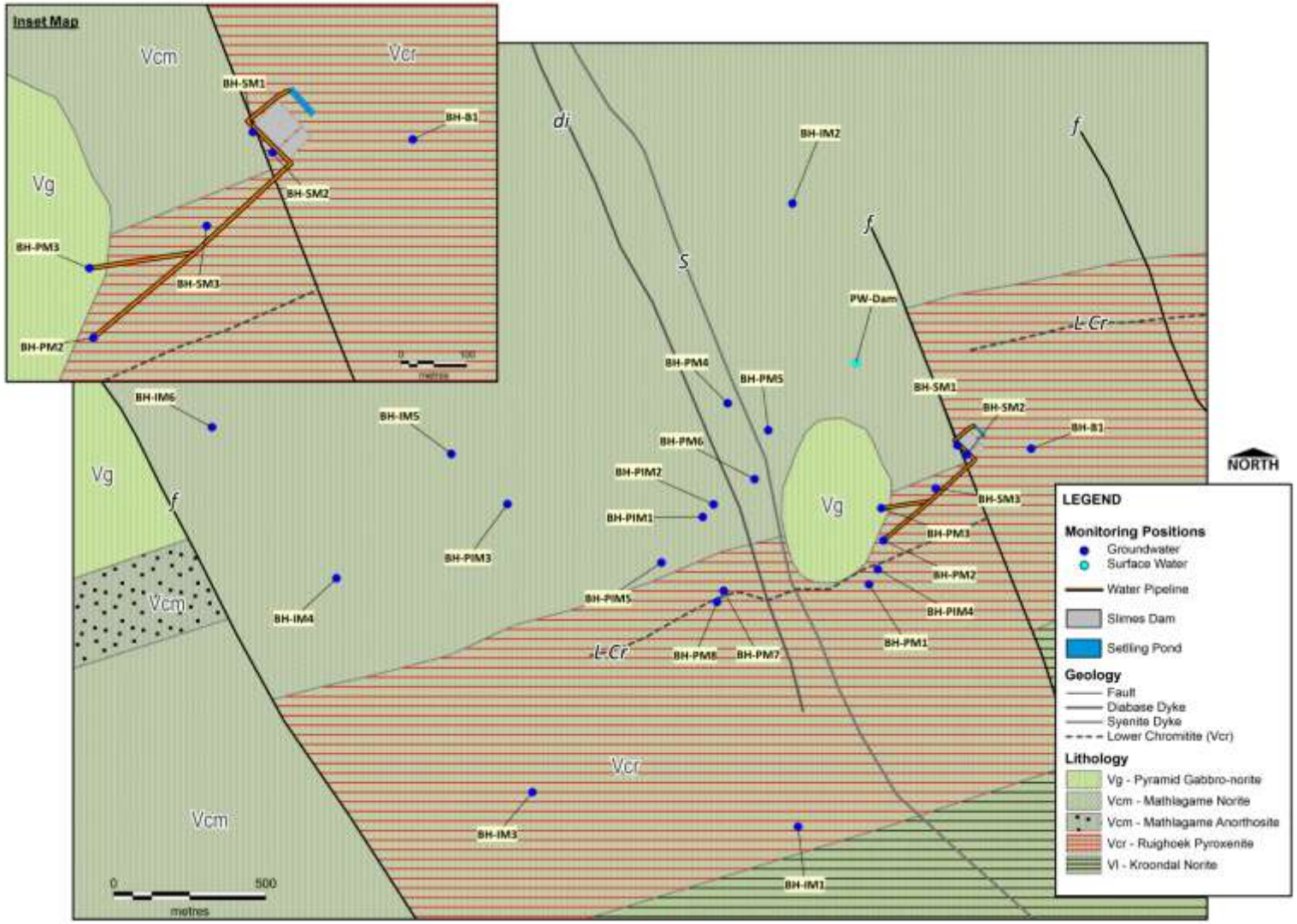


Figure 9: Site geology map.

4.4 Local Hydrogeology

In general, the hydrogeology of the BIC is characterised by a shallow weathered aquifer and a deeper semi-confined fractured bedrock aquifer. In the RLS due to opencast and underground mining operations the water strikes in both aquifers are dewatered at places. The depth of weathering goes up to 15 m b.g.l (Titus et al., 2009). An extensive weathered horizon as well as fracturing and lineaments are characteristic features of crystalline rock aquifers. The effect of erosion and weathering of the BIC improved the groundwater development potential of the shallow weathered aquifer. Crystalline rocks such as the mafic rocks of the RLS will have an unweathered intact matrix which accounts for bulk storage of groundwater in the saturated zone (Davis and Putman. 2013). In the deeper-lying secondary aquifer, groundwater flow occurs in a complex fracture network (Wanner et al., 2011). In the study area, the secondary linear features present are the regional strike-slip fault, a number of -normal faults and a major dolerite dyke.

Dolerite dykes in the BIC were intruded post-emplacement of the BIC. They are magmatic intrusions that are formed by the propagation of magma into open fissures whether vertically or horizontally (as sills) fracturing the native rock at the contact due to the baking effect. The dykes themselves are fractured increasing their secondary permeability. Dolerite dykes are known to extend over long distances but are of limited thickness (Du Plessis and Walvaren, 1990). The dolerite intrusion at the study area outcrops east of the pollution plume and is 10 m thick.

In terms of layering the sequence is an alternating sequence of rocks rich in orthopyroxene (i.e. pyroxenite) and rocks rich in plagioclase (i.e. anorthosite) (Zingg, 1996). The succession between pyroxenite and anorthosite is irregular, at the site anorthosite outcrops to the east of the contamination source and the Cr(VI) contamination plume is confined to the pyroxenite succession into which all the monitoring boreholes are drilled. Hydrogeologically, dolerite dykes represent linear geological features of high permeability which serve as conduits to groundwater flow in the aquifer. Strike-slip faults are considered barriers to groundwater flow, while normal faults may serve as barriers or conduits to flow. Figure 10 displays the influence of normal faults on hydraulic gradients and groundwater flow (Bense et al., 2013). Fault zones create zones of preferential groundwater flow in the zone of deformation. Groundwater movement in the study area is, however, influenced by groundwater abstraction through pumping. The stratigraphic column expected across the study in the context of BIC stratigraphy is shown in Figure 11.

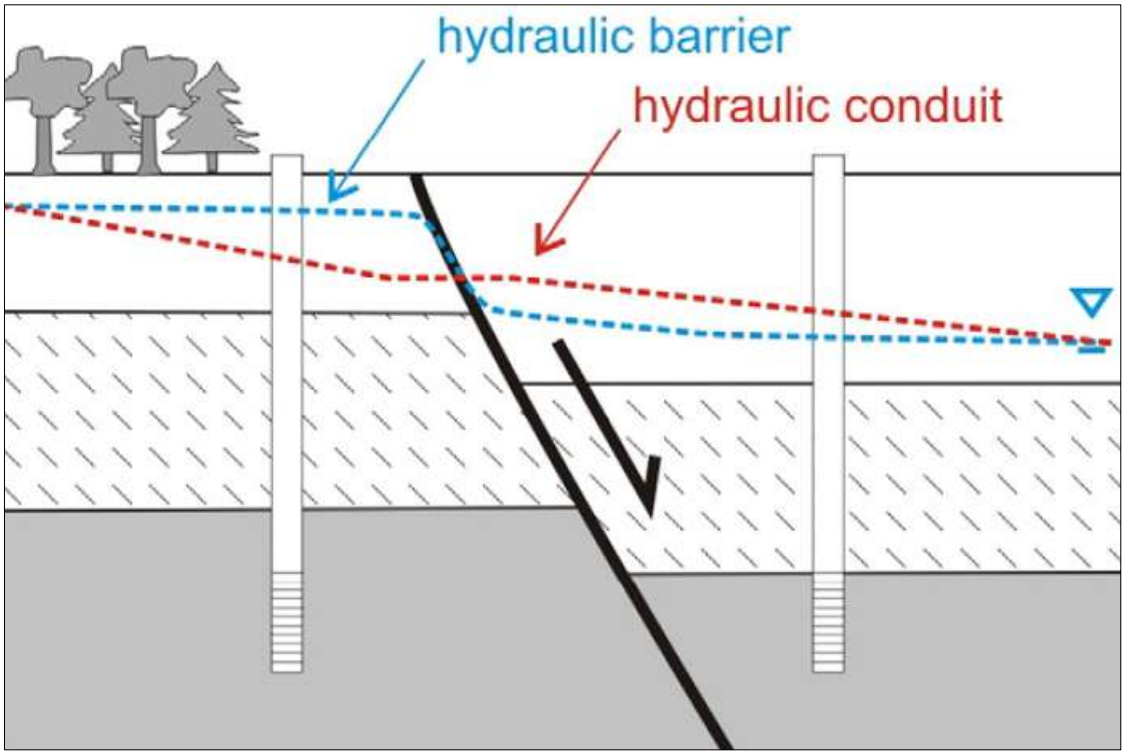


Figure 10: Fault zone potential influences on hydraulic head gradients and groundwater flow (Source: Bense et al., 2013).

Aquifer characterisation techniques include various methods which provide different scale of resolution. The methods include geophysical methods, geotechnical borehole logging and aquifer tests. The estimation of aquifer hydraulic properties through aquifer tests provides precise information on aquifer characteristics from a limited spatial extent. The aquifer tests performed as part of the initial testing programme prior to the implementation of the remedial system are described in a later section and the pumping data is presented graphically in Appendix II. In an aquifer test or pumping test, a borehole is pumped with an electric powered submersible pump at a constant discharge rate. This type of test is known as a constant discharge rate pumping tests as opposed to a step draw down test which is performed at variable pumping rates. Water abstraction through pumping lowers the water table creating a cone of depression, the drawdown is measured and the time that the cone of depression takes to stabilise is used to estimate aquifer parameters. The hydraulic properties or aquifer parameters of interest are hydraulic conductivity, transmissivity, specific storage and the sustainable yield. The properties of fractured aquifers depend on the fracture networks and the porosity of matrix blocks.

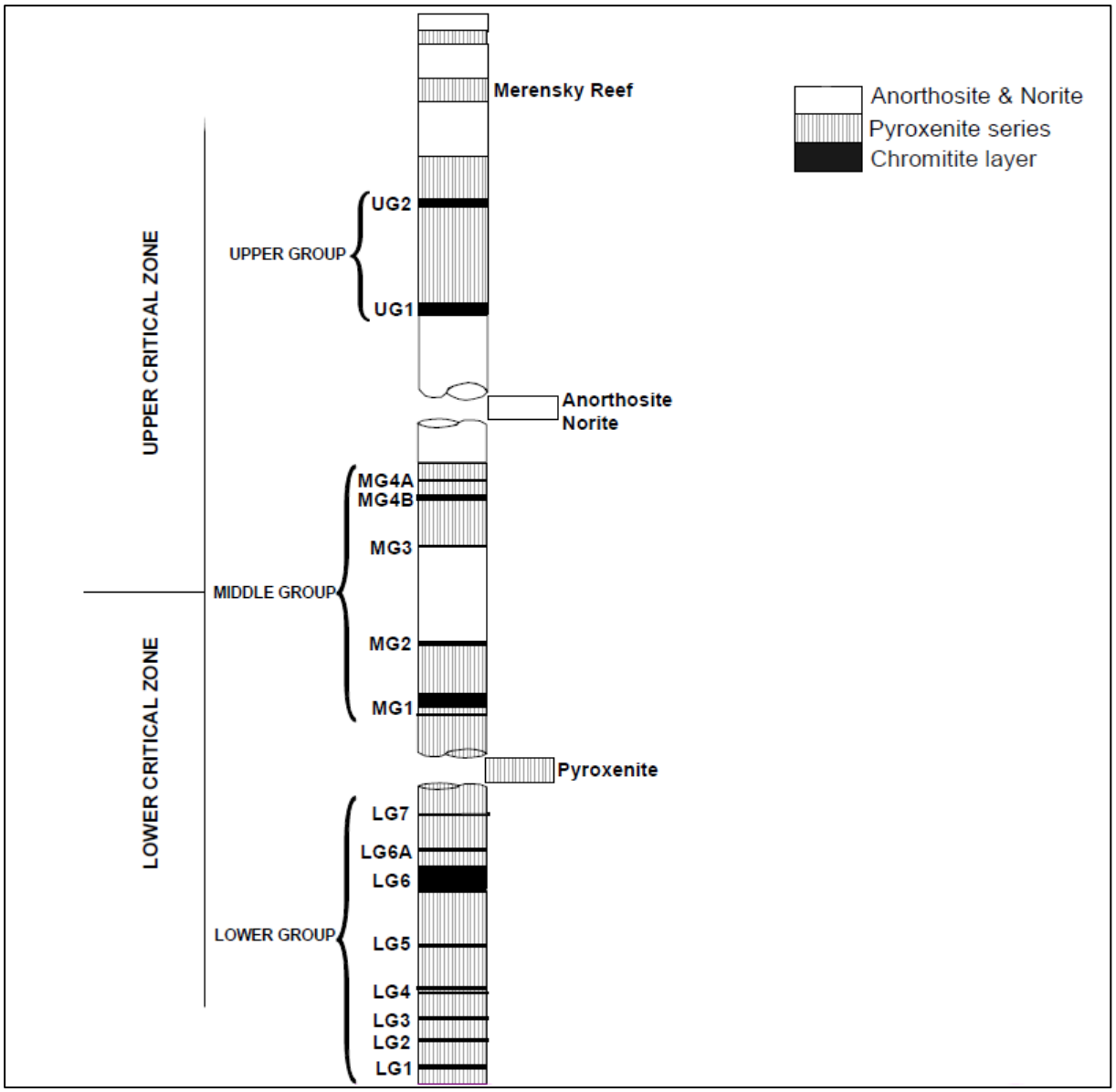


Figure 11: Stratigraphy of the chromitite bearing layers of the RLS (not to scale; Source Cawthorn, 1999).

5. HISTORICAL DATA REVIEW

Groundwater contamination by Cr(VI) was initially picked up in 1997, about a year since the baghouse slimes dam was commissioned. Since then measures were taken to prevent further groundwater contamination by chromate. The leaking baghouse slimes dam was decommissioned in the year 2000 and sealed with polyethylene thermoplastic to prevent leaching by rain water and Cr oxidation. All furnaces used for metallurgical processing of the chromite ore were converted to closed furnaces. There is no evidence suggesting that Cr(VI) dust has been generated since 2009.

Based on site-specific hydrogeological risk assessment and monitoring studies, a remedial action plan was developed. Site characterisation and risk management studies lead to the conclusion that remediation was necessary. The restoration of groundwater to drinking water levels is generally considered impractical and technically not feasible. Corrective action following groundwater resource contamination is based on a risk-based approach. Thus, remediation is required when the contamination poses a risk to the receiving environment and human receptors. The sections that follow summarise the risk management and remedial approach.

5.1 Classification of Contaminated Site

The site assessment and decision-making process was within the framework of the South African National Environmental Waste Act (Act 59 of 2008). The process followed in the decision-making process is schematically presented in Figure 12. Phases 1 and 2 have been completed; this research project is essentially the “control and monitoring” step following the implementation of the remedial design. The baghouse slimes dam was classified with a hazardous rating of 1 (HR1) as a “high risk” waste site. The waste disposal facility was classified as a high-hazard (H:H) facility, which is subject to stringent design criteria and monitoring. It had already been proven that contamination of the underlying aquifer had occurred and groundwater monitoring showed that the Cr(VI) plume had reached privately owned abstraction boreholes. Remediation was deemed necessary to protect critical receptors, i.e. groundwater users downstream of the contamination source. The remedial plans and system design were approved by the South African Department of Environmental Affairs.The hazardous rating (HR) is used to classify hazardous waste into the following categories:

- HR1 : Extremely hazardous waste
- HR2 : High risk hazardous waste
- HR3 : Moderate risk hazardous waste
- HR4 : Low risk hazardous waste

A hazardous rating of 2 is assigned to waste containing highly toxic substances which are not persistent and include some carcinogens. The fate of contaminants in the groundwater regime depends on their mobility, prevalent redox conditions and toxicity. DWAF (1998) classified Cr(VI) as a class 5 and class 6 substance based on its oxidation state and toxicity. Class 5 substances are oxidising agents and Cr(VI) is a very strong oxidising agent. Class 6 substances are toxic and infectious substances, Cr(VI) is highly toxic to living organisms as a mutagen and carcinogen. During remediation, oxidising agents must be eliminated to neutralise their oxidising potential. Chemical treatment is regarded as a technology capable of achieving remedial objectives by DWAF (1998) for chromate contaminated sites.

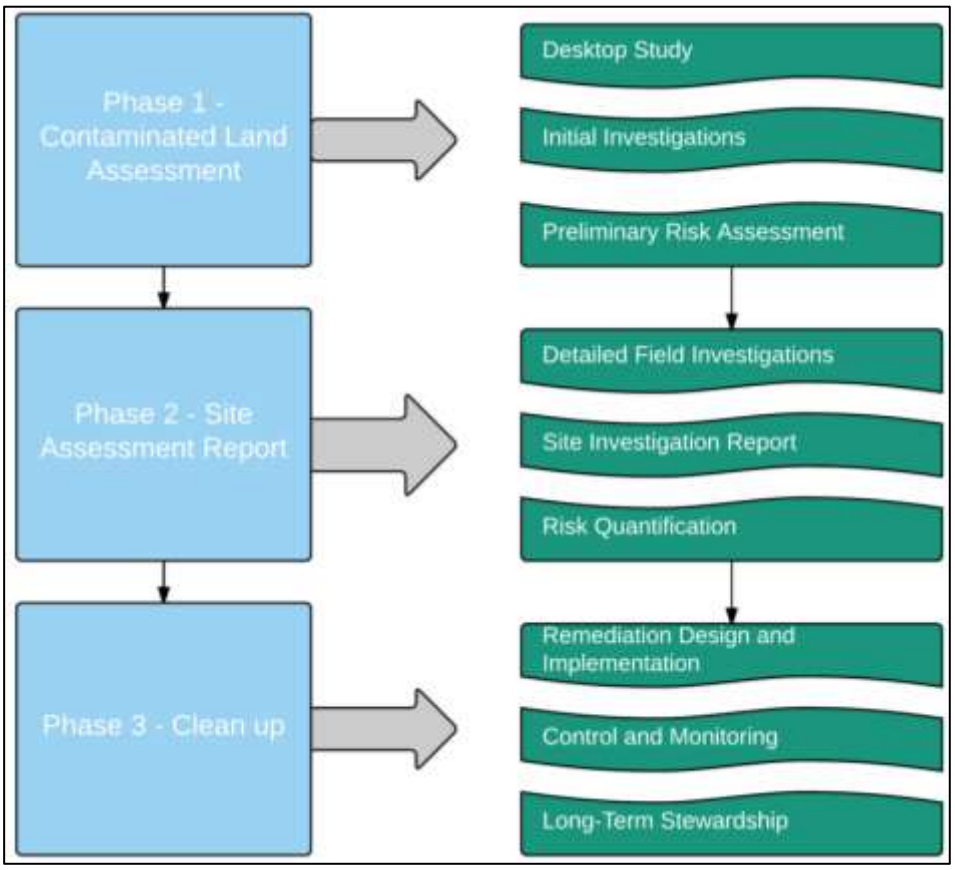


Figure 12: Site assessment as per the best practice guidelines as set by the South African environmental authoroties (DWAF, 1998).

5.2 Initial Testing Programme

Preliminary site investigations aimed to characterise the contaminant source and hydrogeological characteristics of the aquifer. Further, a cost-benefit analysis was also required prior to selecting the most practical and cost-effective remedial technique. The programme followed prior to the implementation of the remedial action plan is detailed below:

- Site maps were prepared to show local topography, drainage, geology, groundwater flow directions and contours of contaminant concentrations relative to the human consumption limits.
- Cr(VI) plume delineation was conducted through a hydrocensus study, development of a monitoring programme, high frequency groundwater and surface water monitoring, monitoring well development and modelling studies.
- Aquifer mapping and characterisation information was reviewed and incorporated into the decision making process.
- The source of contamination was contained and measures were taken to ensure that the potential for Cr(VI) generation all across the operation was eliminated.
- Ex-situ chemical treatment through PAT action was considered as the most practical and least expensive method for aquifer clean up. The system design pre-feasibility study included aquifer tests and engineering design of the system, which are discussed in a later section of this report.

5.2.1 Aquifer tests

Considering the shape, extent and spatial distribution of contaminant concentrations the following system design criteria were considered to optimise the capture zone of the pumping boreholes:

- The optimum number of abstraction boreholes
- Borehole positions
- Optimal and sustainable pumping rate
- Optimal treatment method of abstracted water
- Disposal of treated water

The boreholes that showed the highest concentrations of Cr(VI) and were subjected to the aquifer test are show in Appendix II. The aquifer tests were conducted under steady condition. Constant rate discharge and recovery tests were conducted on four boreholes. The constant discharge

tests were chosen to attain the highest possible accuracy in comparison to step drawdown tests (Singhal and Gupta, 2010). The duration of the pumping tests is always determined by the degree of accuracy required. The purpose of the pump tests was to quantify a sustainable abstraction rate during pumping for treatment. A low degree of accuracy was required and the aquifer tests were carried out until steady-state flow had been reached, i.e. the cone of depression had stabilised.

The water level measurements were taken frequently and with high accuracy at pre-determined intervals using an electronic dip meter. After the pump was switched off the residual drawdown was measured to within 95% of the static water level or until the recovery stabilised. Recovery test data was used as a control on calculations based on the constant rate discharge test.

The long term abstraction value for each borehole was estimated by applying the Flow Characteristic (FC) analytical tool to the drawdown data. A summary of the FC results is shown in Appendix II.

5.2.1.1 BH-PM2

By applying a constant pumping rate of 0.25 l/s a drawdown of 0. 27 m was achieved within 180 min of testing. Therefore, based on the drawdown, a pumping rate of 0.5 l/s was set as long-term abstraction rate.

5.2.1.2 BH-PM3

By applying a constant rate of 0.25 l/s pumping rate a drawdown of 0.14 m was achieved within 210 min of testing. Therefore, based on the drawdown, a pumping rate of 0.2 l/s was set as long-term abstraction rate.

5.2.1.3 BH-SM1

By applying a constant rate of 0.25 l/s pumping rate a drawdown of 0.10 m was achieved within 120 min of testing. Therefore, based on the drawdown, a pumping rate of 0.8 l/s was set as long-term abstraction rate.

5.2.1.4 BH-SM2

By applying a constant rate of 0.25 l/s pumping rate a drawdown of 12.09 m was achieved within 35 min of testing. Therefore based on the drawdown, this borehole was regarded unsuitable for long-term abstraction as it will run dry within minutes even at a very low pumping rate.

Based on the aquifer test results, three boreholes were equipped with low-flow pumps, with a flow rate of less than 0.5 l/s. As safety measure the pumps were to automatically switch of when the

water level reaches pump inlet to prevent pump burnout. Based on the calculated sustainable pumping rates, the following volumes of water will be abstracted:

- BH-PM2: (43.2 m^3/day), (302.4 m^3/week), (9072 m^3/month)
- BH-PM3: (17.3 m^3/day), (121 m^3/week), (3628.8 m^3/month)
- BH-SM1: (67.4 m^3/day), (471.7 m^3/week), (14152.3 m^3/month)
- Total volume abstracted: (127.9 m^3/day), (895.1 m^3/week), (26853.1 m^3/month)

5.3 System Design

Following an initial testing programme which included long-term monitoring, pumping tests and plume characterisation a PAT system was designed and implemented in February 2015. Based on aquifer tests, plume characterisation and monitoring data a full-scale plant was implemented instead of a pilot plant. The abstraction boreholes were selected to capture the highest concentrated parts of the plume. The PAT system infrastructure consisted of the following:

- Three abstraction boreholes equipped with low-flow rate pumps.
- Two settling ponds (pre-treatment and post-treatment).
- One dosing pump.
- Two tanks storing and transmitting aqueous $Fe(II)SO_4$ to the dosing pump.

A schematic representation of the treatment system is presented in below in Figure 13.

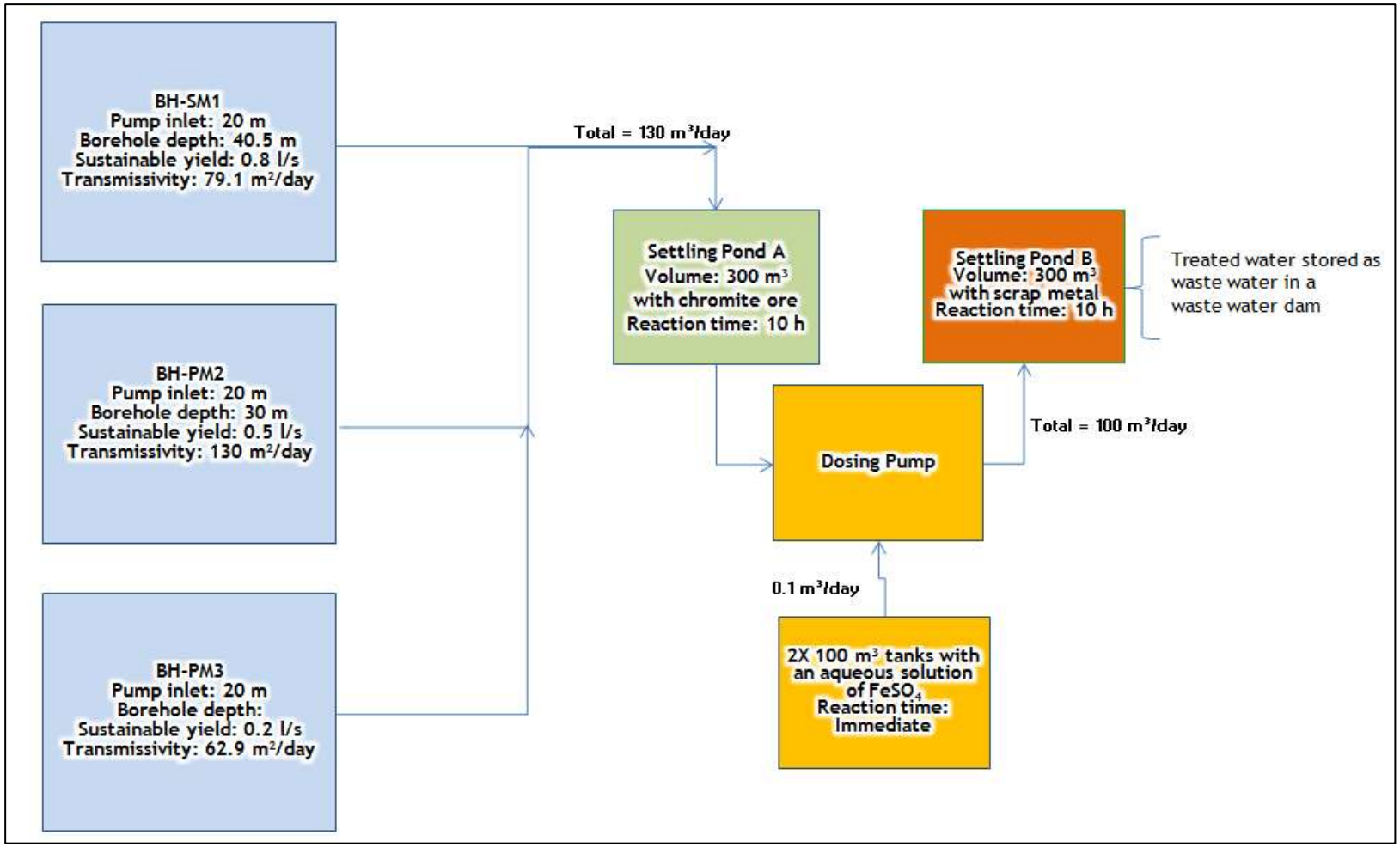


Figure 13: Treatment system design (Geo Pollution Technologies, 2013).

5.4 Objectives of the PAT Technology

Groundwater quality remediation is expected to occur over relatively long period of time. The PAT system was implemented as a medium-term strategy with the following objectives:

- To intercept the Cr(VI) contamination plume during migration to prevent it from impacting on groundwater users downstream of the mine.
- Reduce the Cr(VI) concentration of the abstracted water to below 0.05 mg/ℓ.
- Eventually reduce the Cr(VI) concentrations in the aquifer to below 0.05 mg/ℓ.

5.5 Expected Outcomes

The abstracted contaminated-groundwater is to be treated by reduction of Cr(VI) to Cr(III) followed by the precipitation of Cr_2O_3 or $Cr(OH)_3$. Cr(III) compounds are non-toxic and less soluble in water than Cr(VI) compounds. The treatment system is expected to be highly effective in reducing Cr(VI) to Cr(III) by dissolved Fe(II) (Watts et al., 2015). The complete reduction of Cr(VI) to Cr(III) is expected to occur at a pH of ~8.7, while the solubility of the precipitated $Cr(OH)_3$ is lowest at a pH range of 8 to 11 (Fenglian and Wang, 2011).

Cr(III) is expected to be the dominant form in anaerobic aqueous environments and Cr(VI) in aerobic aqueous environments. The Cr valence state is, however, controlled by water pH, and Cr(III) is more soluble at acidic pH and will precipitate at near neutral and basic pH condition. At neutral pH, dissolved oxygen (DO) controls the proportions between Cr(III) and Cr(VI). It is, thus, important to monitor physico-chemical parameters in the treatments, which are likely to constantly change, as the treatments are open systems (Stanin and Pirnie, 2005). Under basic pH conditions the likelihood of Cr(III) oxidation into Cr(VI) is very high (Hashim et al., 2011).

The use of ferrous sulphate presents some associated disadvantages. Its use increases the total dissolved solids (TDS) content of the process and waste water. Fe(II) is removed by oxidation to Fe(III), which consequently forms ferric hydroxide which precipitates from solution at the pH levels common in waste waters. However, sulphate remains in solution, causing an increase in TDS. The increase in TDS could result in increased scale build-up in pipes, spray nozzles of wet scrubber systems, and other equipment.

Although complete reduction of Cr(VI) to Cr(III) by Fe(II) could be achieved, the increased TDS or sulphate load would result in an increased salinity of surface water and groundwater, following the disposal of treated water.

Dissolved Fe(II) is oxidised by dissolved O_2 at elevated pH levels, ferrous sulphate solutions should be stored in special tanks in bunded areas. The bund walls should be able to contain spillages that might occur and thereby prevent contamination of the environment.

5.6 Implementation of Treatment Technology

The aim of the PAT remedial system was to make it as practical as possible for implementation and easy to operate for responsible personnel. The plant design was only based on the treatment of Cr (VI), other constituents such as SO_4^{2-}, NO_3^- and generally high salinity will not be treated in this remedial process.

5.6.1 Step 1 - Pumped Cr (VI)- contaminated groundwater

Water from boreholes PM2, PM3 and SM1 is abstracted with low flow pumps. A total volume of 130 m^3/day is extracted. This water is pumped into the Settling Pond A. Settling pond A is filled with chromite ore (finest grading possible-10microns or less) which will be the first step in the reaction process. Cr(VI) contaminated groundwater and then reacts with the chromite ore to precipitate Cr(III) compounds. Water quality monitoring was required on a weekly basis along with water level monitoring for the abstracting boreholes.

5.6.2 Step 2 – Settling pond A to Dosing Pump

The water from Settling Pond A (Fig. 13) is pumped into a dosing pump for dosing with soluble Fe(II)-sulphate. For every 100 m^3 of water from Settling Pond A, 0.1m^3 of $Fe(II)SO_4$ is added in the dosing process and the reaction is immediate then the dosed water is released into Settling Pond B. The Eh and pH in the settling ponds were monitored on a weekly basis to ensure that:

- pH remains between 3 and 8.
- Eh is reduced by approximately 0.5 to 1 mV from the initial to the final stage of treatment.

5.6.3 Step 3 – Dosing Pump to Settling pond B

The dosed water from the Settling Pond A is pumped to Settling pond B, which is filled with scrap iron material, to further reduce Cr(VI) to Cr (III). This water should have a Cr(VI) value of below 0.05 mg/ℓ to indicate successful treatment of Cr(VI). The treated water is then collected and stored as waste water to be used in the mine.

5.7 Groundwater monitoring network

Quarterly water quality and level monitoring was conducted regularly by the author (with the help of a geo-technician). The programme utilised a comprehensive network of monitoring boreholes and surface water monitoring points. The groundwater monitoring network was utilised to evaluate the environmental status and trends in water level and water quality at the study and its immediate surrounds. In the context of groundwater immediate surrounds are commonly regarded to extend between 2 and 4 km radially around the potential contamination source for inorganic constituents.

Against national regulations groundwater quality is tested to verify that it is suitable for its intended use, i.e. domestic, livestock watering, irrigation or industrial. In cases where groundwater has been contaminated by anthropogenic sources and its use is potentially harmful to the environment or human health it is often necessary to remediate. Groundwater monitoring is adaptable to a specific project needs and indicator parameters are chosen to represent the environmental status quo of the specific area in respect of the activities that may produce contaminants. In essence groundwater contamination by chromate was detected at the study area in 1997, thus the monitoring programme may be described as an assessment monitoring programme. An assessment monitoring programme was designed so as to collect data that may be needed to formulate remedial actions. Detection monitoring is applied to detect potential impacts on groundwater quality. This study essentially controls monitoring to evaluate the efficiency of remedial action.

The assessment monitoring consists of 13 monitoring boreholes, six privately owned abstraction boreholes and three surface water monitoring points. The monitoring network was developed over more than a decade and has been in its current from since 2013. An assessment-monitoring-network is generally dynamic and is extended over time to accommodate the migration of contaminants and to improve the resolution of data collection. The groundwater monitoring network is expected to be expanded in the future as a result of remedial control monitoring findings. The source-pathway-receptor method was followed in the design of the monitoring network. The conceptual site model is described in terms of source and sinks, migratory pathways and the receiving environment in section.

Monitoring point names reflect the design objectives, background monitoring boreholes are coded – BH-B; source monitoring boreholes are coded – BH-SM; chromate plume monitoring boreholes are coded – BH-PM; Impact monitoring boreholes are coded – BH-IM; and a combination of plume and impact monitoring boreholes are coded – BH-PIM. The monitoring points are listed in Table 3 and displayed in spatial relation to the contamination source in Figure 5. Groundwater monitoring by sampling and water level measurement has been widely proven to the most successful plume delineation technique. It is advantageous in that it can be targeted to specific site limitations and

contaminants of concern. Further the monitoring network design can be adapted to site conditions and limitations. Other plume delineation techniques such as geophysical techniques or sampling probes are limited to one-time events. Groundwater monitoring allows us to evaluate the natural environmental conditions of the subsurface. The environmental statuses of the different areas of the monitoring network are described in a later section.

The monitoring boreholes target different aquifers and are designed to prevent vertical inflows and cross-contamination. Water level fluctuations and the attenuation of contaminants in the shallow weathered aquifer and the deeper fractured aquifer are different due to different hydraulic properties. Sanitary borehole design as applied to the study area is displayed in the attachment in Appendix III.

The objectives of chemical analyses were designed so as to assess contaminant migration in terms of constituents of concern and indicator parameters. Sampling procedures and precise analytical technologies supported by control measures were in place to ensure precise quality data were collected during monitoring. Groundwater monitoring took place quarterly and analytical results were kept in an electronic database. The indicator parameters used to reflect the environmental status of the study area are listed in Table 4. The respective laboratory technologies applied for analyses and sample preservation requirements are described in an earlier section.

Table 3: Monitoring points.

Monitoring point	Longitude	Latitude	Cr^{6+} in mg/l (January 2015)
BH-B1	27.84188	-25.6629	0
PW-DAM	27.83614	-25.6603	0
BH-SM1	27.83945	-25.6628	1.6
BH-SM2	27.83975	-25.663	0.013
BH-SM3	27.83875	-25.664	0
BH-PM1	27.83656	-25.6669	0
BH-PM2	27.83703	-25.6656	1.59
BH-PM3	27.83697	-25.6646	1.59
BH-PM4	27.83193	-25.6615	0
BH-PM5	27.83326	-25.6623	0.647
BH-PM6	27.83281	-25.6638	0.211
BH-PM7	27.8318	-25.6671	0.296
BH-PIM1	27.83111	-25.6649	0.851
BH-PIM2	27.83147	-25.6645	0
BH-PIM3	27.82471	-25.6645	0.016
BH-PIM4	27.83685	-25.6664	0
BH-PIM5	27.82976	-25.6662	0
BH-IM1	27.83423	-25.674	0
BH-IM2	27.83405	-25.6556	0
BH-IM3	27.82287	-25.663	0
Kareespruit (Upstream)	27.83109	-25.6534	0
Kareespruit (Downstream)	27.81682	-25.6564	0

Table 4: Monitored indicator parameters.

Constituent	Units	Media
Al	mg/l	Water
Alkalinity	mg/l	Water
As	mg/l	Water
B	mg/l	Water
Ca	mg/l	Water
Cl	mg/l	Water
CO_3	mg/l	Water
Cr	mg/l	Water
Cr^{6+}	mg/l	Water
EC	mS/m	Water
F	mg/l	Water
Fe	mg/l	Water
HCO_3	mg/l	Water
K	mg/l	Water
Mg	mg/l	Water
Mn	mg/l	Water
Na	mg/l	Water
NH_4	mg/l	Water
NO_3	mg/l	Water
NO_3 as N	mg/l	Water
pH	pH	Water
PO_4	mg/l	Water
Si	mg/l	Water
SO_4	mg/l	Water
SWL (m bgl.)	m	Water
TDS	mg/l	Water
SWL (mamsl)	m	Water

6. RESULTS AND INTERPRETATION

6.1 Conceptual site model

Conceptual site model (CSM) development is an integral step in fate and transport assessments. The CSM incorporates geological, hydrogeological, hydrochemical and biological information to facilitate an effective contaminant transportation assessment (Stanin and Pirnie, 2005). Thus a conceptual hydrogeological model allows for a combined interpretation of data to assess source-pathway-receptor linkages.

The hydrogeology of plutonic and metamorphic provinces is characterised by groundwater circulation in the zone of weathering, and fracture networks in deeper-lying aquifers (Fulton et al., 2005). Fracturing is limited to relatively shallow depths; the limit of fracture formation estimated is to be 30 mbgl across the study area. However the situation is complicated by dewatering of water strikes due to widespread mining in the vicinity of the study area including historic underground mining. The weathering and fracture zones are considered completely mixed reservoirs underlain by low-permeability to impermeable basement rocks. At the study area normal and strike-slip faults, joints, dykes and hydraulic boundaries control groundwater flow systems. Due to extensive and unmetred groundwater abstraction around the study area in close proximity, groundwater flow occurs under non-steady state hydraulic conditions.

The source of contaminated leachate was identified as the baghouse slimes dam. Secondary containment of the Cr(VI)-bearing slimes failed and was leached by rainfall reaching the subsurface. The regolith horizon consists of clays up to 2 m in thickness, which allowed for vertical seepage of contaminated leachate due to cracking caused by high evapotranspiration and low rainfall conditions.

Migration pathways for contaminated leachate were limited to groundwater flow, which is controlled by weathering-enhanced porosity, faults and jointing. The critical receptors are groundwater users downstream of the contamination source, abstracting groundwater for domestic use and large-scale irrigation. The *Kareespruit* and Crocodile River are both located beyond the radius of influence of the chromate plume (>2 km). The chromate plume is not forecasted to reach the *Kareespruit* and Crocodile River based on kinetic rates and the controls on groundwater flow.

A cross-section was created to visualise the conceptual site model in 2D across the contaminated site in relation to the baghouse slimes dam, i.e. the source of contamination. The most representative section was from ENE through the source, pumping boreholes and monitoring boreholes to the Crocodile River, located SSW of the source. The CSM is displayed in Figure 14

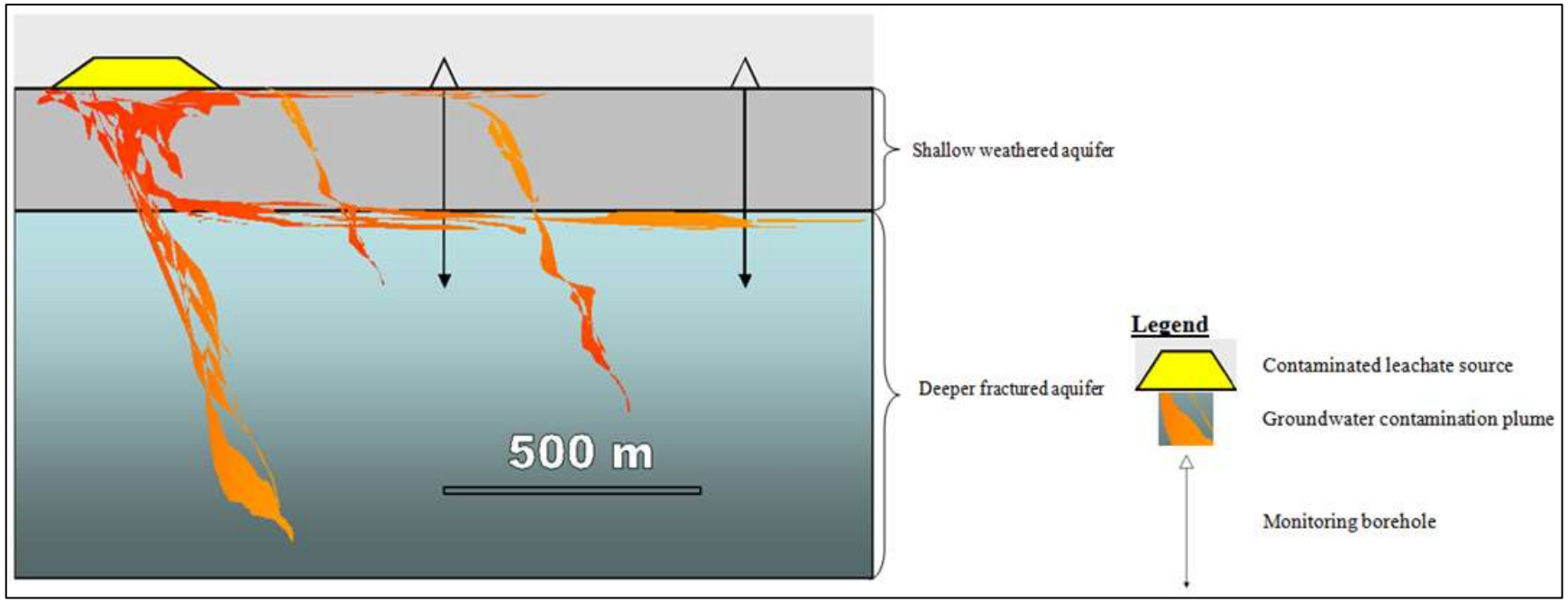


Figure 14: Conceptual groundwater plume shown throun and W-E cross section through the weathered and fractured aquifers, conceptualising the potential flow paths through the subsurface.

6.2 Water Levels

Water levels were measured in all monitoring boreholes prior to the implementation of the PAT system and during operation of the PAT system. Water level elevations are measured in reference to the sea level datum in meters above mean sea level (m.a.m.s.l.). The water levels measured were used to model the groundwater table in the aquifers. Measurement of water level variations in monitoring boreholes is a useful way of determining the degree of connectivity in fracture networks (Cook, 2003).

Periodical monitoring during different seasons (i.e. the wet and dry season) allows for characterisation of the aquifers by examining fluctuations in the monitoring boreholes (Hiscock, 2005). The groundwater table is contoured and resulting maps can be used to understand groundwater flow directions through hydraulic head gradients. Further, monitored groundwater levels are used (including in this study) to calibrate groundwater flow models.

The groundwater level elevations measured prior to the commencement of PAT operation and six months since then were contoured and shown in Figure 16 and Figure 17. Groundwater flow direction should be perpendicular to the contours and inversely proportional to the distance between contours. The inferred groundwater flow directions are shown as flow vectors. The areas where the groundwater table has a shallow hydraulic gradient, the contours are spaced further apart than the areas where the hydraulic gradient is steep. The general direction of flow in the study area downstream of the pollution source westerly towards the Crocodile River located over 4.5 km west. This is similar to surface drainage patterns, as naturally groundwater flows from recharge to discharge points. The study area is located near the western foothills of the Magaliesberg Mountain Range, a recharge area and regional groundwater divide. The primary groundwater discharge area is the Crocodile River and its tributaries. The privately-owned abstraction boreholes downstream of the mine serve as mechanical discharge points.

A comparison of the water levels (m.b.g.l.) measured over the control monitoring period are listed in Table 5 and graphically displayed in Figure 15. Naturally water level fluctuations are expected to be influenced by seasonal precipitation patterns. Hydrological processes have an influence on infiltration and recharge, replenishing aquifer storage. The water levels in the study area have over the entire monitoring period declined, due to the influence of pumping for treatment and irrigation. In the vicinity of the three PAT system's abstracting boreholes water levels have declined by an average of 2 m compared to the same period in 2014. Periodical fluctuations in the fractured aquifer are reflective of the influence of fractures on groundwater flow.

Table 5: A comparison of the water level data measured over a period of a year (July 2014 to July 2015). The difference in water levels after a year of periodical water level monitoring reprents a water level decline for a positive value and vice versa.

Borehole number	SWL (Jul 2014)	SWL (Oct 2014)	SWL (Jan 2015)	SWL (Apr 2015)	SWL (Jul 2015)	Difference (Jul 2015 - Jul 2014)
	mbgl	mbgl	mbgl	mbgl	mbgl	mbgl
BH-B1	9.45	10.06	9.8	12.13	11.95	2.5
BH-PIM1	10.23	10.64	10.94	11.36	11.98	1.75
BH-PIM2	10.65	11.1	11.54	11.34	12.6	1.95
BH-PM1	7.66	7.86	8.55	8.99	9.6	1.94
BH-PM2	11.37	12.13	11.92	12.7	13.67	2.3
BH-PM3	12.07	13.47	12.84	13.93	14.94	2.87
BH-PM4	13.25	13.48	13.68	14.91	15.05	1.8
BH-PM5	14.44	15.23	15.44	15.13	15.31	0.87
BH-PM6	12.87	12.41	13.48	14.8	15.3	2.43
BH-PM7	9.5	6.96	7.16	7.56	7.9	-1.6
BH-SM2	12.99	13.27	11.51	13.79	13.11	0.12
BH-SM3	15.43	16.17	15.7	16.7	-	-

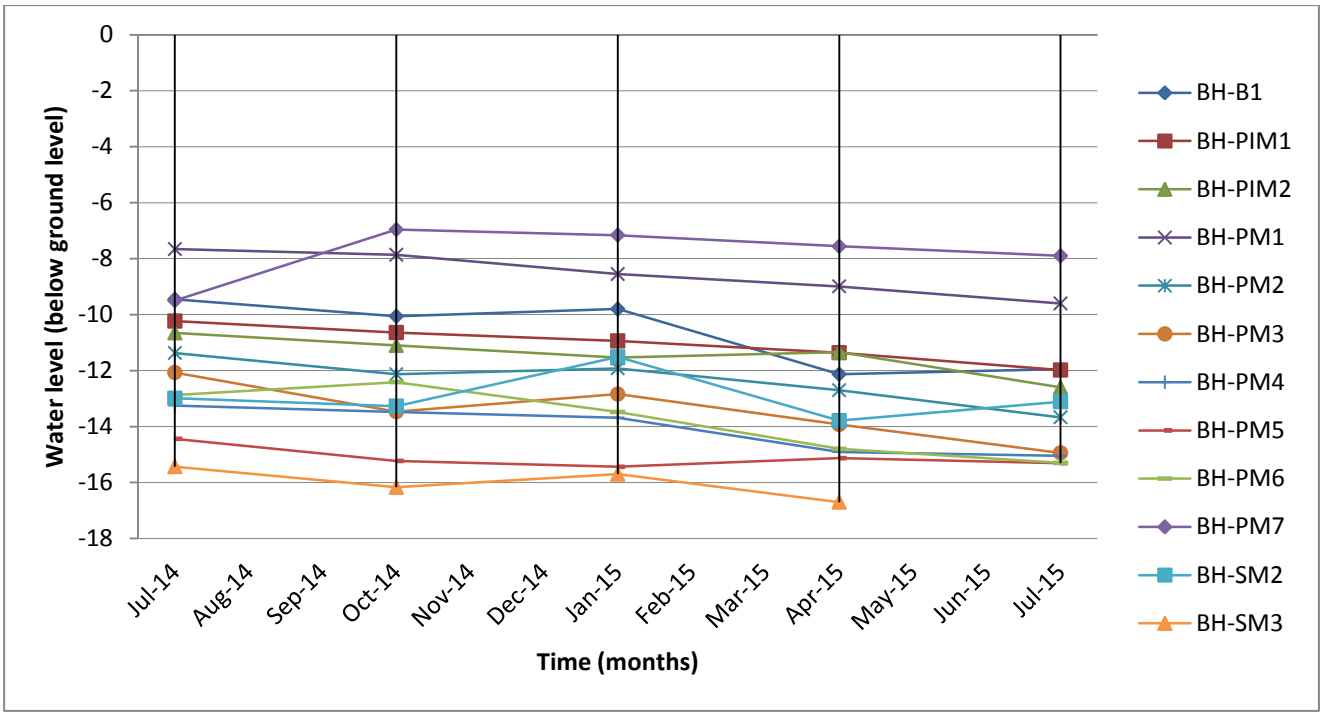


Figure 15: Water level trends over a period of one year showing changes in aquifer storage. BH-SM3 was destroyed in April 2015.

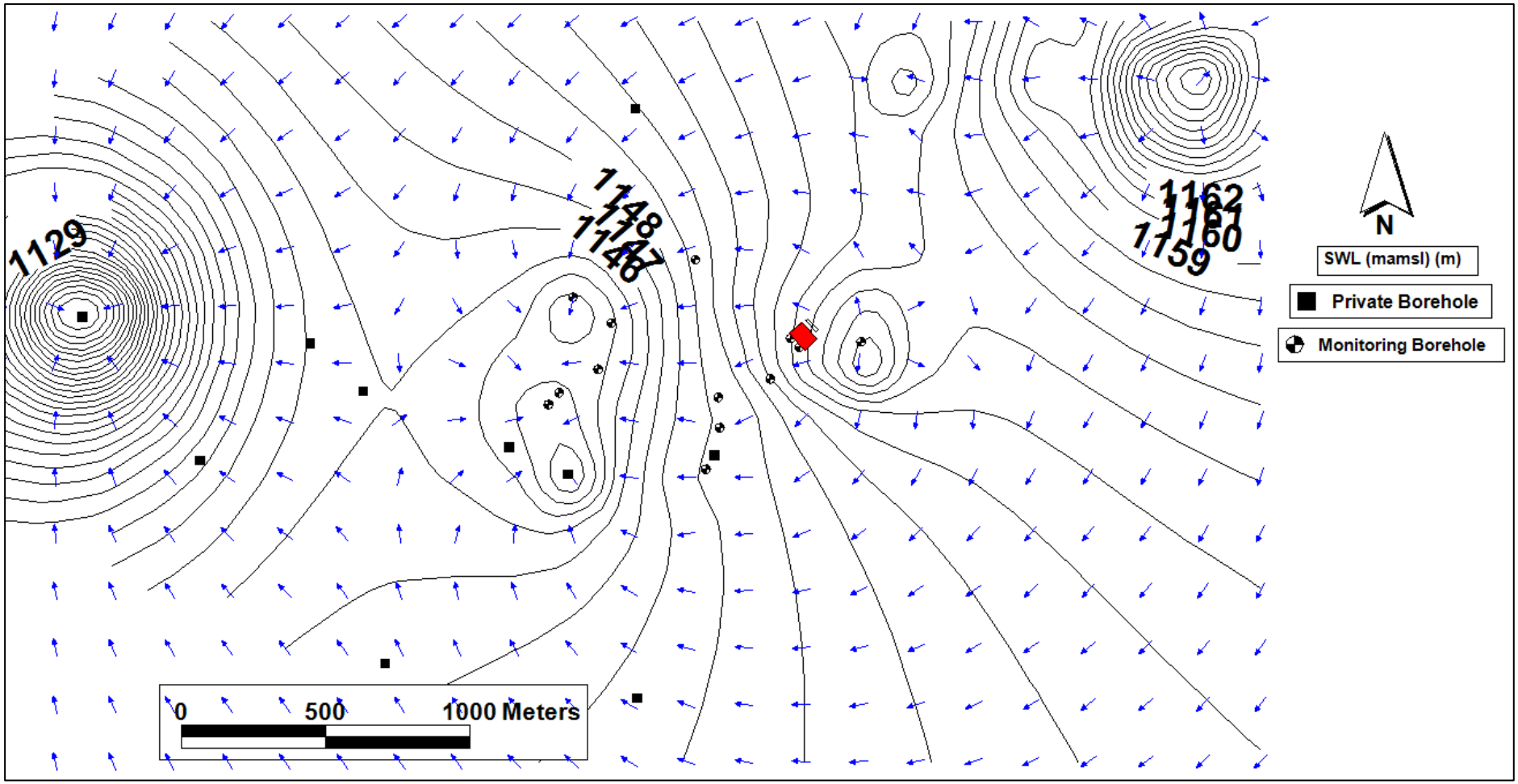


Figure 16: Contoured water level elevations also showing inferred groundwater flow vectors prior to pumping (January 2015).

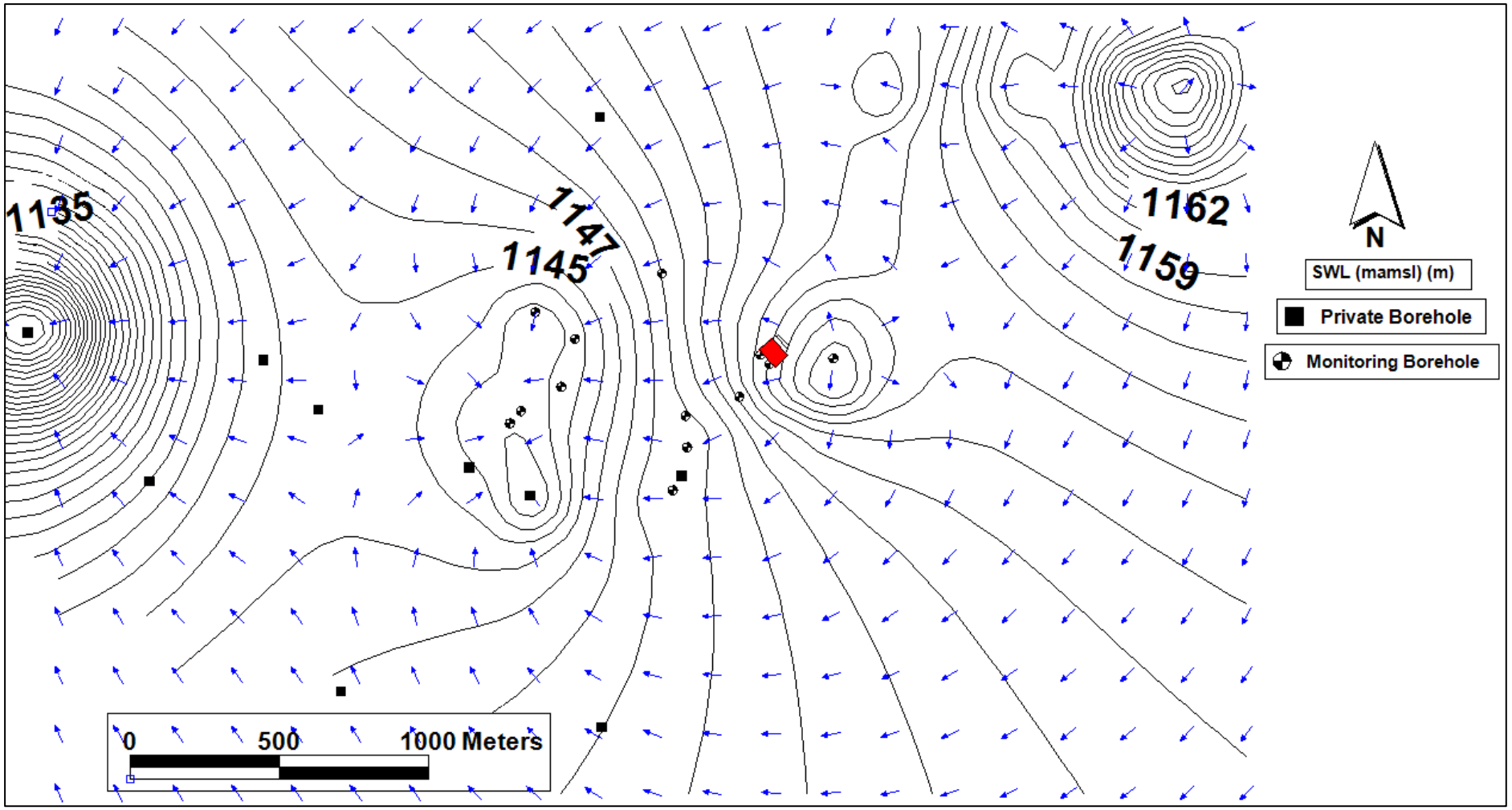


Figure 17: Contoured water level elevations also showing inferred groundwater flow vectorts (July 2015).

6.3 Hydrochemical Characterisation

Groundwater quality monitoring is used to provide an understanding of hydrochemical conditions in hydrogeological studies. Knowledge of the distribution of constituents and trends in concentrations of various constituents drive the decision-making process for managers. Hydrochemical processes are responsible for reactions and processes in the groundwater environment. Groundwater is composed of major ions, viz. Na^+, Ca^{2+}, Mg^{2+}, Cl^-, HCO_3^- and SO_4^{2-} which commonly comprise of over 90% of the total dissolved constituents. Minor ions include K^+, Fe^{2+}, Sr^{2+} and F^- and some trace elements and metal species. In this study, mass concentrations units are reported in mg/ℓ, which is best suited for dilute solutions, while pH is expressed in pH units and electrical conductivity in mS/m.

Major and minor ions are used as geochemical proxies or groundwater tracers by hydrogeologists to study the movement of groundwater and assess the environmental status of groundwater. In fractured aquifers, due to discontinuities, continuous water quality monitoring is the best suited method to assess the environmental status of an area. The spatial distribution of constituents depends on the chemical solubility and mobility of the dissolved species. The likely sources of other elevated constituents other than are listed in Table 6. The source of Cr(VI) pollution was the baghouse slimes dam that leaked leaching chromate contaminated waste water into the subsurface. The dissolved constituents are used in the subsequent sections to characterise the geochemical status of the study are following the implementation of the PAT system.

Table 6: Likely sources of dissolved constituents un the study area.

Dissolved ions in water	Likely local sources
Major ions	
Calcium	Gypsum (hydrated calcium sulphate)
Magnesium	Olivine, pyroxene
Sodium	Clays, feldspars, wastes
Potassium	Feldspar, fertilisers, K-evaporites
Bicarbonate	Soil and atmospheric CO_2
Chloride	Windborne, rain water, pollution
Sulphate	Gypsum and anhydrite, seawater, windborne, oxidation of pyrite
Nitrate	Windborne, oxidation of ammonia or organic nitrogen, pollution
Minor ions	
Iron	Oxides and sulphides, corrosion of iron pipes
Manganese	Oxides and hydroxides
Fluoride	F-bearing minerals (e.g. Fluorite, biotite, etc.)
Trace elements	
Cr	Baghouse dust, tailings and igneous rock weathering under mildly reducing conditions
Zn	Wastes

6.3.1 Water types

The hydrochemical signature of the samples was investigated through Stiff diagrams. Stiff diagram was plotted for major ion concentration on three or four horizontal equidistant axes with major cations on the left-hand side and major anions on the right-hand side. The concentrations were plotted as equivalent charges (meq/ℓ). Stiff diagrams are useful in quickly visualising the spatial distribution of the major groundwater constituents as water signatures (Hiscock, 2005). The Stiff diagrams for the monitoring samples and the treatment ponds have been displayed in Figure 18. The groundwater signatures of the samples vary spatially in the following way:

- Background monitoring: $Mg^{2+}/HCO_3^- + CO_3^{2-}$
- Source monitoring: Mg^{2+} - $Na^+ + K^+/SO_4^{2-}$
- Plume monitoring: $Mg^{2+}/HCO_3^- + CO_3^{2-}$
- Impact monitoring: $Mg^{2+}/HCO_3^- + CO_3^{2-}$

On the Piper diagram compositions in meq/ℓ of all the samples are presented on two separate cation and anion trilinear plots and then projected onto a quadrilateral hydrochemical facies polygon. The Piper diagram is used as a visual display of the chemistry of samples that allows for the identification of spatial trends in pollution (Hiscock, 2005). The explanation of the hydrochemical facies of the Piper diagram is presented in Figure 19 and the analytical data is plotted on the Piper diagram in Figure 20. The hydrochemical facies of the samples vary spatially in this way:

- Background monitoring: Sulphate type sodium type water
- Source monitoring: No dominant cations or anions
- Plume monitoring: Bicarbonate/sulphate type and magnesium/sodium type water
- Impact monitoring: No dominant cations, chloride/bicarbonate type water.

In the mining area sodium and sulphate enrichment is attributed to the impact of chemical extraction from ores, waste water discharge and dewatering of the mine. Chloride enrichment is attributed to leachate from domestic waste and dewatering of the mine. Bicarbonate and magnesium enrichment are indicative of recently recharged water. The groundwater samples plot in the mixing area of the quadrilateral diagram showing evidence of mixing between the primary and secondary aquifers. In the treatment ponds, settling pond A is of a bicarbonate type as the water is exposed to the atmosphere; while settling pond B is enriched in sulphate due to the addition of $Fe(II)SO_4$ for treatment purposes.

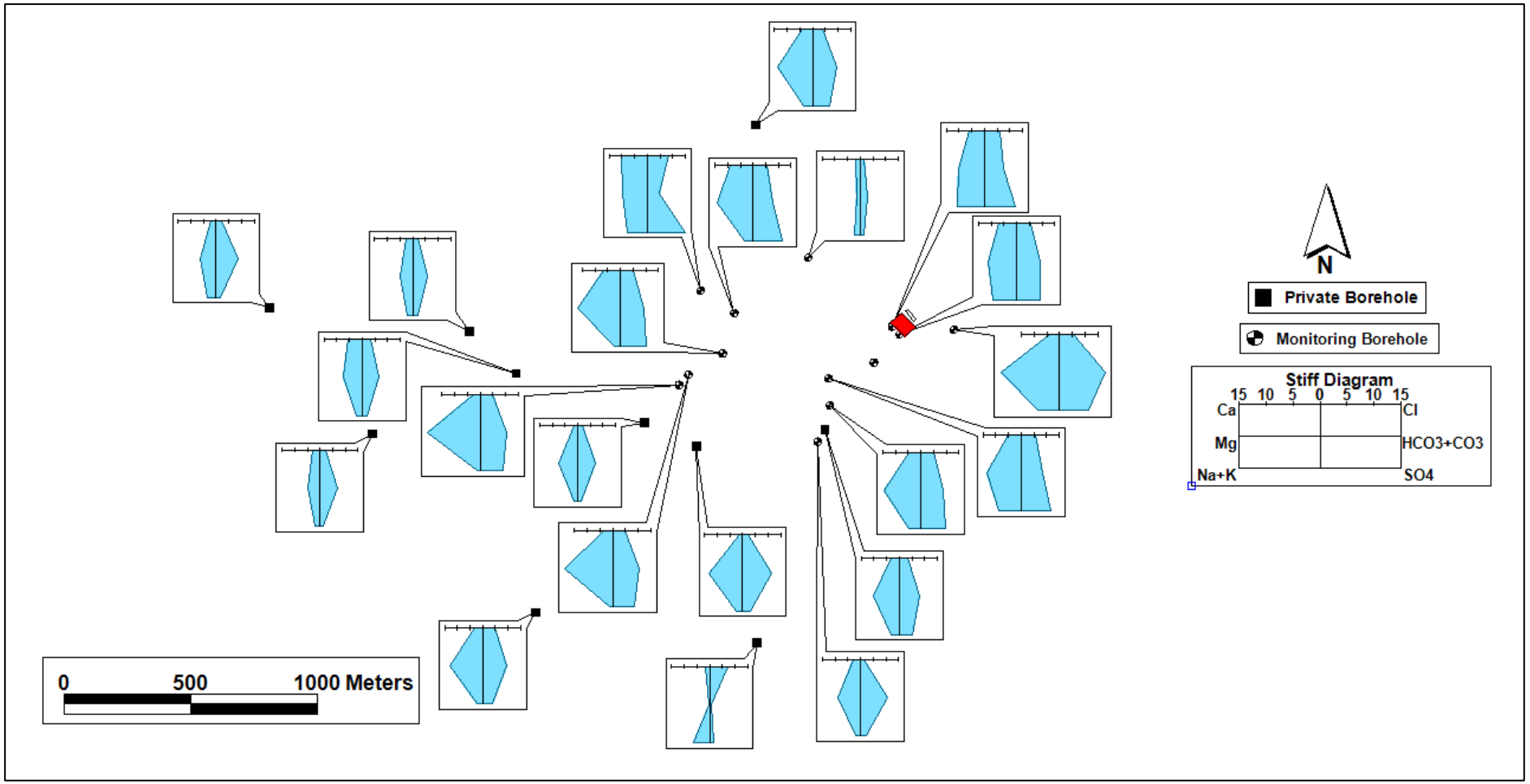


Figure 18: Stiff diagrams showing the spatial distribution of major ions and water signatures in the study area.

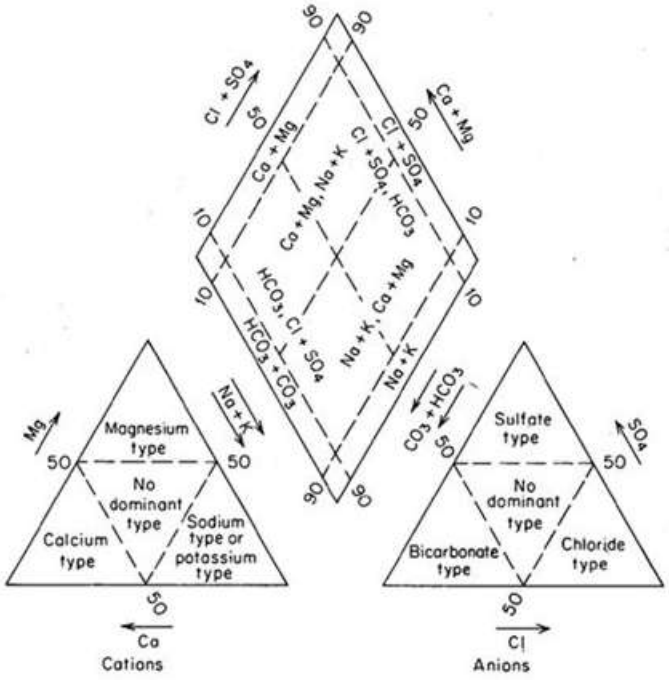


Figure 19: Classification diagram of the hydrochemical facies in the Piper diagram (Hiscock, 2005).

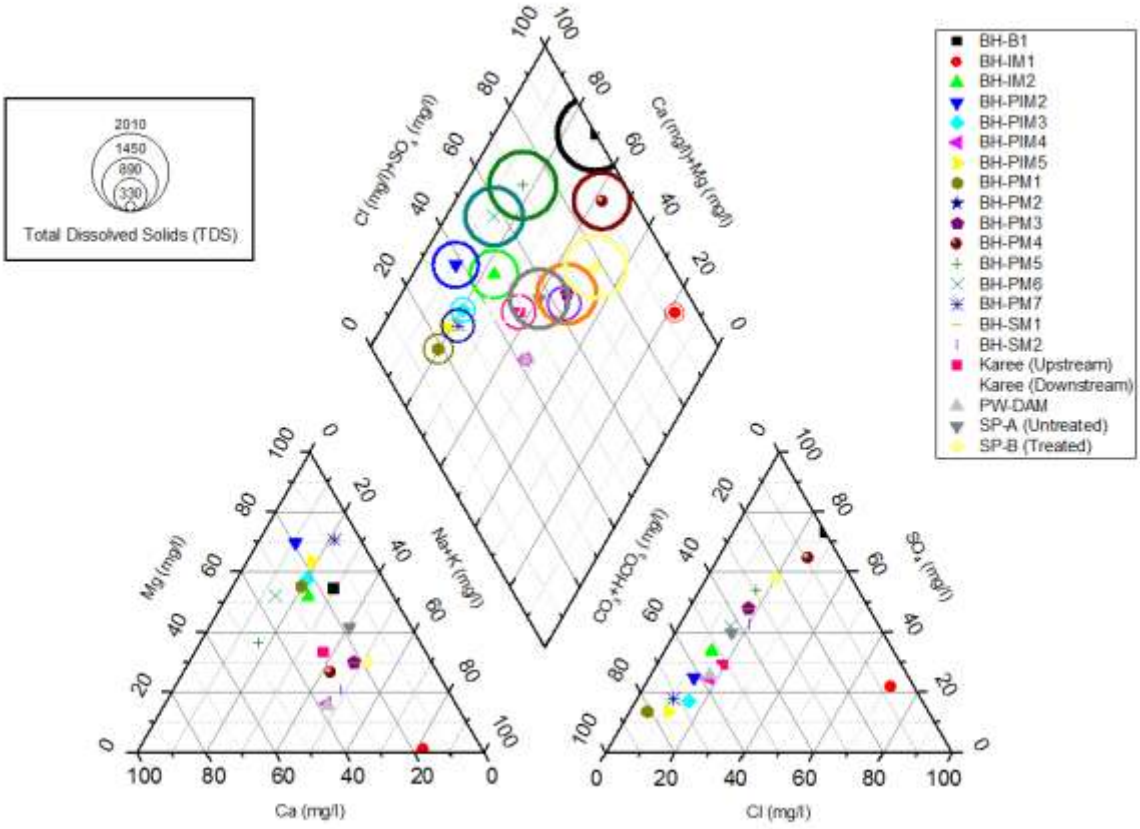


Figure 20: Water samples for groundwater and surface water samples plotted against the Piper diagram.

6.3.2 ^{2}H and ^{18}O

The major factors that can affect the $\delta^{18}O$ and $\delta^{2}H$ isotopic composition of precipitation are season, latitude, temperature, altitude, storm track, and amount of precipitation (Clark and Fritz, 1997). Most of the isotopic variations associated with these factors can be related to isotope fractionation effects that occur during evaporation at the moisture source(s) and during moisture condensation (Clark and Fritz, 1997).

In groundwater $\delta^{18}O$ and $\delta^{2}H$ values are indicative of the changes in the isotopic signature of the recharging water as affected by isotopic fractionation as the water evolves in the atmosphere, surface and subsurface (West et al., 2014). The processes that are responsible for isotopic fractionation cause the isotopic signature of the evolved water to deviate from the global meteoric water line and local meteoric water lines (Geyh, 2000). In this study the stable environmental isotopes, $\delta^{18}O$ and $\delta^{2}H$ are applied to determine the isotopic signature of recharge waters and the evolution of the water in the hydrological cycle. In cases where, $\delta > 0$, the sample is enriched in the isotope relative to the VSMOW standard; and where, $\delta < 0$, the sample is depleted in the isotope relative to the VSMOW standard. The results of the stable isotope analysis are presented in Table 7.

Table 7: Results of the stable isotope analysis.

Sample ID	δ2H‰	2H Standard deviation	δ 18O‰	18O Standard deviation
PW-DAM	-2.75	0.06	-0.80	0.05
BH-B1	-6.90	0.22	-1.17	0.04
BH-SM1	5.83	0.11	1.28	0.04
BH-SM2	9.98	0.13	2.15	0.04
BH-PM1	-19.60	0.09	-3.49	0.07
BH-PM4	-15.09	0.19	-2.83	0.04
BH-PM5	-3.93	0.17	-0.64	0.03
BH-PIM1	-7.54	0.22	-0.79	0.01
BH-PIM4	-1.81	0.16	-0.54	0.03
SP-A	-0.93	0.68	-0.28	0.13
SP-B	-0.66	0.17	0.40	0.04

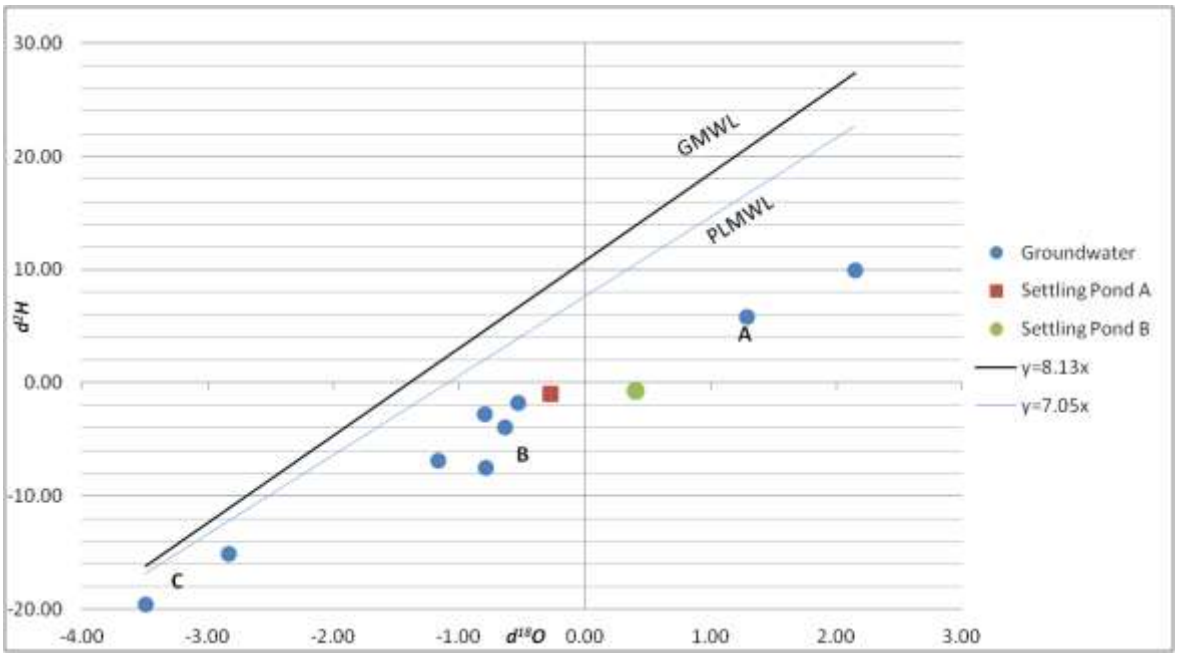


Figure 21: Stable isotope data ($\delta^{18}O$ (‰) vs. $\delta^{2}H$ (‰)) plotted relative to the GMWL and PLMWL.

The $\delta^{18}O$ and $\delta^{2}H$ results of the water samples were plotted on a $\delta^{2}H$ vs $\delta^{18}O$ chart, relative to the Global Meteoric Water Line (GMWL), Craig 1961 and Pretoria Meteoric Water Line (PLMWL) GNIP-IAEA data. The samples deviate from both the GMWL and PLMWL. All groundwater samples show the evidence of evaporation before recharge took place. The groundwater samples can be grouped into three clusters namely, A, B and C. The majority of the groundwater samples plot in cluster B indicative of fresh recharge after evaporation. Cluster C is indicative of recharge following fractionation during cooler temperatures (Winter recharge in this case). Cluster A is indicative of the impact of recharge after strong evaporation process. The treatment ponds show different $\delta^{18}O$ and $\delta^{2}H$ signatures due to higher evaporation losses in Settling Pond B, owing to higher residence times of the treated water before it was transferred from the pond to a wastewater dam. The majority of the groundwater samples, from the shallow primary and deep fractured aquifers plot in the same cluster which is indicative of mixing of waters between the primary and secondary aquifers.

6.3.3 Tritium

Tritium activity is reported in tritium units (TU) where 1 TU is defined as 1 atom of ^{3}H in 10^{18} atoms of ^{1}H (Clark and Fritz,1997). Tritium is radioactive with a half-life of 12.43 years. Tritium is sourced either naturally from the atmosphere by cosmic ray bombardment of nitrogen neutrons; and was added artificially to the atmosphere from thermonuclear device development and testing in the northern hemisphere during the Cold War years, 1952 – 1962 and locally from the Pelindaba nuclear facility (Geyh, 2000). The results of the tritium analysis performed on selected monitoring points are presented in Table 8. According to Clark and Fritz (1997), tritium activity < 5 TU is representative of submodern recharge (pre-1950s); tritium activity ranging between 5 – 15 TU is representative of modern recharge; and tritium activity >15 TU is representative of the influence of nuclear activity or contamination.

Table 8: Results of the tritium analysis for monitoring boreholes.

Sample ID	Tritium (T.U.)	
BH-PIM1	7.1	±0.5
BH-PIM4	6.4	±0.5
BH-PM1	3.5	±0.4
BH-PM4	4.4	±0.4
BH-PM5	4.6	±0.4
BH-SM1	5.3	±0.4
BH-SM2	6.9	±0.5
BH-B1	5.7	±0.4
PW-DAM	7.3	±0.5
SP-A	5.4	±0.4
SP-B	7.2	±0.5
Field blank (SP-B)	7.2	±0.5

The average tritium activity in the Pretoria area is 5.6 ($^{+}/_{-}$ 0.4) T.U (GNIP-IAEA). The majority of the samples have a higher tritium activity than the local average in rainfall. Abiye et al. (2015) reported exceptionally high tritium activity for the Hartbeespoort Dam and Crocodile River and attributed tritium enrichment to contamination by waste water from the nuclear industry in the area. Therefore, recharge of high tritium enriched water used for agricultural purposes from the Hartbeespoort dam might have impacted the groundwater in the study area.

6.4 Assessment of treatment system

The main objective of this study is to assess the efficiency of the dosing system in chemically remediating chromate contaminated groundwater. The remedial technique is a PAT system. A wellfield of three boreholes is used to abstract chromate contaminated groundwater into a temporary storage pond (Settling Pond A, coded as SP-A). In SP-A untreated, contaminated groundwater is reacted with chromite ore to precipitate Cr(III) minerals. Water from SP-A is pumped into a dosing pump and dosed with a solution of $Fe(II)SO_4$ and subsequently pumped into Settling Pond B (SP-B). Cr(VI) is reduced to Cr(III) and $Cr(OH)_3$ is precipitated. The hydrochemistry of the settling ponds was monitored over a 6-month period for the purpose of this study and hydrochemical trends are displayed in Figure 22 for Cr and Cr: Figure 23 for major ions in SP-A; and Figure 24 for major ions in SP-B.

The dosing system has been successful in reducing Cr(VI) to Cr(III) and precipitating $Cr(OH)_3$. The treatment system was designed to treat Cr(VI), other elevated constituents and generally high dissolved ions are not treated in this remedial process. A period of no treatment of Cr(VI) as seen through a concentration higher than the 0 mg/ℓ as intended occurred on 26-May-2015. This was caused by operation error dosing solution was not refilled in time and no treatment by reduction by aqueous Fe(II) occurred. Some treatment may have occurred due to the action of chromite ore precipitating Cr(III) minerals in the treatment ponds.

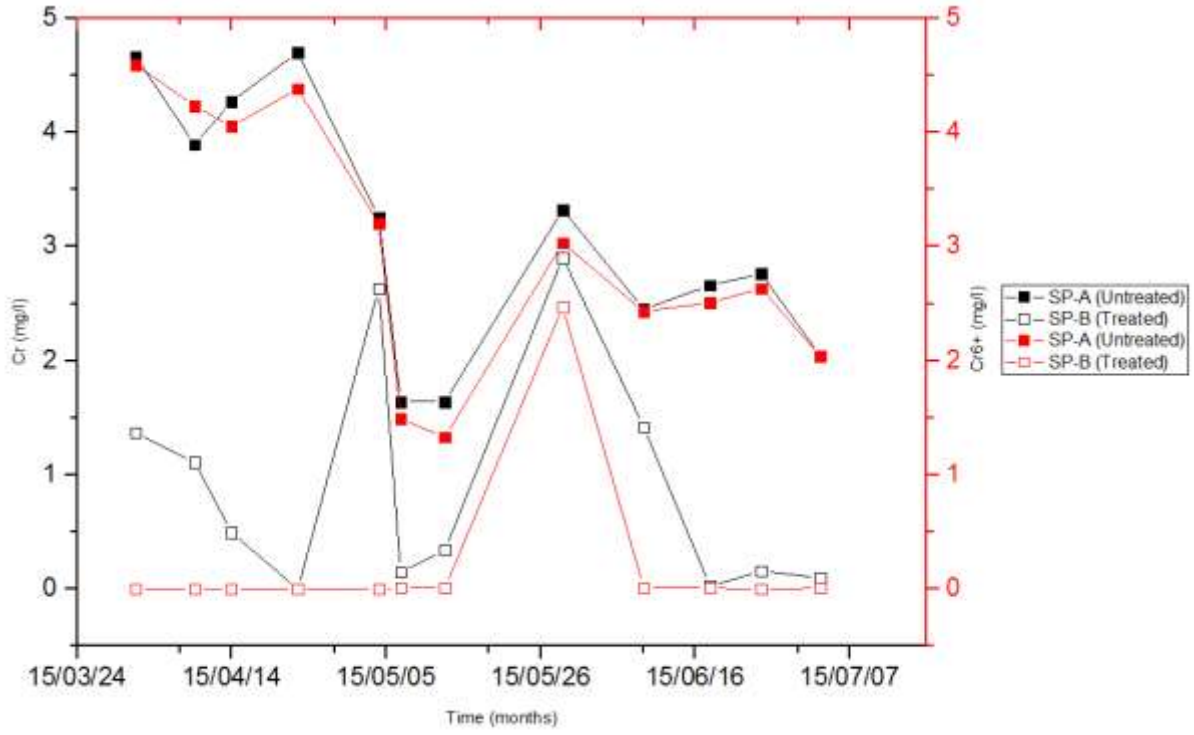


Figure 22: Trends in Cr and Cr(VI) concentrations in the treatment sytem before and after chemical treatment over a six-month period.

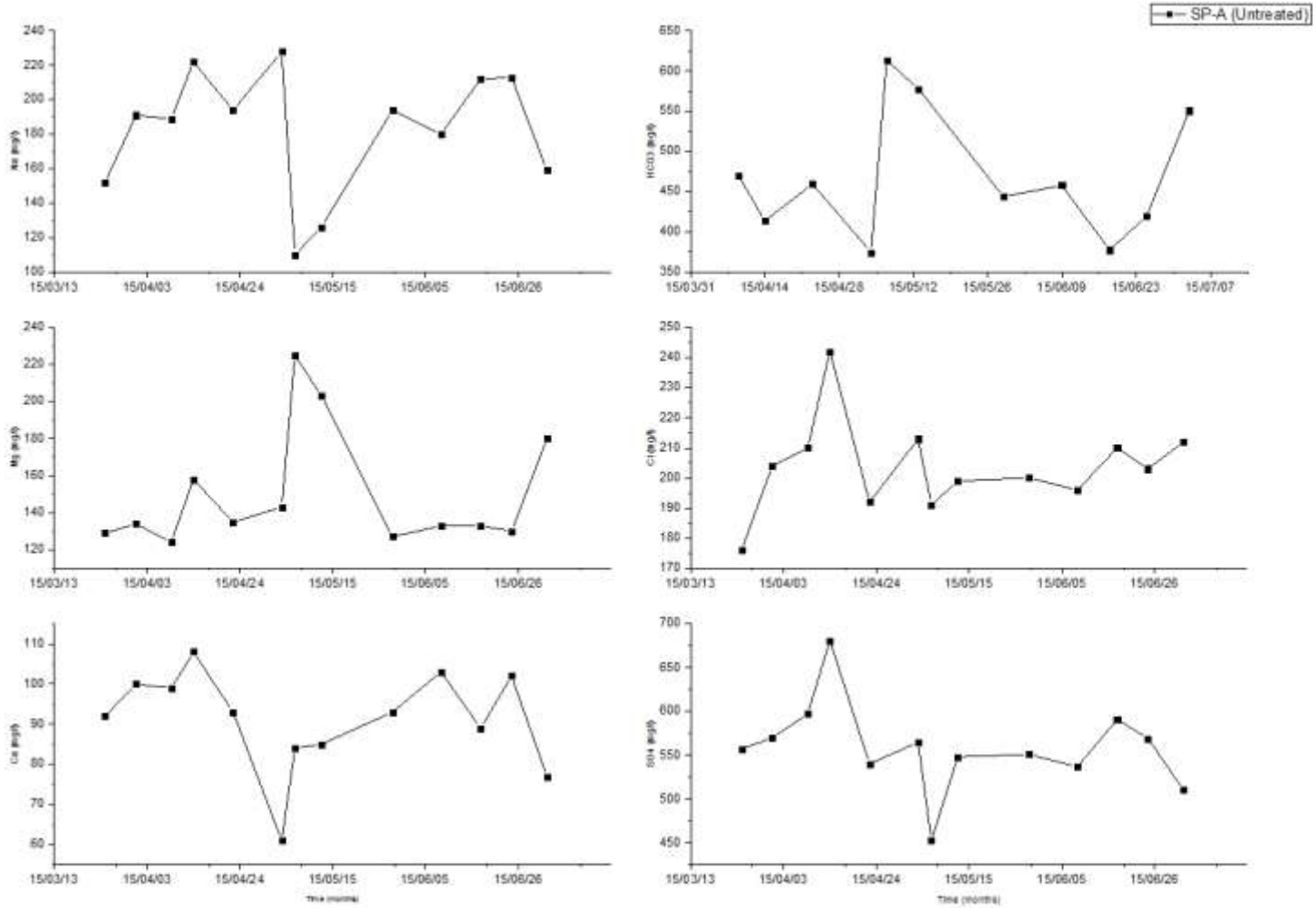


Figure 23: Trends in major ion chemistry before chemical treatment over a six-month period.

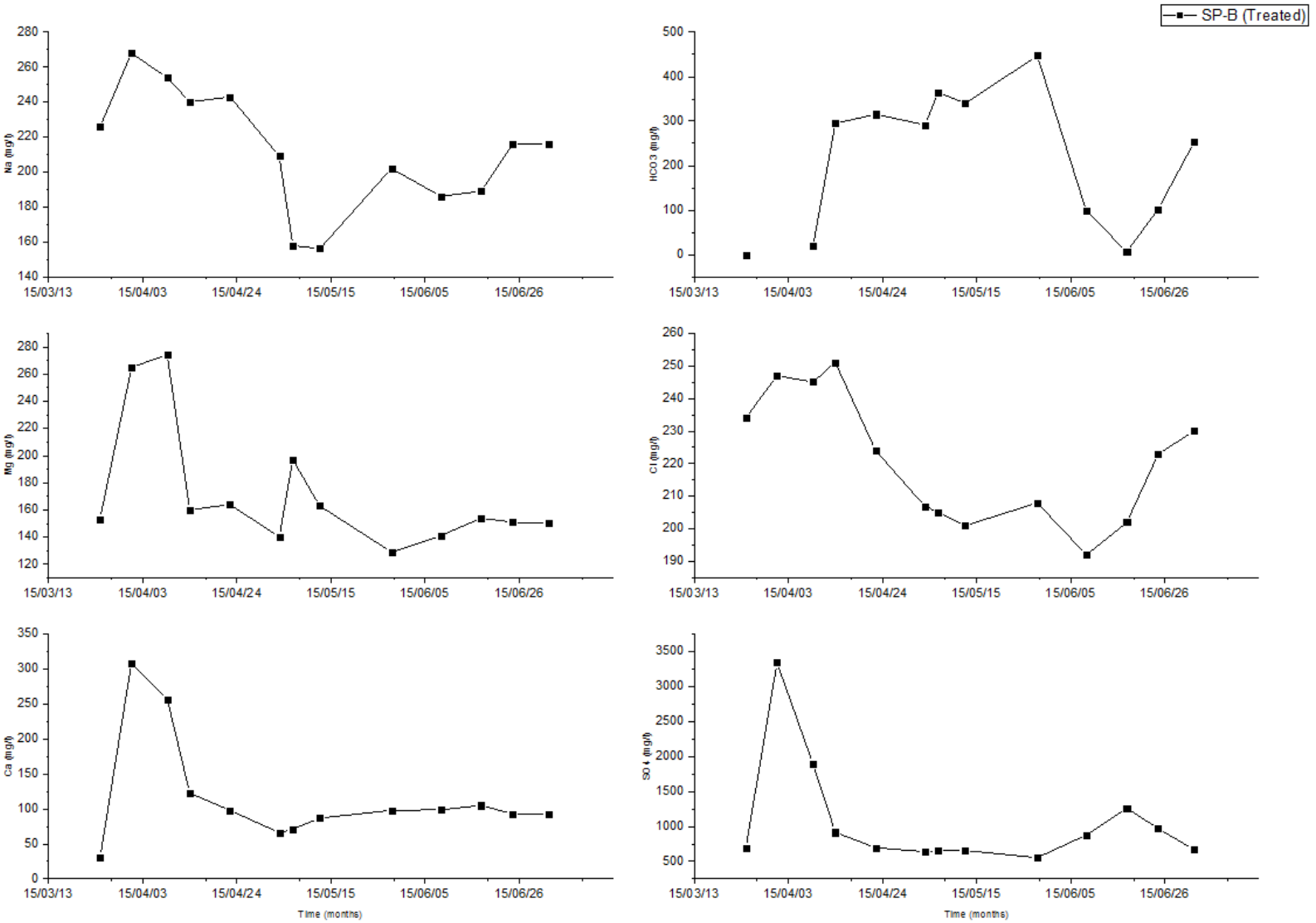


Figure 24: Trends in major ion chemistry after chemical treatment over a six-month period.

Major ions were selected to determine the trends in constituent concentrations of contaminated groundwater that is abstracted and passes through the treatment system. Figure 23 and Figure 24 show trends for major dissolved ions prior to dosing with aqueous $Fe(II)SO_4$ in treatment pond A and after dosing in treatment pond B. Comparison of major cation and anion concentrations indicated that:

- The range of Na^+, Mg^{2+}, Ca^{2+} and Cl^- concentrations is similar before and after treatment.
- The tendency of HCO_3^- concentrations is erratic and tends to increase following extended exposure to the atmosphere.
- Sulphate concentrations increase after treatment as a result of the addition of $Fe(II)SO_4$ for chromate contamination treatment purposes.

6.5 Geochemical Modelling

The purpose of a reaction path modelling is to trace the evolution of aqueous species, and dissolution and precipitation of mineral species over the course of geochemical processes (Watts et al., 2015). The model was constructed to assess the mobility and reactivity of Cr under reducing conditions in the crystalline aquifer(s) and the treatment system. The following parameters where used:

- Volume of Cr (VI) contaminated groundwater = 130 m^3/day,
- Concentration of Cr (VI) contaminated groundwater = 5 mg/l,
- Average hydrochemistry of extracted groundwater,
- TDS of Cr (VI) contaminated groundwater = 2600 mg/l.

During dosing or treatment a volume of 0.13m^3/day $Fe(II)SO_4$ solution should be added to a volume 100 m^3/day of Cr (VI) contaminated groundwater on a daily basis to allow for reduction of Cr (VI) to Cr (III).

In the GWB the result of simulation of the reaction of the chromate anion (CrO_4^{2-}) with Fe(II) is displayed in terms of CrO_4^{2-} concentration in mg/ℓ in Figure 25. The addition of Fe(II) to Cr(VI) contaminated water is thus effective in reducing Cr(VI) to Cr(III) and precipitating $Cr(OH)_3$. The reaction path for the CrO_4^{2-} (dissolved) to Cr_2O_3 (solid) was modelled in the GWB and the results are displayed in Figure 26 in terms of the Cr-compound speciation during treatment in the Eh-pH stability fields of chromium species.

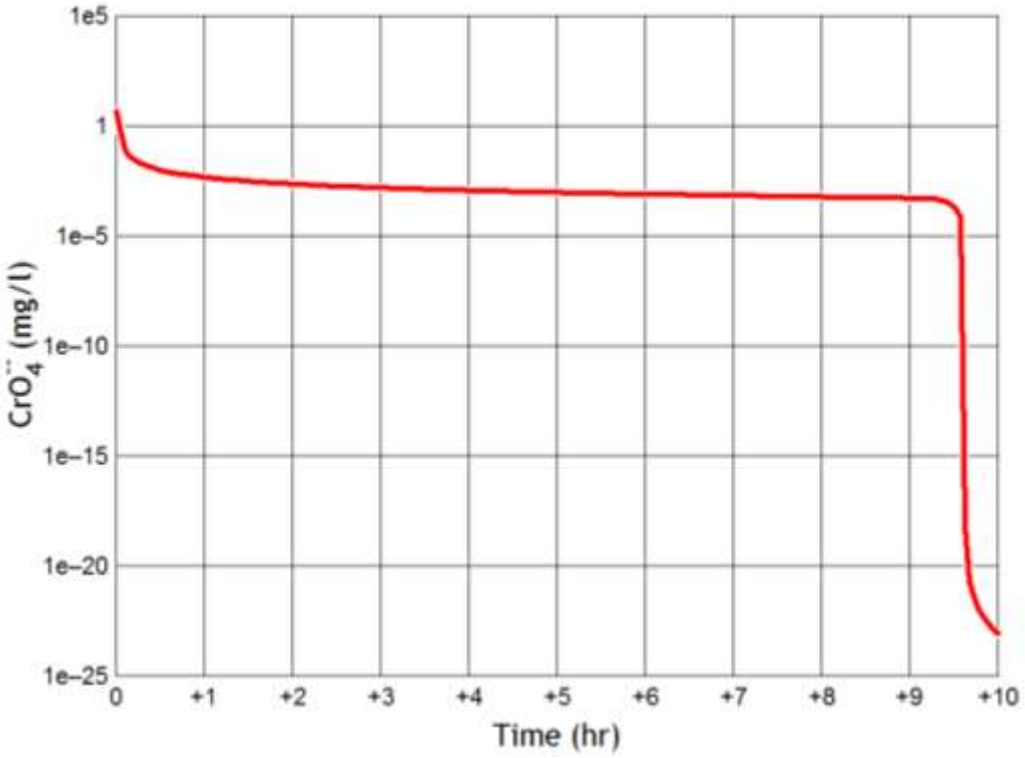


Figure 25: Chemical and mineralogical speciation during treatment (reaction path from CrO_4^{--} aqueous phase to Cr_2O_3 mineral phase).

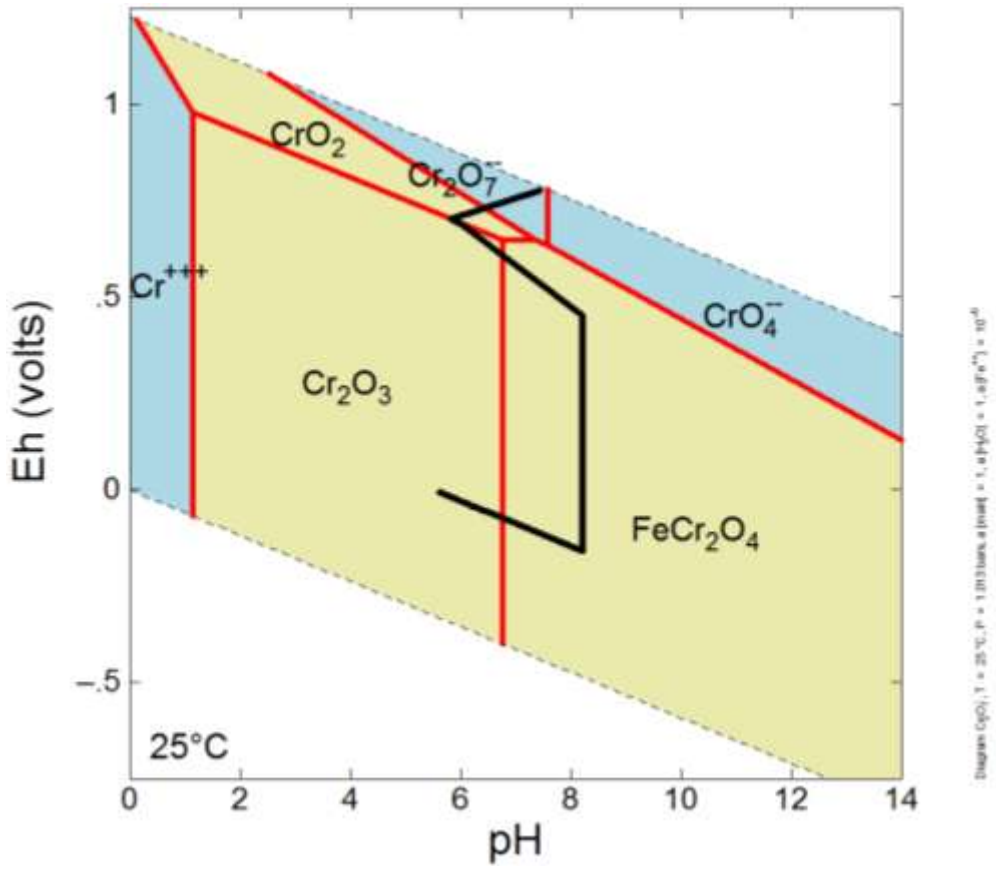


Figure 26: Results of the modelling of the CrO_4^{2-} transition Cr_2O_3 in GWB in terms of chromate concentrations over time.

The simulated reaction path shows that the transformation of CrO_4^{2-} to Cr_2O_3 in the treatment system is not immediate as expected. Each speciation field in the Eh-pH stability diagram represents a different set of reactions (Stanin and Pirnie, 2005). The reaction is irreversible, this is beneficial as the water is abstracted from more reducing conditions, and the treatment is open to atmosphere thus the conditions following dosing with $Fe(II)SO_4$ are oxic and chromate complexes are stable over a wider range of Eh-pH conditions than Cr(III) compounds. This ensures that the efficiency of the dosing system is not reversed in Settling Pond B.

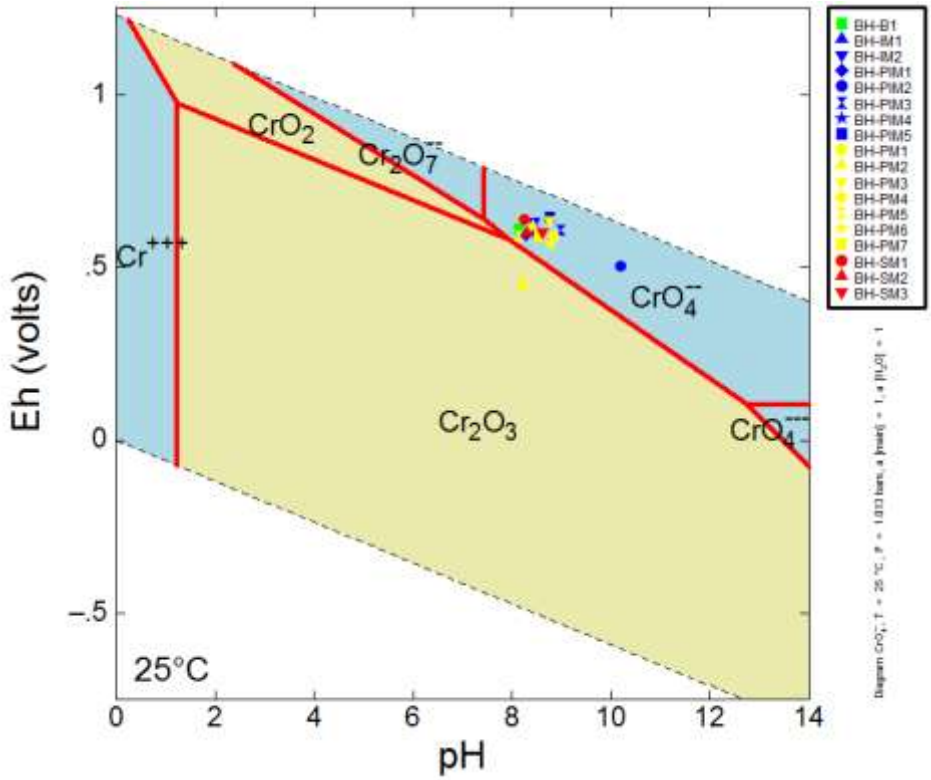


Figure 27: Stability field diagram for Cr species in water at 25°C and 1 atm on Eh and pH axes.

The Eh-pH diagram above (Figure 27) was constructed based on Cr species on the basis that H^+ ions and electrons (e^-) are involved in the aqueous transformations between Cr(III) and Cr(VI). pH determines the influence of the H^+ ions and Eh accounts for the influence of electrons (Robertson, 1975). The majority of the groundwater samples plot in the CrO_4^{2-} stability field Cr(VI) compounds are stable over a wide range of Eh-pH conditions (Stanin and Pirnie, 2005). Cr(VI) is highly soluble at near neutral and alkaline pH waters and can thus be transported over great distances (Stanin and Pirnie, 2005).

6.6 Numerical Modelling

Numerical groundwater modelling is the most commonly used method of simulating groundwater systems (Reilly and Harbaugh, 2004). The aim of the groundwater model is to simulate the groundwater system so as to determine the impact of the PAT system on groundwater flow dynamics, if any. The influence of pumping as part of the PAT system in capturing the chromate plume will be evaluated through modelling flow paths in the plume capture zone.

The numerical model inputs are derived from the CSM of the area under investigation. The CSM simplifies the geological and hydrogeological characteristics of the study area. A clear understanding of aquifer properties and hydrogeological conditions in the study area is used as a guide to accurately represent the *in situ* conditions. The groundwater model was created using the MODFLOW programme in the ModelMuse interface (code).

6.6.1 Assumptions and Limitations

The following assumptions were made during the numerical modelling process:

- A multi-step process is assumed.
- The soil horizon is negligible in modelling groundwater flow paths as the average depth to water level is 8 m.b.g.l.
- Normal faults are modelled as conduits to flow and strike-slip faults as no flow boundaries.
- Streams and rivers are ephemeral and receive a contribution from baseflow.
- The modelled area is part-saturated and mixing between the weathered and fractured aquifers are possible.
- ModelMuse models the unconfined primary aquifer as a convertible aquifer, convertible between a confined and unconfined aquifer.

6.6.2 Boundary Conditions

Groundwater systems are naturally contained by watersheds, hydraulic boundaries and groundwater divides. Boundary conditions are applied in the modelling process to represent *in situ* conditions of mass balance. The concept of mass balance is a fundamental hydrogeological concept to ensure numerical accuracy. In the mass balance approach the net fluxes calculated or specified are compared with changes in storage. Manual calculations may be compared to modelling results to assess the numerical accuracy of the solution. A mass balance error greater than 1% is indicative of modelling or conceptual input errors.

6.6.3 Elevation Data

Elevation data is crucial for developing a credible numerical model, as the groundwater table in its natural state tends to follow topography.

The elevation data was derived from the STRM (Shuttle Radar Tomography Mission) DEM (Digital Elevation Model) database (Rodriguez et al., 2005). The SRTM consisted of a specially modified radar system that flew on-board the Space Shuttle Endeavour during an 11-day mission in February 2000, during which elevation data was obtained on a near-global scale to generate the most complete high-resolution digital topographic database of the earth. Data is available on a grid of 30 metres in the USA and 90 metres in all other areas.

Several studies have been conducted to establish the accuracy of the data, and found that the data is accurate within an absolute error of less than five metres and the random error between 2 and 4 metres for Southern Africa. Over a small area as in this study, the relative error compared to neighbouring point is expected to be less than one metre. This is very good for the purpose of a numerical groundwater model, especially if compared to other uncertainties; and with the wealth of high frequency data collected for the purpose of this study model accuracy is greatly improved.

6.6.4 Aquifer parameters

Although the most relevant aquifer parameters are optimised by the calibration of the model, many parameters are calculated and/or judged by conventional means (Hiscock, 2005). The following fixed assumptions and input parameters were used for the numerical model of this area:

- Recharge = 0.00005 m/d. This value was calculated using the RECHARGE program.
- Evapotranspiration Extinction Depth = 5 m. This depth relates to the expected average root depth of plants in this area.
- The specific storage over the area was taken as 0.000001. This is a typical value for fractured bedrock.
- The effective porosity value of the upper layer was taken as 0.05. This value could not be determined directly and were taken as typical of the fractured anorthosite bedrock (Hiscock 2005).

6.6.5 Calibration of the Model

As the depths to water level were measured during the control monitoring period in the mining and farming area, the numerical model was calibrated using this hydraulic head. The hydraulic conductivity was estimated by manual adjustment. A good fit was obtained for the measured groundwater levels. The final optimised hydraulic conductivities were:

- Horizontal hydraulic conductivity Layer 1= 0.01 m/d
- Horizontal hydraulic conductivity Layer 2= 0.001 m/d
- Horizontal hydraulic conductivity Layer 3= 0.0001 m/d

The horizontal hydraulic conductivity was further decreased by an order of magnitude in each succeeding layer. The calibration graph can be seen in Figure 28. The head error was calculated below 0.8, which can be regarded as acceptable.

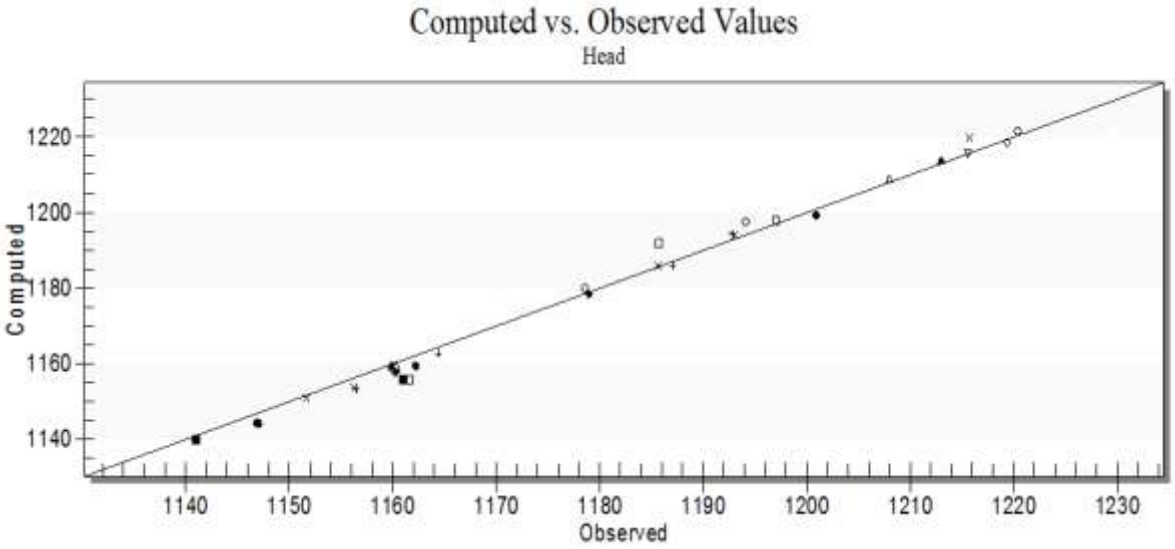


Figure 28: Calibration graph (hydraulic head in m.a.m.s.l.).

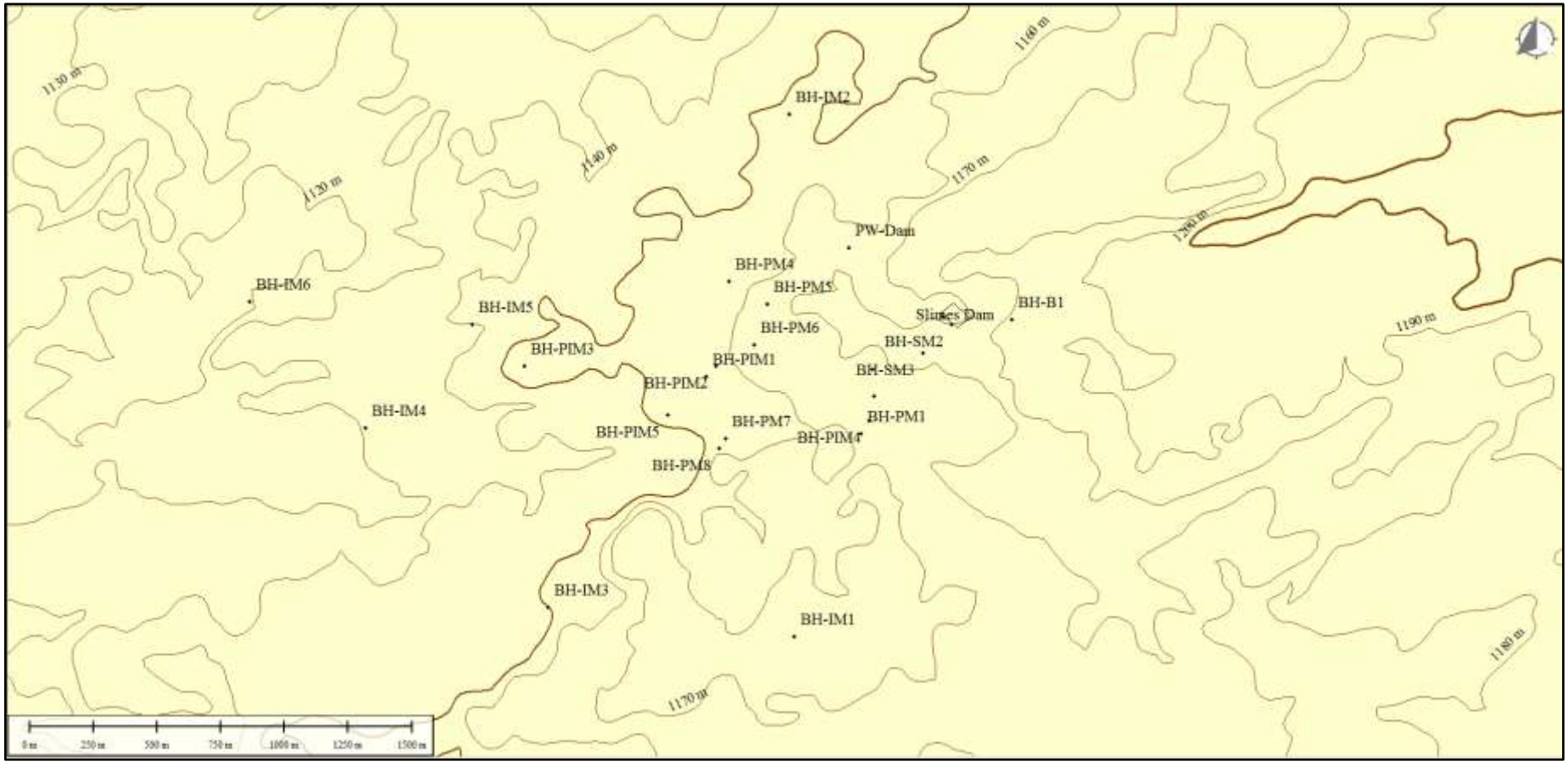


Figure 29: Elevation contours.

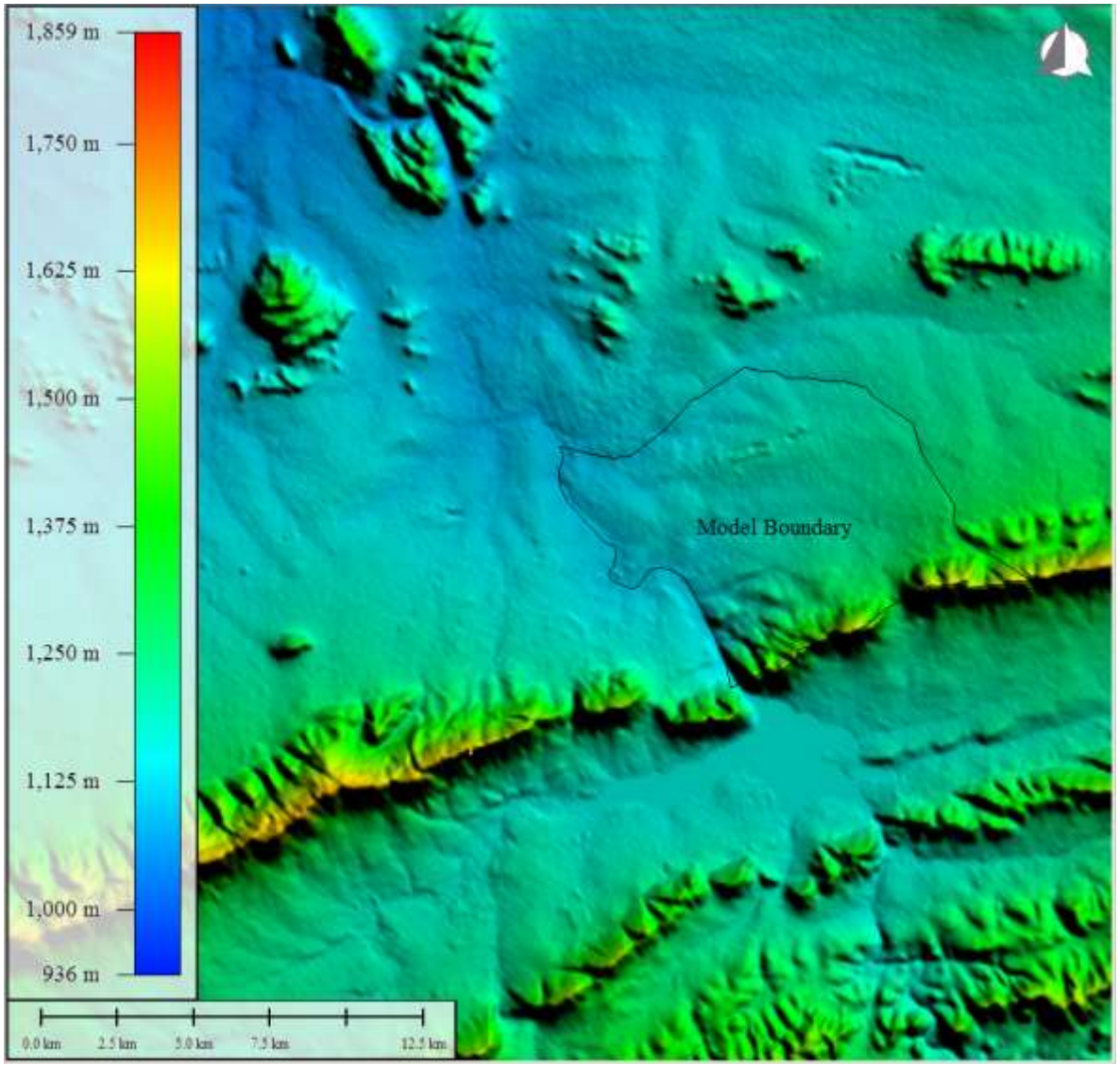


Figure 30: Model boundary.

6.6.6 Groundwater Flow

To obtain an understanding of groundwater flow dynamics in the study area, monitored water levels were used to calibrate the numerical model. Groundwater flow is expected to emulate surface drainage, i.e. flow occurs from topographical high to topographical low areas. High relief areas are generally regarded as recharge areas and groundwater will from recharge areas towards discharge areas such as rivers, streams, pumping boreholes or springs. Mapping of the groundwater table can be useful but will introduce a bias in heterogeneous systems (Cook, 2003). Where, hydraulic gradients tend to be steeper in areas of low permeability and these will dominate groundwater table maps (Cook, 2003). In turn, areas with high conductivity may appear as having shallow gradients while they are responsible for the bulk of groundwater flow (Davis and Putman. 2013).

The aquifers in the study area were conceptualised as an unconfined aquifer whose main source of recharge is precipitation. The modelled flow paths (Figure 31) are similar to the inferred flow vectors (Figure 17) in the targeted area. Fracture flow is the dominant type of flow, the fault zones and dykes create high permeability conduits to flow. Flow paths are parallel to fault lines or the lateral dimensions of dykes; flow occurs along fractures and deformation zones (Bense et al., 2013).

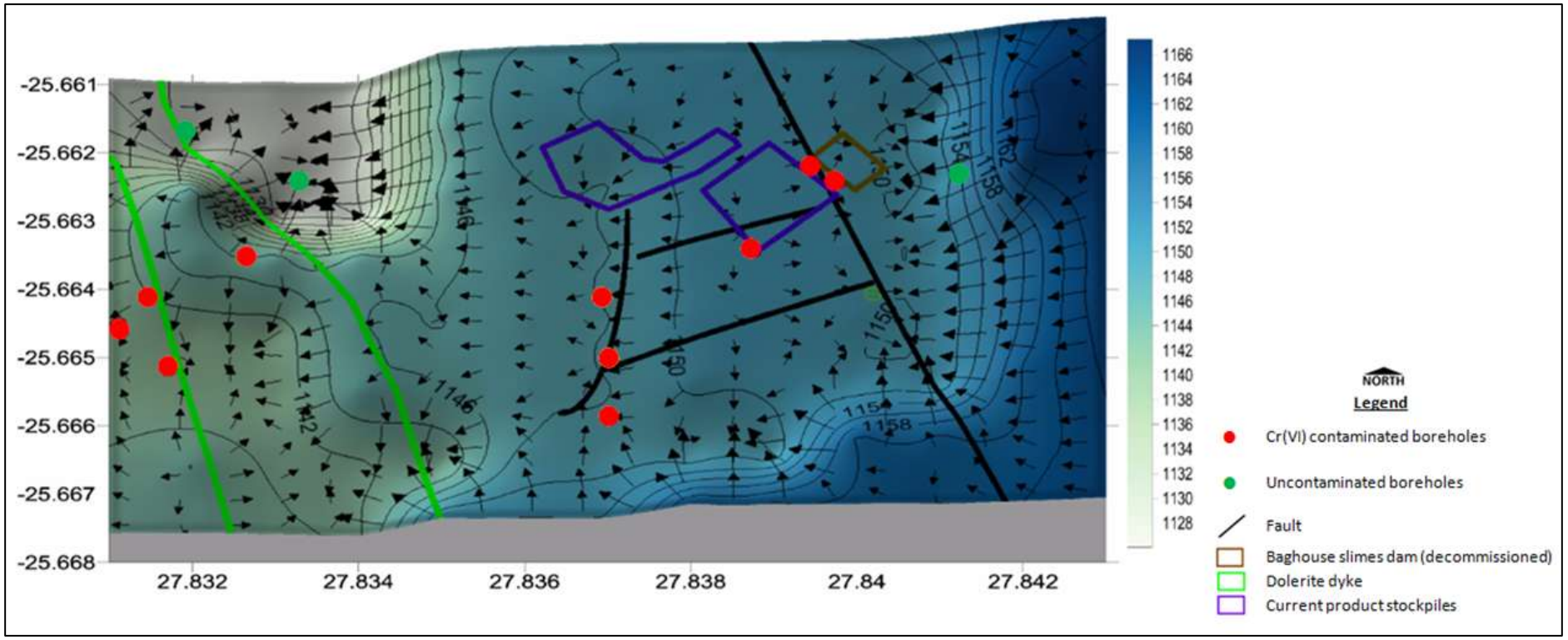


Figure 31: Modelled groundwater head contours showing flow vectors.

7. DISCUSSION

The remedial action was implemented as a risk management measure as the chromate contamination plume had migrated downstream reaching some receptors. To evaluate its efficiency in achieving the short-, medium-, and long-term objectives a SWOT analysis is performed in the subsequent sections. Strengths refer to the advantages and successes of the PAT system; Weaknesses refer to possible improvements that could be implemented to improve efficiency; Opportunities refer to auxiliary benefits that can be gained from the PAT system; Threats refer to obstacles which threaten the success and efficiency of the PAT system.

7.1 Strengths

The PAT system has been successful in reducing Cr(VI) concentrations to below detection limit of the applied analytical technique. The reduction of Cr(VI) concentrations in some of the peripheral sampling points indicates that the PAT system has been successful in capturing the chromate contaminated water through pumping. Groundwater levels have remained more or less stable since the implementation of the PAT system, thus the calculated abstraction rates are sustainable and are not likely to impact groundwater availability negatively. From an engineering perspective, the entire system is able to run automatically. The submersible pumps, dosing systems and PAT pond pumps are fully automated. The settling ponds are equipped with water level sensors that are set up to shut the system down when the settling ponds have reached capacity.

7.2 Weaknesses

The treatment system was designed to treat Cr(VI), other elevated constituents and generally high dissolved ions are not treated in this remedial process. Water with a high TDS and contamination level concentrations of major ions poses a threat to the environment and water users.

7.3 Opportunities

The treatment system was designed to treat Cr(VI), other elevated constituents and generally high dissolved ions are not treated in this remedial process. Instead of storage or disposal of the water treated for Cr(VI) contamination, the water may be used in mineral ore processing, minimising the need to abstract groundwater for processing needs.

7.4 Threats

The plant design was only based on the treatment of Cr(VI), other constituents such as SO_4^{2-}, NO_3^- and generally high salinity could not be treated in this remedial process. Further the addition of SO_4^{2-} and Fe(II) through the action of dosing for Cr(VI) reduction purposes leads to increased SO_4^{2-} in

the treated water. A total of 130 m^3/day (3900 m^3/month) of chromate-contaminated groundwater is abstracted and treated on the surface. The treated water is allowed to settle to allow for the precipitation of $Cr(OH)_3$ following which, the settling pond is emptied and the water is transported to a waste water handling dam and used in the mine. The increase in TDS could result in increased scale build-up in pipes, spray nozzles of wet scrubber systems, and other equipment if the water is used for mine processes. The action of pumping by groundwater users outside of the mine may create flow paths that may affect the efficiency of the PAT system in capturing the chromate plume. The operation of the PAT system needs to be disrupted in order to remove precipitated sludge from the settling ponds. The ponds may need to be fenced off in order to prevent interference from unauthorised mine personnel.

8. CONCLUSIONS

The Cr(VI) contamination originated from leachate due to leakage from a baghouse slimes dam. The contamination plume had migrated off-site reaching privately owned boreholes. This required immediate action and an action plan was developed. Various hydrogeological assessments were conducted after which remedial objectives were formulated and remedial options evaluated according to national regulations. The results of the six-month long monitoring and control exercise for the analysis of a PAT remediation system, show that the system has been successful in chemically treating chromate contamination in the abstracted groundwater.

The hydrogeology of the study area is characterised by a shallow weathered aquifer and a deeper semi-confined fractured bedrock aquifer. In the RLS due to opencast and underground mining operations the water strikes in both aquifers are dewatered at places. The depth of weathering goes up to 15 m.b.g.l. An extensive weathered horizon as well as fracturing and lineaments are characteristic features of crystalline rock aquifers. The effect of erosion and weathering of the BIC improved the groundwater development potential of the shallow weathered aquifer. Crystalline rocks such as the mafic rocks of the RLS will have intact matrix, which accounts for bulk storage of groundwater in the saturated zone. In the deeper-lying secondary aquifer, groundwater flow occurs in a complex fracture network. In the study area, the secondary linear features present are the regional strike-slip fault, a number of normal faults and a major dolerite dyke. The RLS is layered and dips at an average 8° west. Strike-slip faults are regarded as barriers to flow, while normal faults are regarded as conduits to flow. The dolerite dykes are fractured increasing their secondary permeability. They outcrop east of the pollution plume and are 10 m thick.

The PAT infrastructure consists of three abstraction boreholes equipped with low-flow rate pumps; two settling ponds (pre-treatment and post-treatment); one dosing pump; two tanks storing and transmitting aqueous $Fe(II)SO_4$ to the dosing pump. Groundwater quality remediation is expected to

occur over relatively long period of time. The PAT system was implemented as a medium-term strategy to intercept the Cr(VI) contamination plume during migration to prevent it from impacting on groundwater users downstream of the mine.

A comparison of the water levels (m b.g.l.) measured over the control monitoring period showed that water levels in the study area have over the entire monitoring period declined, due to the influence of pumping for treatment and irrigation. In the vicinity of the three PAT system's abstraction boreholes, the water levels in the wells have declined by an average of 2 m compared to the same period in 2014. Periodical fluctuations in the fractured aquifer are reflective of the influence of fractures on groundwater flow.

In the mining area sodium and sulphate enrichment is attributed to the impact of chemical extraction from ores, waste water discharge and dewatering of the mine. Chloride enrichment is attributed to leachate from domestic waste and dewatering of the mine. Bicarbonate and magnesium enrichment are indicative of recently recharged water. The groundwater samples plot in the mixing area of the quadrilateral diagram showing evidence of mixing between the primary and secondary aquifers. In the treatment ponds, settling pond A is of a bicarbonate type as the water is exposed to the atmosphere; while settling pond B is enriched in sulphate due to the addition of $Fe(II)SO_4$ for treatment purposes.

The majority of the groundwater samples are indicative of fresh recharge following precipitation; some are indicative of recharge following fractionation during cooler temperatures (in winter) and some were affected by evaporation losses. The treatment ponds show different $\delta^{18}O$ and $\delta^{2}H$ ratios due to higher evaporation losses in Settling Pond B, due to higher residence times of the treated water before it is transferred from the pond to a wastewater dam. The majority of the groundwater samples, from the shallow primary and deep fractured aquifers plot in the same cluster, which is indicative of mixing of waters between the aquifers. The majority of the samples have a higher tritium activity than the local average in rainfall. In the study area high tritium activity is attributed to contaminated mine water and agricultural return flows.

The dosing system has been successful in reducing Cr(VI) to Cr(III) and precipitating $Cr(OH)_3$. The treatment system was designed to treat Cr(VI), other elevated constituents and generally high dissolved ions are not treated in this remedial process. A period of no treatment of Cr(VI) as seen through a concentration higher than the 0 mg/ℓ as intended occurred on 26-May-2015. This was caused by operation error dosing solution was not refilled in time and no treatment by reduction by aqueous Fe(II) occurred. Some treatment may have occurred due to the action of chromite ore precipitating Cr(III) minerals in the treatment ponds. Sulphate concentrations increase after treatment as a result of the addition of $Fe(II)SO_4$ for chromate contamination treatment purposes.

A geochemical model was constructed to assess the mobility and reactivity of Cr under reducing conditions in the crystalline aquifer(s) and the treatment system. Groundwater flow was modelled numerically and the modelled flow vectors are similar to the contoured water level flow vectors indicating that the PAT wellfield has not negatively impacted on groundwater availability.

The simulated reaction path shows that the transformation of CrO_4^{2-} to Cr_2O_3 in the treatment system is not immediate as expected. The reaction is irreversible, this is beneficial as the water is abstracted from more reducing conditions, and the treatment is open to atmosphere thus the conditions following dosing with $Fe(II)SO_4$ are oxic and chromate complexes are stable over a wider range of Eh-pH conditions than Cr(III) compounds. This ensures that the efficiency of the dosing system is not reversed in Settling Pond B. The modelled flow paths are similar to the inferred flow vectors in the plume capture zone. Fracture flow is the dominant type of flow, the fault zones and dykes create high permeability conduits to flow. Flow paths parallel to fault lines or the lateral dimension of dykes; flow occurs along fractures and deformation zones.

The PAT system has been successful in reducing Cr(VI) concentrations to below detection limit of the applied analytical technique. The reduction of Cr(VI) concentrations in some of the peripheral sampling points indicates that the PAT system has been successful in capturing the chromate contaminated water through pumping. Groundwater levels have remained more or less stable since the implementation of the PAT system, thus the calculated abstraction rates are sustainable and are not likely to impact groundwater availability negatively. From an engineering perspective, the entire system is able to run automatically. The submersible pumps, dosing systems and PAT pond pumps are fully automated. The settling ponds are equipped with water level sensors that are set up to shut the system down when the settling ponds have reached capacity.

The treatment system was designed to treat Cr(VI), other elevated constituents and generally high dissolved ions are not treated in this remedial process. Water with a high TDS and contamination level concentrations of major ions poses a threat to the environment and water users. The increase in TDS could result in increased scale build-up in pipes, spray nozzles of wet scrubber systems, and other equipment if the water is used for mine processes.

9. RECOMMENDATIONS

Taking into account the strengths and weaknesses of the PAT system as a medium-term remedial measure, a long-term strategy must be developed and monitoring must be maintained. There is currently no flow metering to keep track of the volumes of water that pass through the system. Groundwater remediation needs to address the pollution plume as well as the source, there exists an opportunity for the addition of aqueous $Fe(II)SO_4$ to the baghouse slimes dam. Even though the slimes dam has been decommissioned and the leaching through the action of rainwater has been prevented through secondary containment; the treatment by aqueous $Fe(II)SO_4$ will ensure that the accidental leachate is not contaminated with toxic Cr(VI) concentrations.

The extent of the chromate plume is considerably extensive and the development of the PAT wellfield by the addition of other boreholes as abstraction boreholes. Proximal pumping by groundwater users downstream of the mine needs to be quantified through a hydrocensus study detailing groundwater mining and potential receptors within a 2 km radius. The action of pumping by groundwater users outside of the mine may create flow paths that may affect the efficiency of the PAT system in capturing the chromate plume. The extent of the plume vertically and laterally needs to be delineated with the aid of aeromagnetic surveying over the mine and surrounding areas, to map the chromate plume and determine the wellfield development potential. A wellfield downstream of an operating mine serves as a mitigating measure to prevent contamination emanating from the mine from reaching sensitive receptors, such as ecosystems, groundwater users, rivers and their aquatic biota.

Reference list

Abiye, T.A., Mengistu, H., Masindi, K., and Demlie, M. (2015). Surface Water and Groundwater Interaction in the Upper Crocodile River Basin, Johannesburg, South Africa: Environmental Isotope Approach. *South African Journal of Geology* 118.2: 109 – 118.

Barcelona, M. J. (2005). Development and Applications of Groundwater Remediation Technologies in the USA. *Hydrogeology Journal* 13: 288 – 294.

Bense, V. F., Gleeson, T., Loveless, S. E., Bour, O., and Scibek, J. (2013). Fault Zone Hydrogeology. *Earth-Science Reviews* 127:171-12.

Beukes, J. P., Dawson, N. F., and van Zyl, P. G. (2010). Theoretical and practical aspects of Cr(VI) in the South African ferrochrome industry. *The Journal of the South African Institute of Mining and Metallurgy* 10: 743-750.

Cawthorn, G. R. (1999). The Platinum and Palladium Resources of the Bushveld Complex. *South African Journal of Science* 95:481 - 489.

Clark, I. And Fritz, P. (1997). Environmental Isotopes in Hydrogeology. Lewis Publishers. – 328 pp.

Clarke, B., Uken, R., and Reinhardt, J. (2008). Structural and Compositional Constraints on the Emplacement of the Bushveld Complex, South Africa. *Lithos* 111: 21 – 36.

Cole, J., Webb, S. J., and Finn, C. A. (2014). Gravity Models of the Bushveld Complex – Have we Come Full Circle? *Journal of African earth Sciences* 92: 97 – 118.

Cook, P. G. (2003). A Guide to Regional Groundwater Flow in Fractured Rock Aquifers. *CM Digital, Adelaide, Australia*. -115 pp.

Craig, H. (1961). Isotopic variations in meteoric waters. *Science,* 133: 1702 – 1703.

Davis, K. W., and Putnam, L. D. (2013). Conceptual and Numerical Models of Groundwater Flow in the Ogallala Aquifer in Gregory and Tripp Counties, South Dakota, Water Years 1985 – 2009. *Scientific Investigations Report* 2013 – 5069 pp.

Dossing, L. N., Dideriksen, K., Stipp, S. L. S., and Frei, R. (2011). Reduction of Hexavalent Chromium by Ferrous Iron: A Process of Chromium Isotope Fractionation and its Relevance to Natural Environments. *Chemical Geology* 285: 157 – 166.

Du Plessis, C. P. And Walvaren, F. (1990). The tectonic setting of the Bushveld Complex in Southern Africa, Part 1: Structural Deformation and Distribution. *Tectonophysics* 179: 305 – 319.

Department of Water Affairs and Forestry (DWAF). (1996). South African Water Quality Guidelines (Second Edition). Volume 1: Domestic Use, edited by Holmes, S., Council for Scientific and Industrial Research, Pretoria. – 214 pp.

Department of Water Affairs and Forestry (DWAF). (1998). Minimum Requirements for the Handling, Classification and Disposal of Hazardous Waste, Second Edition. Pretoria. The Waste Management Series, - 171 pp.

Department of Water and Sanitation (DWA). (2015). Hydrological Services - Surface Water (Data, Dams, Floods and Flows). Pretoria. 1 screen. Available online. Accessed on April 2015.

Economou-Eliopoulos, M., Antivachi, D., Vasilatos, C., and Megremi, I. (2011). Evaluation of the Cr(VI) and other toxic element contamination and their potential sources: The case of the Thiva Basin (Greece). *Geoscience Frontiers* 3(4): 523 – 539.

Fenglian, F., and Wang, Q. (2011). Removal of heavy metal ions from wastewaters: A review. *Journal of Environmental Management* 92: 407 – 418.

Fulton, J. W., Koerkle, E. H., McAuley, S. D., Hoffman, S. A., and Zarr, L. F. (2005). Hydrogeologic Setting and Conceptual Hydrologic Model of the Spring Creek Basin, Centre County, Pennsylvania. Scientific Investigations Report 2005-5091, - 91 pp.

Geo Pollution Technologies. (2013). Remediation Action Plan. Technical Report. Unpublished.

Geyh, M. (2000). Environmental Isotopes in the Hydrgeological Cycle - Principles and Applications Vol. 4: Groundwater – Saturated and Unsaturated Zone. *Water Resources Programme, International Atomic Energy Agency.* Hannover, - 309 pp.

Guertin, J. (2005). Toxicity and Health Effects of Chromium (All Oxidation States). The Chromium Handbook: Chapter 6: 214 – 232. CRC Press. New York.

Hashim, M. A., Mukhopadhyay, S., Sahu, J. N., and Sengupta, B. (2011). Remediation Technologies for Heavy Metal Contaminated Groundwater. *Journal of Environmental Management* 92: 2355 – 2388.

Hauley, E. L., Deeb, R. A., Michael, C. K., and Jacobs, J. R. G. (2005). Treatment Technologies for Chromium(VI). The Chromium Handbook: Chapter 8: 274 – 308.

Hiscock, K. M. (2005). Hydrogeology: Principles and Practice. Blackwell Science Ltd. Oxford. -405 pp.

International Chromium Development Association (ICDA). (2015). What is Chrome (Internet). Paris. 1 screen. Available online. Accessed on 27 April 2015.

Kitchen, J. W., Johnson, T. M., Bullen, T. D., Zhu, J., and Raddatz, A. (2012). Chromium isotope fractionation factors for reduction of Cr(VI) by aqueous Fe(II) and organic molecules. *Geochemica et Cosmochimica Acta* 89: 190 - 201.

Manahan, S. E. (2000) Environmental Science, Technology and Chemistry. *Environmental Chemistry, - 743 pp.* Boca Raton: CRC Press LLC.

van der Merwe, J. And Cawthorn, R. G. (2005). Structures at the Base of the Upper Group 2 Chromitite Layer, Bushveld Complex, South Africa, on Karee Mine (Lonmin Platinum). *Lithos* 83: 214 – 228.

Motzer, W. E and Todd Engineers. (2005). Chemistry, Geochemistry, and Geology of Chromium and Chromium Compounds. The Chromium Handbook: Chapter 2: 23 - 77. CRC Press. New York.

Mukhopadhyay, B., Sundquist, J., and White, E. (2007). Hydro-geochemical Controls on Removal of Cr(VI) from Contaminated Groundwater by Anion Exchange. *Applied Geochemistry* 22: 370 – 387.

Mustafa, S., Bahar, A., Abdul Aziz, Z., and Suratman, S. (2015). Modelling Contaminant Transport for Pumping Wells in Riverbank Filtration Systems. *Journal of Environmental Management* 165: 159 – 166.

Reilly, T. E., and Harbaugh, A. W. (2004). Guidelines for Evaluating Ground-water Flow Models: *U. S. Geological Survey Scientific Report* 2004-5038, 30 pp.

River Health Programme. (2005). State of Rivers Report: Monitoring and Managing the Ecological State of Rivers in the Crocodile (West)-Marico Water Management Area. *Department of Environmental Affairs and Tourism, Pretoria. State-of-Rivers Report 9.* 159 pp.

Robertson, F. N. (1975). Hexavalent Chromium in the Ground Water in Paradise Valley, Arizona. *Ground Water,* Vol.13, No. 6: 516 – 527.

Rodriguez, E., Morris, C. S., Belz, J. Chapin, E., Martin, J., Daffer, W., and Hensley, S. (2005). An Assessment of the SRTM Topographic Products. *Technical Report JPL D-31639,* Jet Propulsion Laboratory, Pasadena, California.

Schaffer, J., and Herman, C. (2015). Reactions in Aqueous Solutions: Precipitation Reactions. Online. Accessed on 7 July 2015.

Singhal, B. B. S., and Gupta, R. P. (2010) Applied Hydrogeology of Fractured Rocks, Ed. 2. Springer. Dordrecht. - 429 pp.

Stanin, F. T. and Pirnie, M. (2005). The Transport and Fate of Cr(VI) in the Environment. The Chromium Handbook: Chapter 5: 161 - 211. CRC Press. New York.

Theis, T. L., O'Carroll, D. M., Vogel, D. C., Lane, A. B., and Collins, K. (2003). Systems Analysis of Pump-and-Treat Groundwater Remediation. *Practice Periodical of Harzardous, Toxic and Radioactive Waste Management, 7,* No. 3: 177 - 188.

Titus, R., Witthüser, K. and Walters, B. (2009). Groundwater and Mining in the Bushveld Complex. International Mine Water Conference, 2009 October 19 – 23, Pretoria, South Africa. Document Transformation Technologies cc, ISBN Nr.: 978-0-9802623-5-3: 178 – 184.

Trois, C., Marcello, A., Pretti, S., Trois, P., and Rossi, G. (2006). The Environmental Risk Posed by Small Dumps of Complex Arsenic, Antimony, Nickel and Cobalt Sulphides. *Journal of Geochimical Exploration* 92: 83 – 95.

Wanner, C., Eggenberger, U., Kurz, D., and Mader, U. (2011). Reactive transport modelling of Cr(VI) treatment by cast iron under fast flow conditions. *Applied Geochemistry* 26: 1513 – 1523.

Wanner, C., Eggenberger, U., Kurz, D., Zink, S., and Mader, U. (2012). A chromate-contaminated site in southern Switzerland – Part 1: Site characterisation and the use of Cr isotopes to delineate fate and transport. *Applied Geochemistry* 27: 644 – 654.

Watts, M. P., Coker, V. S., Parry, S. A., Thomas, R. A. P., Kalin, R, and Lloyd, J. R. (2015). Effective treatment of alkaline Cr(VI) contaminated leachate using a novel Pd-bionanocatalyst: Impact of electron donor and aqueous geochemistry. *Applied Catalysts B: Environmental* 170-171: 162 - 172.

West, A. G., February, E. C., and Bowen, G. J. (2014). Spatial Analysis of Hydrogen and Oxygen Stable Isotopes ("Isoscapes") in Groundwater and tap water across South Africa. *Journal of Geochemical Exlploration* 145: 213 – 222.

Zingg, A. J. (1996). Recrystallization and the origin of layering in the Bushveld Complex. *Lithos* 37: 15 37.

APPENDIX I: Analytical Data

SiteName	Date	pH	EC mS/m	TDS mg/l	Ca mg/l	Mg mg/l	Na mg/l	K mg/l	MALK mg/l	Cl mg/l	SO4 mg/l	NO3-N mg/l
BH-B1	29-Jan-15	7.50	284.0	1949.0	76.0	278.00	219.00	3.60	948.0	217.0	573.0	3.10
BH-B1	30-Apr-15	7.50	281.0	1890.0	81.0	294.00	203.00	4.60	968.0	209.0	504.0	3.00
BH-B1	30-Jul-15	7.60	252.0	2 010	105.0	356.00	184.00	5.40	940.0	208.0	576.0	2.60
BH-IM1	29-Jan-15	9.00	96.4	508.0	29.0	0.00	144.00	0.00	20.0	241.0	79.0	0.00
BH-IM1	30-Apr-15	8.90	100.0	510.0	29.0	3.00	155.00	0.00	20.0	248.0	62.0	0.00
BH-IM1	30-Jul-15	9.00	96.60	509.00	29.00	2.00	140.00	0.00	20.00	249.00	77.00	0.00
BH-IM2	29-Jan-15	7.90	178.0	1183.0	76.0	162.00	79.00	0.00	468.0	143.0	295.0	33.00
BH-IM2	30-Apr-15	7.80	182.0	1216.0	79.0	177.00	80.00	0.00	476.0	146.0	297.0	34.00
BH-IM2	30-Jul-15	7.80	172.00	1 286	82.00	172.00	78.00	0.00	456.00	146.00	357.00	40.00
BH-PIM2	29-Jan-15	7.70	186.0	1267.0	74.0	230.00	36.00	1.80	572.0	164.0	404.0	3.20
BH-PIM2	30-Apr-15	7.60	202.0	1271.0	57.0	265.00	23.00	0.00	524.0	178.0	411.0	4.80
BH-PIM2	30-Jul-15	7.80	185.0	1 217	63.0	226.00	31.00	4.20	648.0	168.0	316.0	2.10
BH-PIM3	29-Jan-15	8.30	104.0	631.0	37.0	97.00	33.00	0.00	380.0	92.0	100.0	9.80
BH-PIM3	30-Apr-15	8.10	102.0	633.0	40.0	100.00	37.00	0.00	388.0	92.0	86.0	10.00
BH-PIM3	30-Jul-15	8.20	105.0	648.0	39.0	101.00	36.00	0.00	352.0	99.0	108.0	12.00
BH-PIM4	29-Jan-15	8.10	56.6	343.0	42.0	19.00	41.00	7.90	152.0	57.0	77.0	1.70
BH-PIM4	30-Apr-15	7.50	191.0	1241.0	79.0	188.00	86.00	1.50	576.0	140.0	299.0	23.00
BH-PIM4	30-Jul-15	8.40	56.70	331.00	41.00	18.00	43.00	8.50	140.00	52.00	73.00	4.00
BH-PIM5	29-Jan-15	8.00	88.0	521.0	23.0	84.00	35.00	0.00	372.0	71.0	74.0	2.30
BH-PIM5	30-Apr-15	7.90	87.4	501.0	24.0	89.00	40.00	0.00	356.0	65.0	57.0	2.50
BH-PIM5	30-Jul-15	8.10	82.90	475.00	23.00	82.00	24.00	0.00	332.00	62.00	73.00	2.60
BH-PM1	29-Jan-15	7.70	109.0	675.0	64.0	101.00	36.00	3.20	560.0	39.0	96.0	0.00
BH-PM1	30-Apr-15	7.60	121.0	755.0	62.0	124.00	43.00	2.60	604.0	53.0	104.0	1.00
BH-PM1	30-Jul-15	8.00	114.00	785.00	62.00	137.00	47.00	2.20	604.00	49.00	123.00	0.50
BH-PM2	29-Jan-15	7.70	219.0	1559.0	88.0	205.00	115.00	1.10	460.0	200.0	532.0	32.00
BH-PM2	30-Jul-15	8.50	228.0	1584.0	108.0	144.00	196.00	33.00	388.0	195.0	542.0	30.00
BH-PM3	29-Jan-15	7.70	219.0	1559.0	88.0	205.00	115.00	1.10	460.0	200.0	532.0	32.00
BH-PM3	30-Jul-15	8.50	228.0	1584.0	108.0	144.00	196.00	33.00	388.0	195.0	542.0	30.00
BH-PM4	29-Jan-15	7.30	221.0	1496.0	163.0	113.00	166.00	1.60	176.0	284.0	663.0	0.00
BH-PM4	30-Apr-15	7.20	212.0	1354.0	122.0	115.00	188.00	2.10	84.0	285.0	591.0	0.20
BH-PM4	30-Jul-15	7.20	210.0	1 508	127.0	110.00	172.00	2.00	88.0	297.0	746.0	0.00
BH-PM5	29-Jan-15	7.30	194.0	1411.0	161.0	149.00	76.00	0.00	400.0	176.0	484.0	28.00
BH-PM5	30-Apr-15	7.30	246.0	1632.0	222.0	204.00	88.00	0.00	440.0	229.0	604.0	4.50
BH-PM5	30-Jul-15	7.60	222.0	1 798	245.0	191.00	89.00	0.00	356.0	244.0	795.0	4.50
BH-PM6	29-Jan-15	7.60	204.0	1484.0	134.0	198.00	66.00	0.00	464.0	178.0	496.0	30.00
BH-PM6	30-Apr-15	7.50	206.0	1434.0	132.0	208.00	52.00	1.10	460.0	184.0	448.0	30.00
BH-PM6	30-Jul-15	7.90	193.0	1 549	146.0	223.00	58.00	1.40	444.0	191.0	530.0	30.00
BH-PM7	29-Jan-15	7.60	138.0	854.0	19.0	156.00	55.00	0.00	596.0	71.0	141.0	12.00
BH-PM7	30-Apr-15	7.60	142.0	870.0	20.0	168.00	57.00	0.00	568.0	87.0	134.0	14.00
BH-PM7	30-Jul-15	7.90	137.0	876.0	18.0	167.00	51.00	0.00	532.0	98.0	161.0	14.00

SiteName	Date	pH	EC mS/m	TDS mg/l	Ca mg/l	Mg mg/l	Na mg/l	K mg/l	MALK mg/l	Cl mg/l	SO4 mg/l	NO3-N mg/l
BH-B1	29-Jan-15	7.50	284.0	1949.0	76.0	278.00	219.00	3.60	948.0	217.0	573.0	3.10
BH-B1	30-Apr-15	7.50	281.0	1890.0	81.0	294.00	203.00	4.60	968.0	209.0	504.0	3.00
BH-B1	30-Jul-15	7.60	252.0	2 010	105.0	356.00	184.00	5.40	940.0	208.0	576.0	2.60
BH-IM1	29-Jan-15	9.00	96.4	508.0	29.0	0.00	144.00	0.00	20.0	241.0	79.0	0.00
BH-IM1	30-Apr-15	8.90	100.0	510.0	29.0	3.00	155.00	0.00	20.0	248.0	62.0	0.00
BH-IM1	30-Jul-15	9.00	96.60	509.00	29.00	2.00	140.00	0.00	20.00	249.00	77.00	0.00
BH-IM2	29-Jan-15	7.90	178.0	1183.0	76.0	162.00	79.00	0.00	468.0	143.0	295.0	33.00
BH-IM2	30-Apr-15	7.80	182.0	1216.0	79.0	177.00	80.00	0.00	476.0	146.0	297.0	34.00
BH-IM2	30-Jul-15	7.80	172.00	1 286	82.00	172.00	78.00	0.00	456.00	146.00	357.00	40.00
BH-PIM2	29-Jan-15	7.70	186.0	1267.0	74.0	230.00	36.00	1.80	572.0	164.0	404.0	3.20
BH-PIM2	30-Apr-15	7.60	202.0	1271.0	57.0	265.00	23.00	0.00	524.0	178.0	411.0	4.80
BH-PIM2	30-Jul-15	7.80	185.0	1 217	63.0	226.00	31.00	4.20	648.0	168.0	316.0	2.10
BH-PIM3	29-Jan-15	8.30	104.0	631.0	37.0	97.00	33.00	0.00	380.0	92.0	100.0	9.80
BH-PIM3	30-Apr-15	8.10	102.0	633.0	40.0	100.00	37.00	0.00	388.0	92.0	86.0	10.00
BH-PIM3	30-Jul-15	8.20	105.0	648.0	39.0	101.00	36.00	0.00	352.0	99.0	108.0	12.00
BH-PIM4	29-Jan-15	8.10	56.6	343.0	42.0	19.00	41.00	7.90	152.0	57.0	77.0	1.70
BH-PIM4	30-Apr-15	7.50	191.0	1241.0	79.0	188.00	86.00	1.50	576.0	140.0	299.0	23.00
BH-PIM4	30-Jul-15	8.40	56.70	331.00	41.00	18.00	43.00	8.50	140.00	52.00	73.00	4.00
BH-PIM5	29-Jan-15	8.00	88.0	521.0	23.0	84.00	35.00	0.00	372.0	71.0	74.0	2.30
BH-PIM5	30-Apr-15	7.90	87.4	501.0	24.0	89.00	40.00	0.00	356.0	65.0	57.0	2.50
BH-PIM5	30-Jul-15	8.10	82.90	475.00	23.00	82.00	24.00	0.00	332.00	62.00	73.00	2.60
BH-PM1	29-Jan-15	7.70	109.0	675.0	64.0	101.00	36.00	3.20	560.0	39.0	96.0	0.00
BH-PM1	30-Apr-15	7.60	121.0	755.0	62.0	124.00	43.00	2.60	604.0	53.0	104.0	1.00
BH-PM1	30-Jul-15	8.00	114.00	785.00	62.00	137.00	47.00	2.20	604.00	49.00	123.00	0.50
BH-PM2	29-Jan-15	7.70	219.0	1559.0	88.0	205.00	115.00	1.10	460.0	200.0	532.0	32.00
BH-PM2	30-Jul-15	8.50	228.0	1584.0	108.0	144.00	196.00	33.00	388.0	195.0	542.0	30.00
BH-PM3	29-Jan-15	7.70	219.0	1559.0	88.0	205.00	115.00	1.10	460.0	200.0	532.0	32.00
BH-PM3	30-Jul-15	8.50	228.0	1584.0	108.0	144.00	196.00	33.00	388.0	195.0	542.0	30.00
BH-PM4	29-Jan-15	7.30	221.0	1496.0	163.0	113.00	166.00	1.60	176.0	284.0	663.0	0.00
BH-PM4	30-Apr-15	7.20	212.0	1354.0	122.0	115.00	188.00	2.10	84.0	285.0	591.0	0.20
BH-PM4	30-Jul-15	7.20	210.0	1 508	127.0	110.00	172.00	2.00	88.0	297.0	746.0	0.00
BH-PM5	29-Jan-15	7.30	194.0	1411.0	161.0	149.00	76.00	0.00	400.0	176.0	484.0	28.00
BH-PM5	30-Apr-15	7.30	246.0	1632.0	222.0	204.00	88.00	0.00	440.0	229.0	604.0	4.50
BH-PM5	30-Jul-15	7.60	222.0	1 798	245.0	191.00	89.00	0.00	356.0	244.0	795.0	4.50
BH-PM6	29-Jan-15	7.60	204.0	1484.0	134.0	198.00	66.00	0.00	464.0	178.0	496.0	30.00
BH-PM6	30-Apr-15	7.50	206.0	1434.0	132.0	208.00	52.00	1.10	460.0	184.0	448.0	30.00
BH-PM6	30-Jul-15	7.90	193.0	1 549	146.0	223.00	58.00	1.40	444.0	191.0	530.0	30.00
BH-PM7	29-Jan-15	7.60	138.0	854.0	19.0	156.00	55.00	0.00	596.0	71.0	141.0	12.00
BH-PM7	30-Apr-15	7.60	142.0	870.0	20.0	168.00	57.00	0.00	568.0	87.0	134.0	14.00
BH-PM7	30-Jul-15	7.90	137.0	876.0	18.0	167.00	51.00	0.00	532.0	98.0	161.0	14.00

SiteName	Date	F mg/l	Fe mg/l	NH3 mg/l	Cr mg/l	Cr6+ mg/l	Zn mg/l	As mg/l
BH-B1	29-Jan-15	0.200	0.174	0.2	-1.000	0.000	0	0
BH-B1	30-Apr-15	0.000	0	0	0.000	0.017	0	0.012
BH-B1	30-Jul-15	0.200	0.258	0.2	0.000	0.000	0	0
BH-IM1	29-Jan-15	1.800	0	0	-1.000	0.000	0	0
BH-IM1	30-Apr-15	1.400	0.027	0	0.000	0.000	0	0
BH-IM1	30-Jul-15	1.60	0.00	0.00	0.000	0.000	0	0
BH-IM2	29-Jan-15	0.000	0.039	0	-1.000	0.000	0	0
BH-IM2	30-Apr-15	0.000	0.052	0	0.000	0.000	0	0
BH-IM2	30-Jul-15	0.00	0.06	0.00	0.000	0.000	0.041	0
BH-PIM2	29-Jan-15	0.000	15	2	-1.000	0.000	0	0
BH-PIM2	30-Apr-15	0.000	0.306	0.7	0.948	0.899	0	0
BH-PIM2	30-Jul-15	0.000	17	11	0.120	0.000	0	0
BH-PIM3	29-Jan-15	0.000	0	0.4	-1.000	0.016	0	0
BH-PIM3	30-Apr-15	0.000	0	0.2	0.000	0.000	0.034	0
BH-PIM3	30-Jul-15	0.000	0.142	0	0.000	0.021	0	0
BH-PIM4	29-Jan-15	0.200	0	0.3	-1.000	0.000	0	0
BH-PIM4	30-Apr-15	0.000	0	0	0.612	0.598	0	0
BH-PIM4	30-Jul-15	0.20	0.05	0.00	0.000	0.000	0	0
BH-PIM5	29-Jan-15	0.000	0	0	-1.000	0.000	0	0
BH-PIM5	30-Apr-15	0.000	0	0	0.000	0.000	0	0
BH-PIM5	30-Jul-15	0.20	0.00	0.00	0.000	0.000	0	0
BH-PM1	29-Jan-15	0.000	3.93	0.2	-1.000	0.000	0	0
BH-PM1	30-Apr-15	0.000	0.691	0.3	0.000	0.000	0	0
BH-PM1	30-Jul-15	0.00	15.00	0.00	0.000	0.000	0	0
BH-PM2	29-Jan-15	0.000	0.072	0	-1.000	1.590	0	0.012
BH-PM2	30-Jul-15	0.600	0.0	0.2	1.780	1.780	0	0
BH-PM3	29-Jan-15	0.000	0.072	0	-1.000	1.590	0	0.012
BH-PM3	30-Jul-15	0.600	0.0	0.2	1.780	1.780	0	0
BH-PM4	29-Jan-15	0.200	31	0.5	-1.000	0.000	0	0
BH-PM4	30-Apr-15	0.000	31	1	0.000	0.000	0.052	0
BH-PM4	30-Jul-15	0.000	21	1	0.000	0.000	0	0
BH-PM5	29-Jan-15	0.000	0.307	0	-1.000	0.647	0	0.023
BH-PM5	30-Apr-15	0.000	0.04	0.2	0.226	0.220	0	0
BH-PM5	30-Jul-15	0.000	0.134	0.4	0.035	0.036	0	0
BH-PM6	29-Jan-15	0.000	0.524	0.2	-1.000	0.211	0	0
BH-PM6	30-Apr-15	0.000	0.143	0.2	0.274	0.256	0	0
BH-PM6	30-Jul-15	0.000	0.341	0.3	0.377	0.377	0	0
BH-PM7	29-Jan-15	0.000	1.87	0	-1.000	0.296	0	0
BH-PM7	30-Apr-15	0.000	0.044	0	0.473	0.422	0	0
BH-PM7	30-Jul-15	0.000	0.437	0	0.515	0.515	0	0

SiteName	Date	F mg/l	Fe mg/l	NH3 mg/l	Cr mg/l	Cr6+ mg/l	Zn mg/l	As mg/l
BH-B1	29-Jan-15	0.200	0.174	0.2	-1.000	0.000	0	0
BH-B1	30-Apr-15	0.000	0	0	0.000	0.017	0	0.012
BH-B1	30-Jul-15	0.200	0.258	0.2	0.000	0.000	0	0
BH-IM1	29-Jan-15	1.800	0	0	-1.000	0.000	0	0
BH-IM1	30-Apr-15	1.400	0.027	0	0.000	0.000	0	0
BH-IM1	30-Jul-15	1.60	0.00	0.00	0.000	0.000	0	0
BH-IM2	29-Jan-15	0.000	0.039	0	-1.000	0.000	0	0
BH-IM2	30-Apr-15	0.000	0.052	0	0.000	0.000	0	0
BH-IM2	30-Jul-15	0.00	0.06	0.00	0.000	0.000	0.041	0
BH-PIM2	29-Jan-15	0.000	15	2	-1.000	0.000	0	0
BH-PIM2	30-Apr-15	0.000	0.306	0.7	0.948	0.899	0	0
BH-PIM2	30-Jul-15	0.000	17	11	0.120	0.000	0	0
BH-PIM3	29-Jan-15	0.000	0	0.4	-1.000	0.016	0	0
BH-PIM3	30-Apr-15	0.000	0	0.2	0.000	0.000	0.034	0
BH-PIM3	30-Jul-15	0.000	0.142	0	0.000	0.021	0	0
BH-PIM4	29-Jan-15	0.200	0	0.3	-1.000	0.000	0	0
BH-PIM4	30-Apr-15	0.000	0	0	0.612	0.598	0	0
BH-PIM4	30-Jul-15	0.20	0.05	0.00	0.000	0.000	0	0
BH-PIM5	29-Jan-15	0.000	0	0	-1.000	0.000	0	0
BH-PIM5	30-Apr-15	0.000	0	0	0.000	0.000	0	0
BH-PIM5	30-Jul-15	0.20	0.00	0.00	0.000	0.000	0	0
BH-PM1	29-Jan-15	0.000	3.93	0.2	-1.000	0.000	0	0
BH-PM1	30-Apr-15	0.000	0.691	0.3	0.000	0.000	0	0
BH-PM1	30-Jul-15	0.00	15.00	0.00	0.000	0.000	0	0
BH-PM2	29-Jan-15	0.000	0.072	0	-1.000	1.590	0	0.012
BH-PM2	30-Jul-15	0.600	0.0	0.2	1.780	1.780	0	0
BH-PM3	29-Jan-15	0.000	0.072	0	-1.000	1.590	0	0.012
BH-PM3	30-Jul-15	0.600	0.0	0.2	1.780	1.780	0	0
BH-PM4	29-Jan-15	0.200	31	0.5	-1.000	0.000	0	0
BH-PM4	30-Apr-15	0.000	31	1	0.000	0.000	0.052	0
BH-PM4	30-Jul-15	0.000	21	1	0.000	0.000	0	0
BH-PM5	29-Jan-15	0.000	0.307	0	-1.000	0.647	0	0.023
BH-PM5	30-Apr-15	0.000	0.04	0.2	0.226	0.220	0	0
BH-PM5	30-Jul-15	0.000	0.134	0.4	0.035	0.036	0	0
BH-PM6	29-Jan-15	0.000	0.524	0.2	-1.000	0.211	0	0
BH-PM6	30-Apr-15	0.000	0.143	0.2	0.274	0.256	0	0
BH-PM6	30-Jul-15	0.000	0.341	0.3	0.377	0.377	0	0
BH-PM7	29-Jan-15	0.000	1.87	0	-1.000	0.296	0	0
BH-PM7	30-Apr-15	0.000	0.044	0	0.473	0.422	0	0
BH-PM7	30-Jul-15	0.000	0.437	0	0.515	0.515	0	0

SiteName	Date	pH	EC mS/m	TDS mg/l	Ca mg/l	Mg mg/l	Na mg/l	K mg/l	MALK mg/l	Cl mg/l	SO4 mg/l	NO3-N mg/l
SP-A (Untreated)	25-Mar-15	7.60	212.00	1471.00	92.00	129.00	152.00	29.00	-1.00	176.00	557.00	-1.00
SP-A (Untreated)	01-Apr-15	7.8	228.0	1572.0	100.0	134.0	191.0	36.0	-1.00	204.0	570.0	
SP-A (Untreated)	09-Apr-15	7.6	221.0	1239.0	99.0	124.0	189.0	34.0	387.0	210.0	597.0	25.0
SP-A (Untreated)	14-Apr-15	8.6	256.0	1780.0	108.0	158.0	222.0	51.0	352.0	242.0	681.0	24.0
SP-A (Untreated)	23-Apr-15	8.0	221.0	1525.0	93.0	135.0	194.0	41.0	380.0	192.0	540.0	23.0
SP-A (Untreated)	04-May-15	8.5	227.0	1544.0	61.0	143.0	228.0	43.0	316.0	213.0	565.0	23.0
SP-A (Untreated)	07-May-15	7.4	214.0	1495.0	84.0	225.0	110.0	1.3	504.0	191.0	453.0	29.0
SP-A (Untreated)	13-May-15	7.8	215.0	1582.0	85.0	203.0	126.0	12.2	476.0	199.0	548.0	28.0
SP-A (Untreated)	29-May-15	8.1	219.0	1538.0	93.0	127.0	194.0	41.0	368.0	200.0	551.0	25.0
SP-A (Untreated)	09-Jun-15	7.4	219.0	1425.0	103.0	133.0	180.0	35.0	376.0	196.0	537.0	3.5
SP-A (Untreated)	18-Jun-15	8.7	225.0	1587.0	89.0	133.0	212.0	42.0	324.0	210.0	591.0	26.0
SP-A (Untreated)	25-Jun-15	8.4	227.0	1588.0	102.0	130.0	213.0	40.0	352.0	203.0	569.0	27.0
SP-A (Untreated)	03-Jul-15	8.3	201.0	1564.0	77.0	180.0	159.0	16.0	460.0	212.0	511.0	30.0
SP-B (Treated)	11-Feb-15	4.2	241.0	1578.0	59.0	114.0	217.0	65.0	-1.0	185.0	475.0	60.0
SP-B (Treated)	25-Mar-15	7.8	245.0	1568.0	31.0	153.0	226.0	45.0	-1.0	234.0	692.0	
SP-B (Treated)	01-Apr-15	6.1	490.0	5139.0	308.0	265.0	268.0	56.0	-1.0	247.0	3342.0	
SP-B (Treated)	09-Apr-15	6.7	513.0	2140.0	257.0	274.0	254.0	47.0	15.0	245.0	1890.0	3.1
SP-B (Treated)	14-Apr-15	8.0	278.0	1991.0	123.0	160.0	240.0	49.0	244.0	251.0	915.0	24.0
SP-B (Treated)	23-Apr-15	7.8	256.0	1734.0	98.0	164.0	243.0	49.0	260.0	224.0	694.0	24.0
SP-B (Treated)	04-May-15	7.6	225.0	1544.0	66.0	140.0	209.0	42.0	240.0	207.0	639.0	22.0
SP-B (Treated)	07-May-15	7.4	228.0	1609.0	71.0	197.0	158.0	18.5	300.0	205.0	660.0	27.0
SP-B (Treated)	13-May-15	7.7	222.0	1575.0	87.0	163.0	156.0	29.0	280.0	201.0	656.0	26.0
SP-B (Treated)	29-May-15	8.2	222.0	1566.0	98.0	129.0	202.0	42.0	372.0	208.0	553.0	25.0
SP-B (Treated)	09-Jun-15	6.4	231.0	1589.0	99.0	141.0	186.0	35.0	80.0	192.0	878.0	2.3
SP-B (Treated)	18-Jun-15	5.0	275.0	1967.0	105.0	154.0	189.0	40.0	5.0	202.0	1262.0	3.3
SP-B (Treated)	25-Jun-15	7.3	250.0	1862.0	93.0	151.0	216.0	44.0	84.0	223.0	969.0	26.0
SP-B (Treated)	03-Jul-15	7.6	248.0	1645.0	92.0	150.0	216.0	41.0	208.0	230.0	667.0	28.0

SiteName	Date	F mg/l	Fe mg/l	NH3 mg/l	Cr mg/l	Cr6+ mg/l
SP-A (Untreated)	25-Mar-15	0.80	0.03	0.00	2.19	2.05
SP-A (Untreated)	01-Apr-15	0.7	0.029	0	4.66	4.59
SP-A (Untreated)	09-Apr-15		0.0	0.0	3.9	4.2
SP-A (Untreated)	14-Apr-15	1.2	1.1	0.2	4.3	4.1
SP-A (Untreated)	23-Apr-15	0.7	0.16	0.2	4.7	4.38
SP-A (Untreated)	04-May-15	0.5	0.699	0.2	3.25	3.2
SP-A (Untreated)	07-May-15	0.2	0.025	0.2	1.64	1.49
SP-A (Untreated)	13-May-15	0.2	3.65	0.2	1.64	1.33
SP-A (Untreated)	29-May-15	0.7	0.801	0	3.32	3.03
SP-A (Untreated)	09-Jun-15	0.7	0.5	0.2	2.45	2.43
SP-A (Untreated)	18-Jun-15	0.7	0.334	0.2	2.66	2.51
SP-A (Untreated)	25-Jun-15	0.9	0.16	-1.00	2.76	2.63
SP-A (Untreated)	03-Jul-15	0.4	0.16	-1.00	2.04	2.04
SP-B (Treated)	11-Feb-15	2.7	27.0	97.5	0.3	0.0
SP-B (Treated)	25-Mar-15	0.7	19.0	0.2	1.2	0.0
SP-B (Treated)	01-Apr-15	0.3	1800.0	0.7	1.4	0.0
SP-B (Treated)	09-Apr-15		600.0	0.5	111.0	0.0
SP-B (Treated)	14-Apr-15	1.2	14.0	0.5	0.5	0.0
SP-B (Treated)	23-Apr-15	0.7	14	0.2	0.0	0.0
SP-B (Treated)	04-May-15	0.5	37.0	0.2	2.63	0.0
SP-B (Treated)	07-May-15	0.2	27	0.2	0.147	0.012
SP-B (Treated)	13-May-15	0.3	64	0.2	0.343	0.01
SP-B (Treated)	29-May-15	0.8	3.84	0	2.9	2.47
SP-B (Treated)	09-Jun-15	0.7	163	0.2	1.42	0.01
SP-B (Treated)	18-Jun-15	0.5	164	0.2	0.025	0.01
SP-B (Treated)	25-Jun-15	0.8	31	-1.00	0.158	0
SP-B (Treated)	03-Jul-15	0.7	7.71	-1.00	0.099	0.01

APPENDIX II: Aquifer Test Analysis

Summary

Main

BH-SM1

Applicable	Method	Sustainable yield (l/s)	Std. Dev	Early T (m^2/d)	Late T (m^2/d)	S	AD used
☑	Basic FC	1.02	0.32	105	79.1	5.00E-03	7.0
☐	Advanced FC			105	79.1	1.00E-03	7.0
☑	FC inflection point	0.01	0.00				0.1
☑	Cooper-Jacob	1.18	0.76		37.7	5.00E-03	7.0
☐	FC Non-Linear						7.0
☑	Barker	0.91	0.25	K_f = 47	S_s =	2.00E-03	7.0
	Average Q_sust (l/s)	0.78	0.53	b = 1.06	Fractal dimension n =	2.00	

Recommended abstraction rate (L/s)	0.78	for 24 hours per day		
Hours per day of pumping 24	0.78	L/s for	24	hours per day
Amount of water allowed to be abstracted per month	2021.76	m^3		
Borehole could satisfy the basic human need of	2696	persons		
Is the water suitable for domestic use (Yes/No)	No			

Summary

Main

BH-SM2

Applicable	Method	Sustainable yield (l/s)	Std. Dev	Early T (m^2/d)		Late T (m^2/d)		S	AD used
☑	Basic FC	0.01	0.00	0		0.4		5.00E-03	8.4
☐	Advanced FC			0		0.4		1.00E-03	8.4
☑	FC inflection point	0.01	0.00						4.0
☑	Cooper-Jacob	-0.11	0.07			0.3		5.00E-03	8.4
☐	FC Non-Linear								8.4
☑	Barker	0.00	0.00	K_f =	1		S_s =	1.45E-03	8.4
	Average Q_sust (l/s)	-0.02	0.06	b =	0.64	Fractal dimension n =		1.67	

Recommended abstraction rate (L/s)	0.02	for 24 hours per day	
Hours per day of pumping	24	0.02	L/s for 24 hours per day
Amount of water allowed to be abstracted per month		51.84	m^3
Borehole could satisfy the basic human need of		69	persons
Is the water suitable for domestic use (Yes/No)	No		

Summary

Main

BH-PM2

Applicable	Method	Sustainable yield (l/s)	Std. Dev	Early T (m^2/d)		Late T (m^2/d)		S	AD used
☑	Basic FC	0.70	0.13	3953		395.3		5.00E-03	1.6
☐	Advanced FC			3953		395.3		1.00E-03	1.6
☑	FC inflection point	0.15	0.00						0.2
☑	Cooper-Jacob	0.32	0.21			62.9		5.00E-03	1.6
☐	FC Non-Linear								1.6
☑	Barker	0.37	0.03	K_f =	87		S_s =	1.50E-06	1.6
	Average Q_sust (l/s)	0.39	0.23	b =	1.12	Fractal dimension n =		1.95	

Recommended abstraction rate (L/s)	1.08	for 24 hours per day	
Hours per day of pumping	24	1.08 L/s for 24 hours per day	
Amount of water allowed to be abstracted per month	2799.36	m^3	
Borehole could satisfy the basic human need of	3732	persons	
Is the water suitable for domestic use (Yes/No)	No		

Summary

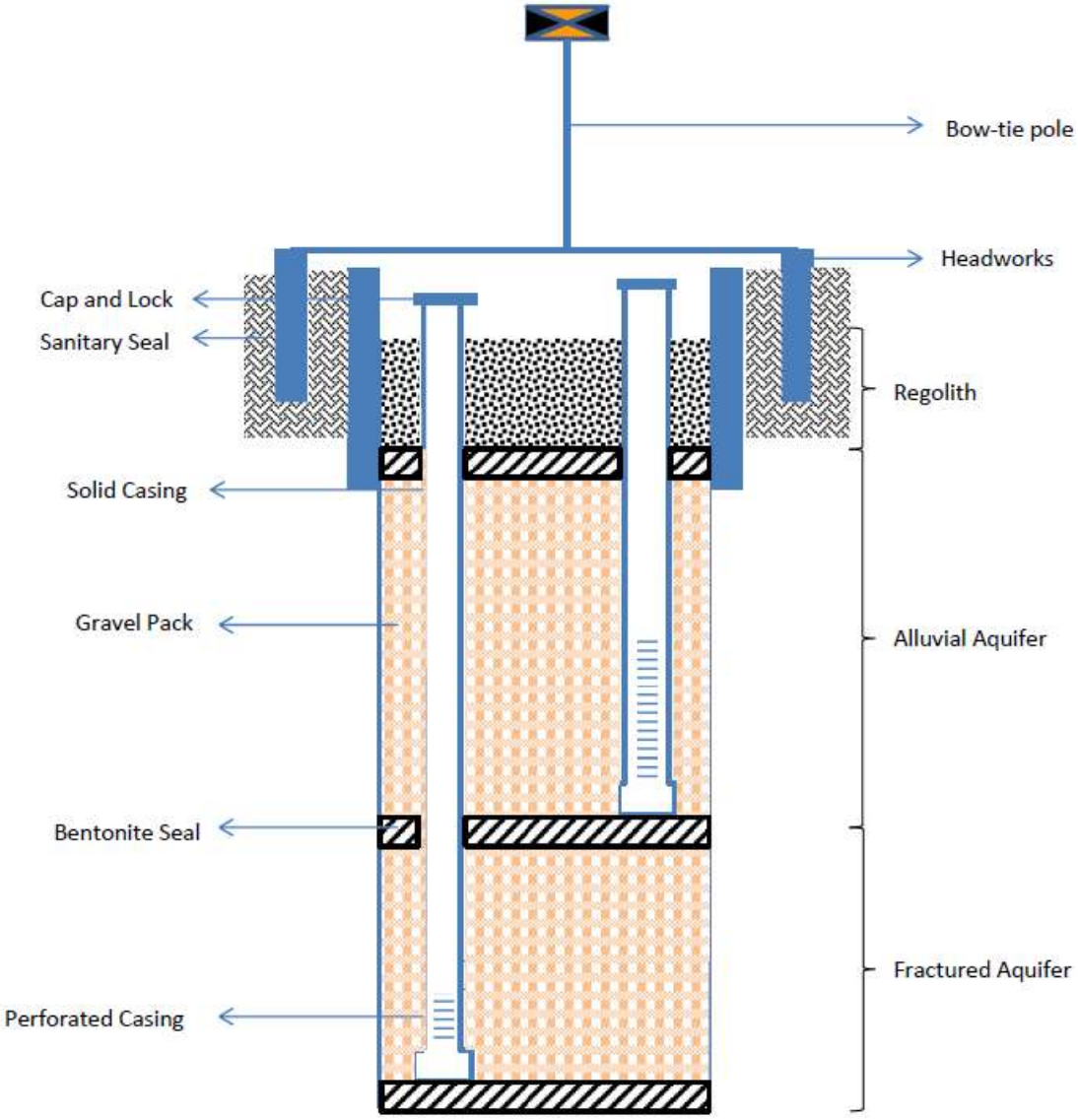
Main

BH-PM2

Applicable	Method	Sustainable yield (l/s)	Std. Dev	Early T (m^2/d)	Late T (m^2/d)	S	AD used
☑	Basic FC	0.23	0.08	132	131.8	5.00E-03	0.9
☐	Advanced FC			132	131.8	1.00E-03	0.9
☑	FC inflection point	0.02	0.01				0.1
☑	Cooper-Jacob	0.29	0.19		138.2	5.00E-03	0.9
☐	FC Non-Linear						0.9
☑	Barker	0.21	0.06	K_f = 303	S_s =	2.00E-03	0.9
	Average Q_sust (l/s)	0.19	0.12	b = 0.33	Fractal dimension n =	2.00	

Recommended abstraction rate (L/s)	0.20	for 24 hours per day	
Hours per day of pumping: 24	0.20	L/s for 24	hours per day
Amount of water allowed to be abstracted per month	518.4	m^3	
Borehole could satisfy the basic human need of	691	persons	
Is the water suitable for domestic use (Yes/No)	No		

APPENDIX III: Borehole Construction


Bow-tie pole
Headworks
Cap and Lock
Sanitary Seal
Regolith
Solid Casing
Gravel Pack
Alluvial Aquifer
Bentonite Seal
Fractured Aquifer
Perforated Casing